UNIVERSITY OF STELLENBOSCH

Relationship of historical copper mining to the transport and accumulation of trace metals and salts in semi-arid environments: An example from the Buffels River, Northern Cape, South Africa.

Thesis presented in fulfilment of the requirements for the degree Master of Science in Geology/Environmental Geochemistry Stellenbosch University

Alexander Dunford

March 2016

Supervisor: Dr. Jodie Miller

Co-supervisor: Dr. Catherine Clarke

Faculty of Science

Abstract

The town of Kleinzee, located in the Northern Cape, South Africa exists solely to mine alluvial diamonds found in the Buffels River. Given the very low precipitation of the area (generally <150mm/yr) groundwater is the principal supply of domestic and industrial water to the town. In an effort to increase the water supply needed, the town installed an underground membrane across the Buffels River approximately 5.5km upriver from the town. However, climatic conditions, long term copper and diamond mining and poor groundwater management practices have combined to produce very poor quality groundwater within the Buffels River Valley. The purpose of this study is to look at the impact of the membrane on the quality of both the shallow groundwater system as well as the soils within the river bed. To do this, 46 sites were selected for soil analysis starting below the membrane and continuing above the membrane upriver for a distance of approximately 5 km. Additionally, a further 15 groundwater samples were collected at the end of the wet season in October when groundwater was available. Cation and anion analysis of the shallow groundwater and the saturated paste extracts shows significant peaks in SO_4^{2-} and Mg^{2+} immediately above the membrane in the sediments in addition to Na^{+} and Cl^{-}, diminishing upstream away from the membrane. Cu^{2+} and Zn^{2+} did not show an elevated concentrations in the groundwater or sediments above the membrane as originally thought. Experiments on atacamite, a Cu^{2+}-hydroxide, which forms naturally in the Spektakel soils within the Buffels River Valley, indicates that although generally stable at moderate pH, large rain events may increase the solubility of atacamite resulting in its transport downstream. However, the source of sulphate is probably linked to processing of Cu^{2+} ores further up the river valley. The transport mechanism of the groundwater salts and trace metals is via dissolution mobilization. The membrane is accumulating trace metals and salts in sediments behind the membrane and not in groundwater found behind the membrane. Thus accumulation is due principally to evaporative concentration.

Keywords: Atacamite, Buffels River, membrane, shallow groundwater

Declaration

I declare that *Relationship of historical copper mining to the transport and accumulation of trace metals and salts in semi-arid environments: An example from the Buffels River, Northern Cape, South Africa* is my own work, that it has not been submitted for any degree or examination in any other university, and that all the sources I have used or quoted have been indicated and acknowledge by complete references.

Full name: Alexander John Dunford Date: March 2016

Acknowledgements

I would first like to thank my supervisor Dr Jodie Miller who provided me with insight to the study area, suggestions, reading of drafts and the opportunity to do this study. I would also like to thank Dr Catherine Clarke my co-supervisor for her help and input into my study. Furthermore I like to thank the NRF for the financial assistance I received.

The central analytical facilities staff at the University of Stellenbosch must also be thanked for analysing the data. The contributions from Riana Rossouw (Department of Earth Sciences, Stellenbosch University), Matt Gordons (Department of Soil Sciences, Stellenbosch University), Dr Maritjie Stander, Dr Cynthia Sanchez-Garrido, and Dr Remy Bucher from iThemba laboratory with the analytical analysis are highly acknowledged. I would like to acknowledge the South African Weather Bureau for the historical weather records of Namaqualand. Nigel Robertson for his assistance in the Soil Science Department with various sediment experiments. Acknowledgement should also be given to the farmers in the area and William MacDonald from the De Beers mine for access to the study area.

Thanks to fellow masters student, Kelley Swana who provided help and company with field work and various laboratory experiments. Lastly I would like to thank my family and friends for their involvement and encouragement throughout the years.

Contents

Table of Figures

List of Tables

1. INTRODUCTION

1.1. General Introduction

Salinization of groundwater in semi-arid and arid environments is becoming a critical issue for water resource management worldwide (Borrok & Engle, 2014). According to Rose (2004) salinization of groundwater and soil affects 7% of the world's total land mass, with most of this being in arid and semi-arid regions. In Africa these regions are predominantly in poor and rural areas where clean drinking water is important for the sustainability of the town. However various other means of salinization are also likely. Dissolution of old marine sediments or rock mass is also known to increase salinity. Coastal areas are also likely to have ingress of marine waters due to over pumping of groundwater used for agriculture. The most serious issue associated with high salt contents in groundwater and soils is that it leads to non-potable water. In poor areas infrastructure is not well maintained and knowing the source and the transport mechanisms of salts and trace metals through the hydrosphere is essential for long term management and protection of groundwater resources (Herczeg, et al., 2001).

Numerous studies regarding groundwater salinization throughout Africa as well as other arid and semi-arid regions have been conducted (Bennett & Hanor, 1987; Bridgman, et al., 2008; Campbell, et al., 1992). Salinization and the associated chemical evolution of groundwater in the north central Namibia is thought to be the result of concentration by evaporation, dissolution of saline sediments and mixing with older saline groundwater (Shanyengana, et al., 2004). This process and mechanism is the same as those found in the Northern Cape, South Africa (Adams, et al., 2004). Groundwater salinity in the Namaqualand, Northern Cape, has been reported by several researchers who studied the groundwater in this region (Adams, et al., 2004; Pietersen, et al., 2009; Leshomo, 2011). A more regionally specific investigation was done by Nakwafila (2015) where the salinity of the Buffels River was investigated. The results from this showed that the source of the salinity in the Buffels River was due to dissolution of the host rocks and subsequent concentration through evaporation. The results were used to help in understanding the mechanisms and sources of salinity in alluvial aquifers along the Buffels River.

Acosta et al. (2011) discussed how the increase of salinity in groundwater increased the mobility of heavy metals such as Cu^{2+}, Cd^{2+}, Pb^{2+} and Zn^{2+}. This happens through various methods but the main mechanism regulating Cu^{2+} mobility was the formation of Cu-sulphate, followed by competition with magnesium, calcium and chloride. The higher mobility of heavy metals linked to salinity globally is thought to be one of the main processes causing land degradation (Acosta, et al., 2011). Due to historical copper mining in Namaqualand there is a possibility of heavy metal mobilisation into surrounding groundwater and sediments. Le Roux (2013) conducted a study which was to characterise

the chemical environment within the Spektakel soils surrounding the Spektakel mine, Namaqualand, in order to understand and predict the conditions needed for the formation and stability of secondary Cu^{2+} minerals in the soil. The overall conclusion Le Roux (2013) made was that the current chemical conditions are conducive for the formation and stability of atacamite. However a reduction in the soil pH would allow for dissolution of atacamite and result in leaching of large quantities of Cu^{2+} into the surrounding water bodies.

There has been no research on the effects historical mining has had on the groundwater in the region. Significant research has been done on salinization and trace metal transport and accumulation throughout arid and semi-arid environments (Du Laing, et al., 2008; Pestana, et al., 1997) however; nothing has been done on the area selected for this study; the lower reaches of the Buffels River just outside of Kleinzee. These results are particularly important for the town of Kleinzee and surrounding farms which tap into the groundwater as a source of domestic water. The possible accumulation and mobility of trace metals associated with the high salinity found in the groundwater has also not been fully researched in the lower reaches of the Buffels River, which is the aim of this study.

This study was interested in the impact artisanal Cu mining had on the region and groundwater quality.. The town of Kleinzee is one of the many rural centres that rely on the highly saline water of the Buffels River. The town of Kleinzee is situated at the end of the 9,249km^2 Buffels River catchment, where it flows into the Atlantic Ocean (Benito, et al., 2010). The valley is rich in historical copper deposits, however today the Okiep copper district hosts very little mining due to fluctuating copper prices (Cairncross, 2004). According to local farmers who border onto the membrane and use the groundwater source, the mining is believed to have contributed to the increased salinity in the area. It is also thought to possibly be adding trace metals into the soil and groundwater. These heavy metals could potentially add to the issue of potable water in the area due to the health implication of high trace metal concentrations in drinking water (Acosta, et al., 2011; Lim, et al., 2008).

The source of the salts in the Buffels River are still being debated and several different explanations have been proposed. One explanation for the source of the salts is due to dominant Na-Cl rainfall chemistry and by the preferential dissolution and leaching of the more evaporitic salts during infiltration (Adams, et al., 2004). Another proposed source of these salts is thought to be derived from the dissolution of rocks found in the valley (Nakwafila, 2015). Nakwafila (2015) states that the groundwater samples have high $^{87}Sr/^{86}Sr$ ratios which links them to the dissolution of K-feldspar, hornblende and micas found in the Rietberg granites. Much of the salt in the landscape is dissolved sodium chloride found in groundwater and sediments (Rengasamy, 2006; Herczeg, et al., 2001). Highly saline groundwater furthermore allows for the easier mobility of heavy metals through groundwater (Zhao, et al., 2013).

In 1996, the town of Kleinzee placed a plastic membrane across the Buffels River with the idea to dam groundwater that could be used by the rural town as their water supply. The membrane across the Buffels River gave an ideal opportunity to study the possible mobilisation of the trace metals. This is because the membrane could also act as a concentrator of: (1) dissolved metals that are transported down the river in the shallow groundwater; (2) dissolved salts also transported down the river in the shallow groundwater; and (3) heavy metal contaminated particulate matter and sediment during storm and other episodic flood events.

Furthermore this study examines the formation and mobility of copper in the form of the mineral atacamite [$Cu_2(OH)_3Cl$] which is found at the Spektakel mine (Clarke, et al., 2014; Le Roux, 2013). The use of atacamite in leaching and other mobility studies has allowed for the understanding of copper mobility in the sediments surrounding the Buffels River. Various leaching and titration experiments will be used to recreate possible environments in which trace metals can be transported. The investigation of the mobilisation of trace metals and salinity in the Buffels River catchment is important to help in understanding how trace metals are mobilised in the study area. This mobilisation is important in supporting the understanding of possible accumulation.

In this study, the role of the membrane in accumulating salts and trace metals will be examined to assess whether trace metals are currently being or have in the past been transported down the river system. The idea will be to test whether trace metals are transported as particulate matter and/or as dissolved species. The water source behind the membrane needs to be understood as an accumulation of certain metals and high salt content in the groundwater could have a detrimental effect on the general public currently consuming the water (Karim, 2011; WHO, 2008). The results gathered will help to develop appropriate management strategies for the Buffels River system and are particularly important in the possibility of climate change that will result in higher average temperatures and lower precipitation rates (Fauchereau, et al., 2003).

1.2. Aims and Objectives

This study will investigate the transportation and accumulation of trace metals in the shallow groundwater of the Buffels River. The role of the membrane across the river inland of Kleinzee will be assessed and the implications for management of groundwater in the mining regions in arid to semi-arid environments will be discussed. In order to do this, several objectives and key questions have been identified.

1. To characterise the nature and spatial distribution of sediments in the Buffels River above and below the membrane.

1.1. What is the distribution of the sediment grain sizes in the Buffels River 5 km upstream and 0.5 km downstream from the membrane with respect to depth in the Buffels River?

1.2. What is the composition of different sediment size fractions above and below the membrane with respect to depth in the Buffels River?

1.3. Are all sediment size fractions likely to aid in accumulation of trace metals, and if not which sediments are more likely to host trace metals?

2. To characterise the nature and distribution of salts in the Buffels River upstream and downstream from the membrane.

2.1. What is the concentration of the salt load in shallow groundwater and adhering to sediments in the Buffels River?

2.2. Does the composition of salts found in shallow groundwater and adhering to sediments vary in the Buffels River?

2.3. Is the concentration and composition of the salts in sediments and shallow groundwater homogeneous throughout the study area?

3. To characterise the nature and distribution of trace metals in the Buffels River upstream and downstream from the membrane.

3.1. Are the trace metals found both above and below the membrane, and if so what is the spatial distribution with proximity to the membrane and does this differ above and below the membrane?

3.2. Are the trace metals more accumulated in the upper sediments (0-30cm) and groundwater, or more in the lower sediments (below 30cm from surface) and groundwater and how does this relate to the variation in sediment size with depth?

3.3. What could the potential source of the trace metals be?

4. To determine the mechanism(s) by which salts and trace metals are transported in the Buffels River Valley.

4.1. By what mechanism are salts and trace metals transported down the Buffels River, for example as particulate matter or dissolved ions?

4.2. What role does the membrane in the Buffels River play in accumulating salts and trace metals, and what impact does this have for groundwater quality?

4.3. What are the implications for management of groundwater resources in this area and other areas with small scale mining activities?

1.3. Salinization

Water salinization refers to an increase in Total Dissolved Solids (TDS) and in the overall chemical content of water and sediments (Richter & Kreitler, 1993). Several classifications have been put into place for the ranking of groundwater salinity levels (Carpenter, et al., 1974; Freeze & Cherry, 1979). These classifications vary in class names, values used and parameters used. The classification used in this study is the one defined by Freeze and Cherry (1979) where EC is used to determine TDS at 25 °C using the following equation:

$$TDS\left(\frac{mg}{l}\right) = EC\ \left(\frac{mS}{m}\right)@25℃\ \times 6.5$$

1.3.1. Types of Salinity

Salinity is separated into two main types depending on the salt mobilisation process and where the salt is mobilised to. These are known as primary and secondary salinity types, and are discussed below:

1.3.1.1. Primary Salinity

Primary salinity is a naturally occurring process caused by weathering of rocks, wind and rainfall depositing salt over thousands of years. These salt deposits have an influence on the sediment and groundwater. According to McDowell (2008) and Bridgman et al. (2008) this form of salinity occurs more often in arid environments where evaporation is high and regional rainfall is low. The high evaporation and low rainfall allows for the concentration of salts in groundwater and sediments. Semi-arid and arid regions are more likely to be affected by primary salinization due to these two main circumstances.

1.3.1.2. Secondary Salinity

Secondary salinity occurs as a result from anthropogenic activities which cause a change in the hydrological cycle. These changes are mostly due to agricultural and industrial activities, and are characteristically localised because of this. The following are examples of secondary salinity:

(a) Dryland Salinity

Dryland salinity is broadly the result of the interplay between three processes: (1) groundwater recharge, (2) groundwater movement and (3) groundwater discharge (Scanlon, et al., 2002). Scanlon et al. (2002) state that it is common in areas where deep-rooted perennial vegetation are replaced by crops and pastures that have shallow root systems in non-irrigated areas. These crops utilise less groundwater and decrease the annual evapotranspiration as well as an in increase in recharge to the

water table. This increase in recharge leads to the water table rising and capillary action brings salts to the surface from deep soils, resulting in salinization (Borrok & Engle, 2014). Phillips et al. (2003) point out that dryland salinity may also be caused by the exposure of naturally saline soils and sodic soils due to agricultural preparation or any other earth works.

(b) Irrigation Salinity

Rising groundwater levels due to increased irrigation for agriculture can allow salts in the non-saturated zone to become mobilised. The mobilisation of these salts can then contaminate the groundwater leading to salinization. Alternatively the salts can move to the surface where evaporation allows for the concentration of salts (Van Weert, et al., 2009). According to Ghassemi et al. (1995) this is also the most common form of secondary salinization.

(c) Urban Salinity

Urban salinization is groundwater salinization in urban areas, which is generally caused by urban development (Slinger & Tenison, 2007). This includes activities such as over-watering of parks and leaking of pipes which results in the groundwater level to rise. The rise in groundwater then allows for the mobilisation of salts in the landscape which are then redistributed into the near soil surface. This in turn allows for salinization to occur. Other anthropogenic sources of salts in urban environments are sewage and building materials which mobilise into groundwater.

(d) Industrial Salinity

Industrial salinity is caused by industrial processes such as mining, and large factories. Mining activities often concentrate salts in industrial waste waters. These waste waters are often not handled well and lead to contamination of groundwater and soil. This contamination can lead to accumulation and salinization of the sediments and groundwater. Early mining activities often were not correctly monitored and regulated. This has resulted in abandoned mines being a source of salts to the water resources (Hohne & Hansen, 2008).

1.3.2. Sources of Salt

According to Phillips et al. (2003) groundwater salinity results from the addition of solutes to the groundwater and from concentration processes of dissolved constituents through evapotranspiration. Salt sources can be from a natural origin, or a secondary, anthropogenic, source. Examples of natural sources are halites and seawater intrusion, while an anthropogenic source could be mining waste. Different sources of salts are able to be separated according to their chemical composition. Sodium chloride salts dominate most of the saline waters in the world however other ions such as calcium, magnesium, sulphate and bicarbonate are also found in specific locations throughout the world (Rengasamy, 2006). Examples include Austria where sulphate salts are common, Colorado USA where

bicarbonate salts dominate and England where magnesium sulphate or “Epsom salts” are usually found (Rengasamy, 2006).

1.3.2.1. Rainfall

Rainwater contains low concentrations of salts owing to the distillation effect of evaporation from the ocean. This low salt rainwater is then deposited over coastal areas. These salts are predominantly sodium chloride which is the ocean water signature. The small amount of salt being deposited during each rainfall slowly accumulates on land and is often further concentrated due to evaporation (Shanyengana, et al., 2004). This salt is then dissolved by recharge water and leaches through to the groundwater causing salinization (Rengasamy, 2006). Furthermore, Richter and Kreitler (1993) state that precipitation interacts with atmospheric gases and particles increasing the salt concentration in the precipitation water.

1.3.2.2. Marine Salts

Salinity from marine salts can originate through various sources discussed below.

(a) Connate Saline Groundwater

Connate saline groundwater is found in sediment formations that have a marine origin. These sediments were deposited in seawater and often have trapped pockets of seawater within interstitial spaces (Van Weert, et al., 2009). These pockets of highly saline water interact with precipitation when it flows through the sediment formation. Connate saline waters are prevailing in deeper aquifers as precipitation in shallow aquifers flushes out the formational water and dilutes the salinity (Monjerezi, 2012). This suggests that salinity might increase with depth (Vengosh, et al., 2002).

(b) Seawater Intrusion (Ingress)

Seawater intrusion is common for coastal aquifer and is caused by changes in hydraulic heads. Coastal aquifers are hydraulically connected to ocean waters and over abstraction removes groundwater and causes a decrease in the hydraulic head (Wicks & Herman, 1996; Wicks, et al., 1995.). This decrease results in an up-coning of saline seawater which fills the aquifer (Kim, et al., 2003; Vengosh, et al., 2002; Park, et al., 2005). Groundwater in coastal aquifers flows towards the sea, but due to over pumping of coastal aquifers the fresh water head decreases in comparison to the sea water head. This in turn allows for seawater intrusion (Carreira, et al., 2014).

(c) Marine Transgression (Natural or Anthropogenically Induced) and Incidental Flooding

These two forms of marine salts are caused by natural changes of sea level. Marine transgression happens over a longer period of time, geological scale. Transgression and regression of the geology causes coastal lowlands to become flooded by the sea (Hanor & Evans, 1988). This process takes a long

time, before a regression period occurs, causing salinization of the coastal aquifers. Incidental flooding is a much shorter time scale, an example of this is a tsunami event (McLeod, et al., 2010). The coastal areas are flooded with seawater which causes salinization to the groundwater aquifers.

1.3.2.3. Natural Terrestrial Salts

Natural terrestrial salts cause salinization through the following ways:

(a) Evaporation at or Near Land Surface

In arid to semi-arid environments, evaporation is a significant salinization process. This is due to the high evaporation rates in comparison to the low rainfall rates. The low precipitation amounts aren't enough to flush the accumulated salts (Deverel & Gallanthine, 1989; Yechieli & Wood, 2002). Concentration of saline groundwater is mostly found in shallow surface aquifers, as deeper aquifers are less impacted by evaporation.

(b) Dissolution of Naturally Occurring Soluble Minerals

Sediment basins often contain evaporites at great depths, which may be dissolved by regional or local groundwater recharge (Bennett & Hanor, 1987; Macpherson, 1992). These stored evaporates can get into contact with groundwater moving through the geology. The mobilization of evaporites by the dissolution of soluble salts such as gypsum and halite minerals leads to an increase in salinization of groundwater (Herczeg, et al., 2001).

(c) Aeolian Deposits

Wind-blown sea-salts caused by salts being blown off the ocean surface and onto the soil surface of coastal land also causes salinization. Precipitation flushes these surface salts into the groundwater where they mix and cause an increase of salinity. Strong winds are also known to carry mineral matter which mix with droplets in the atmosphere and dissolve into the precipitation. This precipitation then falls and infiltrates the groundwater through recharge (Richter & Kreitler, 1993).

(d) Geological Sources

Geological sources of salinity are from the lithological make-up of the aquifer. Compact layers of clay and shale are great filters and sieve out dissolved large ions in the groundwater flowing through them. These ions result in salinization of the groundwater at this geological contact (Whitworth & Fritz, 1994). An additional source of saline groundwater can be found where geothermal water is present. The geothermal groundwater contains minerals which become part of the groundwater present in the aquifer (Richter & Kreitler, 1993). The final geological source of salts in groundwater is due to the weathering of the aquifer geology. This allows for the mobilisation of ions found in the geology which

dissolve in the groundwater. Deeper aquifers which have a long residence times dissolve the ions out of the aquifer which then allows for salinization of the groundwater found within the aquifer.

1.3.2.4. Anthropogenic Salts

Anthropogenic pollution is caused by human activities. These include road salt, domestic, industrial and agricultural waste water, oil spills and brines from mining or desalination plants. This pollution causes an addition of salt-load in groundwater as it infiltrates the soil and mixes with the groundwater. Anthropogenic salts are usually more localised than the others. The shallow and high permeability characters of alluvial aquifers makes them more vulnerable to anthropogenic salt sources (Carreira, et al., 2014).

1.4. Trace Metals

Metals including lead (Pb^{2+}), chromium (Cr^{2+}), arsenic (As), zinc (Zn^{2+}), cadmium (Cd^{2+}), copper (Cu^{2+}) and mercury (Hg^{2+}) can cause significant damage to the environment and human health as a result of their mobilities and bioavailability (Mulligan, et al., 2001). The sources of trace metals are through natural and anthropogenic processes, however as industry grows, the anthropogenic sources are exceeding the natural concentrations. The sources and health risks are briefly discussed below:

1.4.1. Source of Trace Metals

Trace metals have various sources, which can be broken up into four main groups according to Pacyna et al. (1995). These groups are atmospheric input, aquatic input, and terrestrial input and output. Below is an outline of each:

(a) Atmospheric Trace Metals

i. Anthropogenic sources

The source of these trace metals is predominantly through pyrometallurgical processes in the metal industries (Pacyna, et al., 1995). This is when minerals and metallurgical ores and concentrates are thermally treated to change the physical and chemical properties. Smelting, roasting, calcining and refining are some examples of this gaseous pollution. This action is a major source of atmospheric As^{3+}, Cd^{2+}, Cu^{2+}, Sb^{3+}, Pb^{2+}, and Se (Pacyna, et al., 1995). Another source of anthropogenic trace metals in the atmosphere is combustion of coal for electricity generation or industrial, residential, or commercial use is a source for anthropogenic As^{3+}, Cr^{2+}, Mn^{2+}, Sb^{3+}, and Ti. Motor vehicles are a source of Pb^{2+}, while the iron and steel industry produce Cr^{2+} and Mn^{2+}.

ii. Natural Sources

Natural sources of atmospheric trace metals include wind-borne soil particles, volcanoes, sea-salt spray, and wild forest fires (Nriagu, 1989). According to Pacyna et al. (1995) volcanoes account for 40-

50% of the As^{3+}, Cr^{2+}, Cu^{2+}, Ni^{2+}, Pb^{2+} and Sb^{3+} produced through natural sources. Salt aerosols accounted for <10% of trace metals from a natural source globally, while soil derived dust emissions accounted for 20-30% of the Cu^{2+}, Mo, Ni^{2+}, Pb^{2+}, Sb^{3+} and Zn^{2+} released into the atmosphere annually. The study performed by Nriagu (1989) suggests that human activities generate more trace metals than natural sources, and this shift would cause significant alterations in the natural bio-geochemical cycling of trace metals.

(b) Sources of aquatic input of trace metals

Aquatic input of trace metals includes pollution into aquatic ecosystems such as rivers, streams, lakes, and oceans. The source of this pollution is from waste-water effluents from mining and smelting, and dumping of raw sewerage (Pacyna, et al., 1995). The atmospheric pollutants also often find their way into water sources through precipitation which contains atmospheric trace metals. Once these trace metals have entered into the water cycle they can enter soils where they can accumulate through evaporation and adsorption (Nriagu, 1989).

(c) Terrestrial input and output of trace metals

A study by Nriagu and Pacyna (1988) was the first assessment of worldwide emissions and the effect on soils by trace metals. The source of trace metals in soils is stated to be from various sources, however the two predominant sources were through municipal and industrial waste dumps, in addition to ash residue from coal combustion. Municipal waste is a source for Cu^{2+}, Hg^{2+}, Pd^{2+}, and Zn^{2+} with noticeable Cd^{2+}, Pd^{2+}, and V being a source from the atmosphere (Pacyna, et al., 1995). Sewage sludge is not seen as a global source of trace metals contamination, however on a local scale it is often an important source for soil and groundwater contamination (Nriagu & Pacyna, 1988). In rural and poor communities sanitation is often poor; this makes sewage an important trace metal source on a local scale.

1.4.2. Health Implications

Global mining activities since the mid-1800s have accelerated metal cycling in aquatic systems. Historical mining lacked correct environmental procedures, and have more often than not been abandoned without any form of rehabilitation. Naturally enriched ore bodies can contribute relatively minor increases in trace metal content in water systems, however mining and extraction of minerals from ore rock have highly increased trace metal content in groundwater (Axtmann & Luoma, 1991; Cantor, 1997; Moore & Luoma, 1990).

Although some metals such as iron (Fe^{2+}), copper (Cu^{2+}), manganese (Mn^{2+}) and zinc (Zn^{2+}) are essential for living organisms in specific concentrations, higher concentrations are toxic (Kavcar, et al., 2009). Ingestion of drinking water containing high concentrations of trace metals have been known to have

an adverse effect on health ranging from shortness in breath to several types of cancer (Muhammad, et al., 2011). Arsenic (As^{3+}) is one of the more hazardous trace metals as it is both toxic and carcinogenic. Non-essential metals are also known to accumulate in the tissue of organisms, these include cadmium (Cd^{2+}), Lead (Pb^{2+}), Mercury (Hg^{2+}) and silver (Ag^{+}) (Muhammad, et al., 2011). These non-essential metals cause various adverse health problems such as brain development (Lau, et al., 1998).

Various studies have been done on the effects that certain trace metals have on the body. Experimental data in humans and animals showed that Cd^{2+} may cause cancer in humans (IARC, 1993). Chromium (Cr^{3+}) is known for causing liver and kidney problems (Knight, et al., 1997). Cobalt (Co^{3+}) through the consumption of contaminated food and water is known to cause abnormal thyroid artery, polycythemia, over production of red blood cells and coronary artery problems (Rober & Mari, 2003). High Cu^{2+} and Mn^{2+} in drinking water is known to cause metal health issues which include Alzheimers (Dieter, et al., 2005). Wasserman et al. (2006) has shown that high Mn^{2+} contamination in drinking water affects the intellectual functions of children. Ni-sulfate and Ni-chloride have been known to cause cardiac arrest, while Pb^{2+} in toxic quantities is known to cause headaches, irritability, abdominal pain, nerve damages, kidney damage, blood pressure, lung cancer, stomach cancer and gliomas (Jarup, 2009).

In light of the above studies, trace metal accumulation in groundwater and sediments would likely impact on the health of inhabitants of Kleinzee. Groundwater is often used as potable water without taking trace metal concentrations into account. This is an important aspect of groundwater and sediments especially in historical mining areas where rehabilitation was not taken into account. These effects are not quantified at present and are not within the scope of this study.

1.5. Geological Context

The study area forms part of the Okiep region which is situated in the central portion of the semi-arid Namaqualand area of the Northwestern Cape Province in South Africa. The greater part of the copper district consists of mountainous terrain cut through by sand filled valleys. The general altitude is approximately 900m to 1300m at the interior plateau but much lower along the coastal belt. The Spektakel mine lies on the lower escarpment at approximately 200 m above sea level. There is an abundance of mineral wealth in the area, and the valley has several small scale mines spread throughout.

1.5.1. Geological Background

The Namaqualand is part of the Namaqua-Natal Metamorphic Province (NNMP), an arcuate belt of Palaeoproterozoic to Mesoproterozoic mixed supracrustals and orthogneisses that wrap around the western and southern sides of the Archaean Kaapvaal Craton (Hartnady, et al., 1985). There are two parts to the NNMP, the Natal Sector in the south east of South Africa and the Namaqua Sector in the north west of South African and southern Namibia. The study area is located in Namaqualand which is within the Namaqua Sector of the NNMP. The Namaqua Sector is made up of six different terranes and subprovinces, and consisting broadly meta-sedimentary and meta-igneous rocks (Petterson, 2008). The orientation of each terrane or sub-province corresponds to the regional fabric for each terrane, with the direction of orogenic accretion being generally eastwards towards the Kaapvaal Craton via stacking of south vergence thrust blocks. The region is affected by the Palaeoproterozoic Orange River Orogeny and subsequently by the Mesoproterozoic Namaquan Orogeny. The Namaqua Orogeny is associated with the planetary wide formation of accretionary belts associated with the formation of the supercontinent Rodinia (Hartnady, et al., 1985).

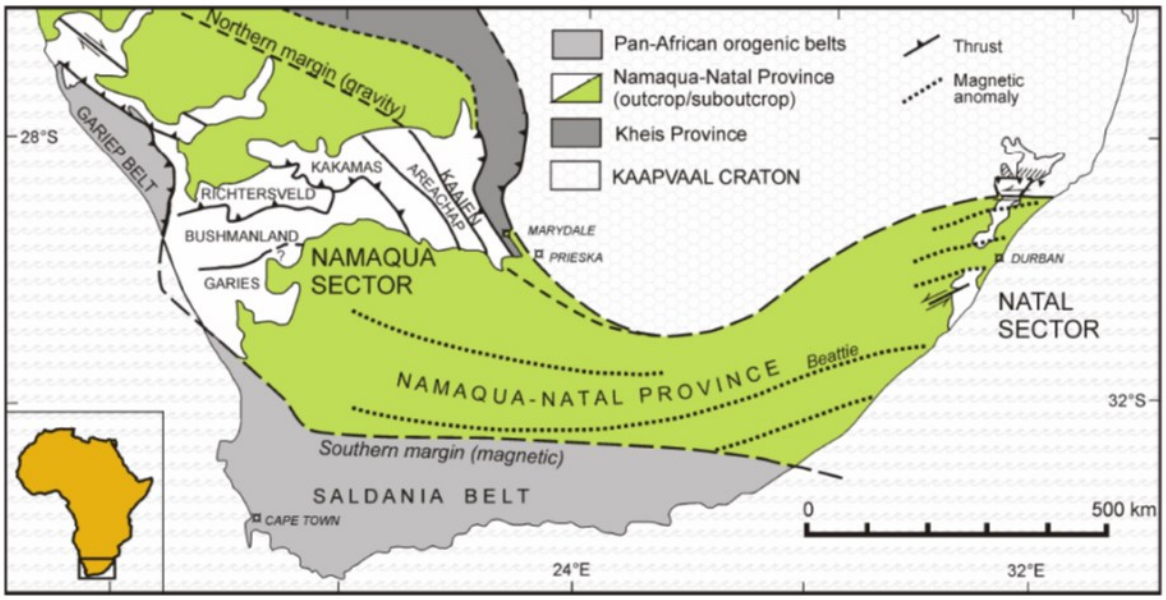

Figure 1: *The Namaqua-Natal province in relation to the Kaapvaal craton. (Petterson, 2008).*

Throughout the Namaqua Sector there are several tectono-stratigraphic domains. These domains are bounded by major sheer zones and are divided into Bushmanland, Richtersveld, Gordonia and Kheis tectonic Subprovinces. The Richtersveld Subprovince is dominated by the Richtersveld Magmatic Arc which is a Palaeoproterozoic arc of intrusive and associated volcanic rocks. These intrusive and volcanic rocks underwent deformation and low-grade (greenschist-facies) metamorphism during the latter part of the Orange River Orogeny (Thomas, et al., 1993). The other subprovinces experienced polyphase deformation, metamorphism and voluminous plutonic activity during the Namaquan Orogeny

between 1200-1000 Ma (Clifford & Barton, 2012). The largest of these subprovinces is the Bushmanland Subprovince which is composed of para- and orthogneisses, amphibolites, psammo-pelitic schists, quartzites, calc-silicate rocks and voluminous granites and granitic gneisses of the Little Namaqualand Suite and the Spektakel Suite (Thomas, 1989). The Bushmanland Subprovince is divided into Aggeneys, Okiep, and Garies Terranes (Eglington, 2006) characterised by upper amphibolite to granulite facies metamorphic grade (Reid, et al., 1997). The northern Aggeneys and Okiep terranes are characterised by rich base metal deposits, while the southern Garies terrane has smaller base metal deposits (Clifford & Barton, 2012). The Buffels River is located within the Okiep Terrane.

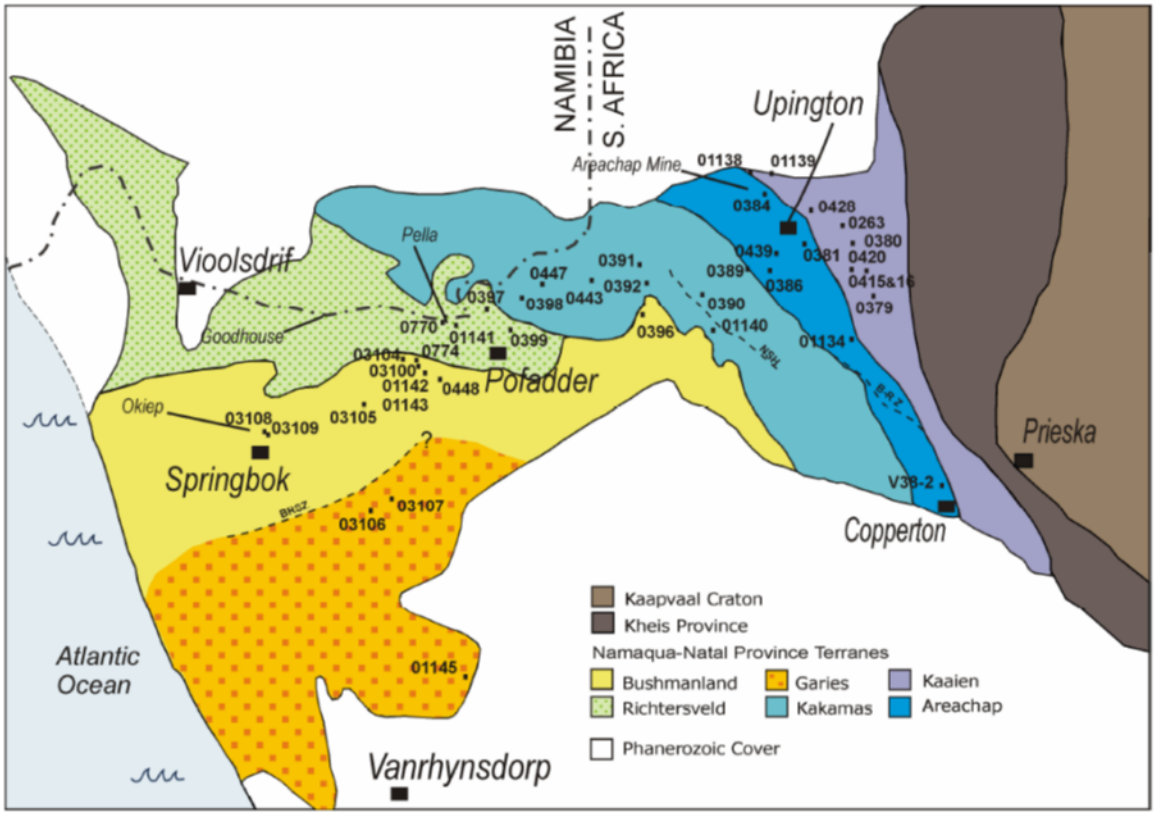

Figure 2: *The Bushmanland province in relation to the Namaqua Sector (Petterson, 2008).*

1.5.2. Geology of the Buffels River

The geology of the Buffels River consists of bedrock made of impermeable sedimentary rocks, granites and granite gneisses of the Little Namaqualand Suite (Clifford, et al., 2004; Marais, et al., 2001). These rocks are intersected by younger faults possibly associated with Karoo volcanism or possibly even neotectonics (Thomas, et al., 1993). Granites found in the Spektakel area are Concordia Granites, ~1170 Ma sheet-like granites composed of quartz, microcline, plagioclase, biotite and garnet (Thomas, et al., 1996). The Concordia Granites are intrusive into the Nababeep Gneiss which is a quartz-feldspar gneiss (Clifford & Barton, 2012). The lack of fabric in the main body of the granites indicates a late to post tectonic timing of the intrusions. The area where the membrane is situated is surrounded by weathered biotite-rich gneissic rocks of the Gladkop Suite on either side of the river cutting (Thomas,

et al., 1996). The river bed itself consists of highly weathered but mature sediments, dominated by sand, but also small lithic fragments of the surrounding gneisses and granites and a small proportion of mica and clay material.

1.5.3. Historical Mining

Copper mineralisation is found within the Okiep Copper District, and is hosted by gneisses associated with the Namaqua Metamorphic Complex. The copper was worked and refined in Namaqualand by the indigenous Namaqua people long before the first Dutch settler Pieter van Meerhof made contact with them in 1661 (Cairncross, 2004; Clifford & Barton, 2012). Through trade with the local tribes the Dutch settlers soon realised the rich mineral wealth of the area (Miller, 1995). Simon van der Stel, a Dutch commander and governor of the Cape Colony identified copper and named the area Koperberg in 1685 (Clifford & Barton, 2012). The deposits were small and remote; but William Paterson, a Scottish explorer and Francois LaValliant, a French explorer drew maps in 1779-1791 to show the general locations to be mined (Cairncross, 2004). Dutch settlers had discovered and started mining by 1685 in the Koperberg area to the east of Springbok. Organised mineral exploration in the area only began in the 1840's because to the remoteness of the area (Gibson & Kisters, 1996). By 1852 the first proclaimed copper district, Okiep, had started at Springbokfontien (now known as Springbok). The early period of mining in the area made use of hand cobbing as the only means of extraction (Cairncross, 2004). Hand cobbing involves mining by physically breaking the ore to further process only the best pieces. These early mining techniques were crude and little to no consideration was given to the environmental impacts the mining would have.

In the 1940s the area had a revival of mining due to large scale exploration for other mineable copper deposits led by the Okiep Copper Company. This revival meant the mining process had become more efficient, and by 1950 the froth flotation method had become a more efficient extraction method (Smalberger, 1975). As a result of exploration work by this company, over 30 copper deposits have been found ranging in size from 0.2 Mt to 37.5 Mt with grades ranging between 1.7 to 14% Cu (Cairncross, 2004). By 2002 most of the mining in the area by the Okiep Copper Company ceased due to the closure of the Nigramoep mine (Clifford & Barton, 2012). The total copper production in the district from 1852 till 2002 amounted to two million tons (Clifford & Barton, 2012).

Re-exploration of the mines vary as the copper price fluctuates. The current mining method used is done by leaching an acidic solution through the mined ore. The Spektakel mine found east of the study area uses an acidic leachate, mostly sulphuric acid, which is sprayed over the copper ore which is piled up (Eriksson & Destouni, 1997). The leachate allows for the mobilization of the copper in solution which can then be easily collected by precipitating out the copper from the leached solution and purified

further (Smith, 2002). This mining practice would allow for easy contamination of the ground water through run off from the ore pile although the mine places thick plastic liners between the leached material and the ground to avoid contamination (Smith, 2002). The mine also monitors possible contamination of the groundwater in the area by testing various boreholes placed at the lower reaches of the mine between the leaching areas and the Buffels River. This allows for accurate monitoring of possible acid movement from the mining process into the surrounding groundwater.

Total copper production from 1940 to 1998 amounted to 105.6 Mt of ore at 1.75% (Cairncross, 2004). The 1.75% copper suggests that a large amount of waste material must have been left behind which is important for this environmental study (Cairncross, 2004). The remaining waste material would be in slimes dams and tailings dumps. These sources could over time leak allowing material into the hydrological system. If the copper price were to increase sufficiently it could be viable to mine the tailings dumps, however the copper prices has not reached this point. Due to the fluctuation of the copper price small scale mines open and close depending on the profitability, the low grade ore means that there is a fine line between making a profit and a loss each month. The Spektakel mine is one of these mines that only produce when it is financially viable.

Diamond mining is also found in Kleinzee just west of the study area along the coast. The diamond mining is done by working through the coastal sands to find alluvial diamonds. The Springbok mine was the first formal mine opened in South Africa, 15 years later Daniel Jacob's children picked up a 21.75-carat diamond in the Orange River (Clifford & Barton, 2012). The source of the diamonds are from weathered Kimberlites found inland which are transported down river towards the ocean.

There is no literature that shows the minerals present close to the membrane study area, this is due to no mining activity, other than diamond mining close to the membrane site. However some of the mines further upstream from the study area have indicated the major sulphide minerals to be the primary copper minerals of the Buffels River Valley. These consist of bornite, chalcopyrite, and chalcocite. Other minerals associated with the ore are vallerite, millerite, niccolite, molybdenite, linnaeite, melonite, sylvanite, hessite, coloradoite and tetradymite. The main secondary copper minerals observed by Gadd-Claxton (1981) are chrysocolla and subordinate malachite and brochantite.

1.6. Hydrogeological Framework

Namaqualand is a region of water scarcity due principally to the low to very low rainfall and high evaporation rate found in the area. The small amount of groundwater found in the area is classified as moderately to severely saline (Adams, et al., 2004). Currently water from the Orange River to the north is transferred to major towns and mining areas to help aid water supply (Pietersen, et al., 2009). The water being transported is mixed with the water found in the area to dilute the saline

groundwater. The water being supplied is still a valuable resource, and not everyone has full access to this potable water source.

Figure 3: *The view looking from the inland plateau down the river catchment. The town of Buffelriver is just to the left.*

1.6.1. The Buffels River Catchment

The Buffels River in the Northern Cape is approximately 250km long and cuts its way from the Kamiesberg Mountains inland on the Bushmanland Plateau towards the coast in a western direction (Figure 4). The smaller feeder rivers Modderfontein and Schaap help in the drainage of the area (Benito, et al., 2010). The lower escarpment is drained by a number of sandy streams and rivulets that mainly flow westward toward the ocean and link up to create the larger Buffels River. All the streams and rivers are intermittent drainages which rarely flow even during winter rainfall. The total drainage area is 9249km^2 and extends from the Kamies Mountains in the east to the Atlantic Ocean in the west (Benito, et al., 2010). The large Kamies Mountains force coastal fronts to move to higher altitudes which results in orographic precipitation. This precipitation is the main source of water for the river catchment (MacKellar, et al., 2007). Although larger towns such as Kleinzee and Buffelsriver have water piped from the Orange River, smaller communities are reliant on the alluvial aquifers for potable water (Adams, et al., 2004).

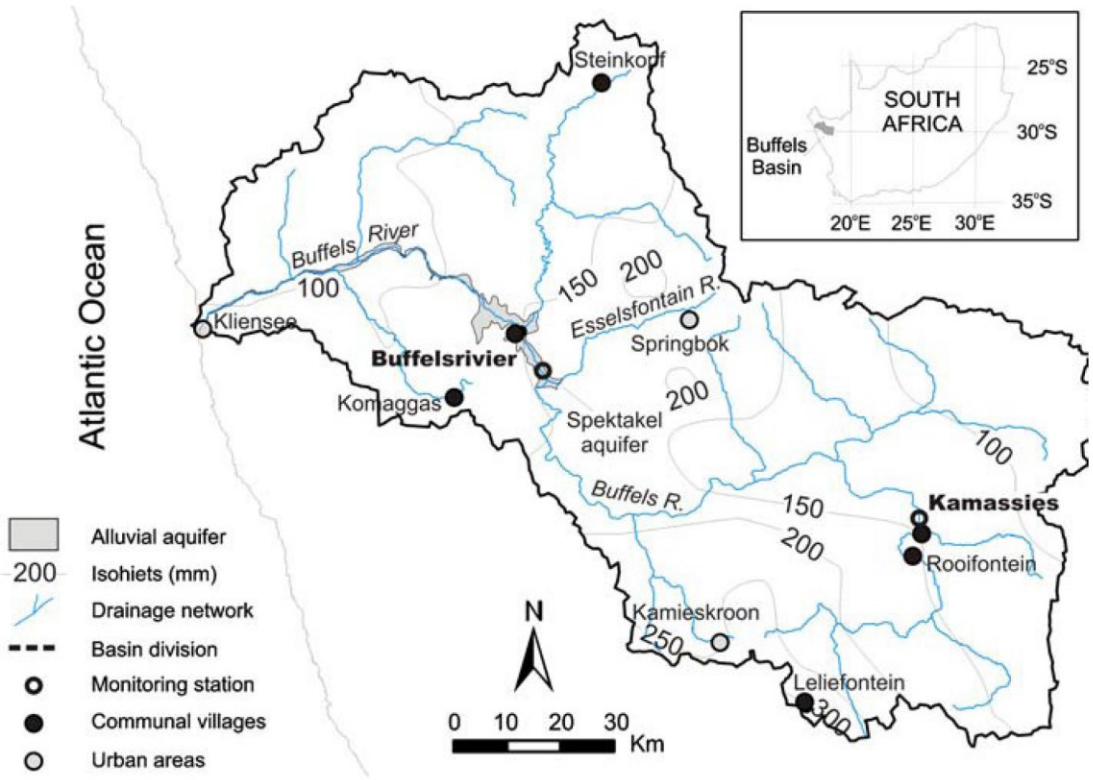

Figure 4: *Buffels River basin showing the full extent of the shallow alluvial aquifers (Benito et al., 2010)*

The groundwater in the area is predominantly used for farming of livestock but it is also used as potable water by poorer communities that do not have access to the water supplied from the Orange River. Shallow wells are often dug within the river bed and used to access water for migrating herds of livestock. Farms within the valley use windmills to pump water into storage facilities used for the livestock (Desmet, 2007). The water found in the area varies between surface water and a few meters below the surface of the riverbed (Desmet, 2007). The groundwater is known by the locals and researchers to be saline to very saline, and anecdotally farmers have described it as getting worse over the past few years (Nakwafila, 2015). In some cases farmers refused to personally drink the water. Salinization is thought to be caused by flushing of salts from shallow soils that are then enriched by further evaporation (Benito, et al., 2010). The origin of the salts in the soils has been postulated as dry deposition of ocean salts blown inland. The timescale of the deposition is however not fully understood and known.

1.6.2. Aquifers within the Buffels River Catchment

The Buffels River valley is composed of impermeable metasedimentry rocks, basic granites and ultrabasic intrusive rocks (Benito, et al., 2010). These rocks have been cut by several basement faults and the Buffels River is composed of alluvial fill from the surrounding geology. The Buffels River catchment area is divided into several aquifers due to rock outcrops forming natural barriers

disconnecting the alluvial aquifers. These aquifers in the upper and middle catchment are very small with only two sizeable aquifers located in the lower Buffels River (Figure 4). The Spektakel aquifer is situated where the river emerges from the mountains and onto the coastal plain. The second aquifer is the Kleinzee aquifer, which is situated at the river mouth where river flows into the Atlantic Ocean (Benito, et al., 2010). The Spektakel aquifer was used by the Okiep Copper Company for mining operations during 1947-1974 and by the surrounding community in the Town of Buffels River and outlying private farms. The quality of the Spektakel aquifer further inland varies from good 1000 ppm total dissolved solids (TDS) to poor 6700 ppm (Benito, et al., 2010). The Spektakel aquifer is a 14.6 km long sand filled basin formed from the erosion of granite bedrock. The total water bearing capacity of the aquifer is 20.83 Mm^3, of which 11.33 Mm^3 are recoverable (Marais, 1981).

There are two main types of aquifers found in the area (Benito, et al., 2010). The one type of aquifer is shallow. These recharge by the direct filtration of precipitation, reaching the shallow water tables. The recharge rates in these aquifers are limited by the ability of the aquifers to store and transmit water. These aquifers are mostly unconfined, and are susceptible to contamination. The second type of aquifer is deep. These aquifers recharge by transmission of water along faults and cracks as well as by losses from the overlying shallow aquifers (Scanlon, et al., 2002). Most deep aquifers are confined and occur at stagnant conditions at deeper depths as they are not replenished by recent recharged water and may have been there for thousands to millions of years (Van Weert, et al., 2009).

The shallow aquifers get recharged through the rainfall in the winter months. Flash flooding every couple of years flushes the system by recharging the aquifers, the deeper groundwater will however remain the same as the flooding recharges and dilutes the shallow groundwater in the aquifer. Flooding events also carry muddy waters that seal the land surface and obstruct water infiltration. On average a complete or significant recharge occurs every 4 to 10 years (Benito, et al., 2010). This recharge according to Van Wreet et al. (2009) does not occur at stagnant conditions at deeper depths as the deep groundwater is not replenished by recent recharged water and therefore may have been there for thousands to millions of years.

1.7. Climate, Precipitation and Geomorphology

The Buffels River Valley is categorised as an arid to semi-arid area (Adams, et al., 2004). The precipitation found in the valley is gentle winter rainfall caused by frontal systems from the Atlantic Ocean. The majority of the rainfall is higher in the mountainous areas. Figure 5 shows the Buffels River valley, with the higher escarpment in the east, and the coastal plateau in the west. Also highlighted in Figure 5 are the towns of Kleinzee at the coast, Buffelsriver at the base of the mountainous area, and Springbok further east.

Figure 5: *Google Earth image showing the Buffels River catchment. The towns of Springbok, Buffelsriver, and Kleinzee are highlighted. The membrane is situated just upstream from the town of Kleinzee, seen here by the red line.*

1.7.1. Geomorphology

In general, Namaqualand can be divided into three main geomorphologies: (1) the coastal lowlands (this study); (2) an intermediate escarpment zone; and (3) the Bushmanland Plateau. The coastal lowlands are characterised by recent sands underlain by crystalline basement rocks that crop out sporadically within the river bed (Adams, et al., 2004). The escarpment zone hosts exposed domes of granite, weathered minerals (Extending to 54-60 m), fractured rocks and alluvium filled valleys (Adams, et al., 2004; Partridge & Maud, 1987). The Namaqualand weathered zones show signs of wetter periods, which would have existed over long periods of time. Adams et al. (2004) showed the groundwater plots in the kaolinite stability field indicating that kaolinite formed due to incongruent dissolution of alumina-silicate materials such as kyanite, silimanite, andalusite and thus indicates a relatively advanced weathering stage for the area (Adams, et al., 2004).

1.7.2. Climate

The region's climate is semi-arid with and average maximum and minimum temperatures of 29.5 °C and 10.0 °C respectively (SAWB, 2013). Maximum temperatures rarely exceed 37°C in the summer but sub-zero temperatures are common in the winter months (Hahn, et al., 2005). The western Namaqualand receives winter rainfall while the eastern Namaqualand receives rainfall during the summer (Adams, et al., 2004). This is due to a frontal weather systems being the source of the winter rainfall in the western parts of the Namaqualand (Benito, et al., 2010).

The average rainfall determined from WeatherSA records (Figure 6) from 1 January 2009 to 25 August 2015 show Kleinzee with an average annual precipitation of 82.3 mm per annum. The town of Buffelsriver in the valley has an annual precipitation of 158.2 mm per annum, while the Springbok weather station recorded 224.1 mm per annum. The average mean annual precipitation for the area has been described as reliable and predictable over each year by Hoffman and Cowling (1987). The 2005-2006 Buffels River flows recorded at the town of Buffelsriver, just upstream from the study area, lasted 40 days and coincided with the passage of a coastal front (Benito, et al., 2010). However, according to oral historical records 35 floods of greater or similar magnitude since 1890 have been recorded (Benito, et al., 2010), and the area sometimes experiences extremely wet years, where precipitation can increase to above 400 mm in the Kamiesberg Mountains inland to the south east (Cowling, et al., 1999).

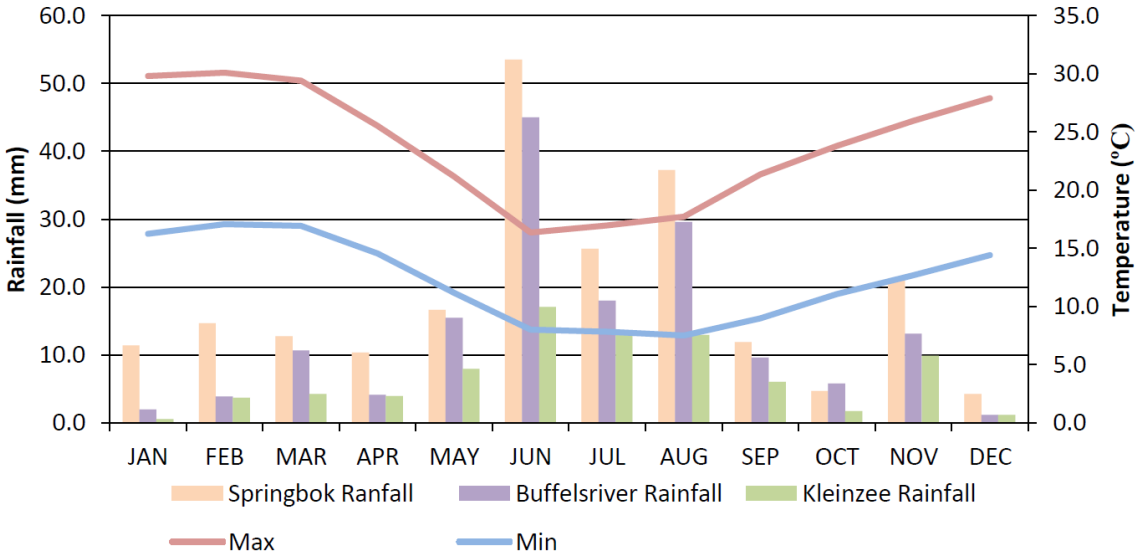

Figure 6: *Rainfall and temperature data collected by Weather SA from Kleinzee, Buffelsriver and Springbok. These are averages from 1 January 2009 – 25 August 2015. The temperature data was only collected from Springbok weather station.*

1.7.3. Evaporation

The Namaqualand region is known for its high evaporation rates, Adams et al. (2004) states that the evaporation rates are on average 12-15 times that of the annual precipitation, and in some cases can be as high as 22 times (Figure 7). The high evaporation rates impact the groundwater and result in evaporitic salts at the surface and subsurface. These surface salts lead to high salinity throughout the Namaqualand region. Campbell et al. (1992) have observed evaporation up to a depth of 91cm from surface level at Kleinzee. Evapotranspiration is also high in the region especially where an area is densely vegetated with a shallow water level. In areas with more sparse vegetation and a deeper groundwater level the evapotranspiration is lower (Van der Sommen & Geirnaert, 1988).

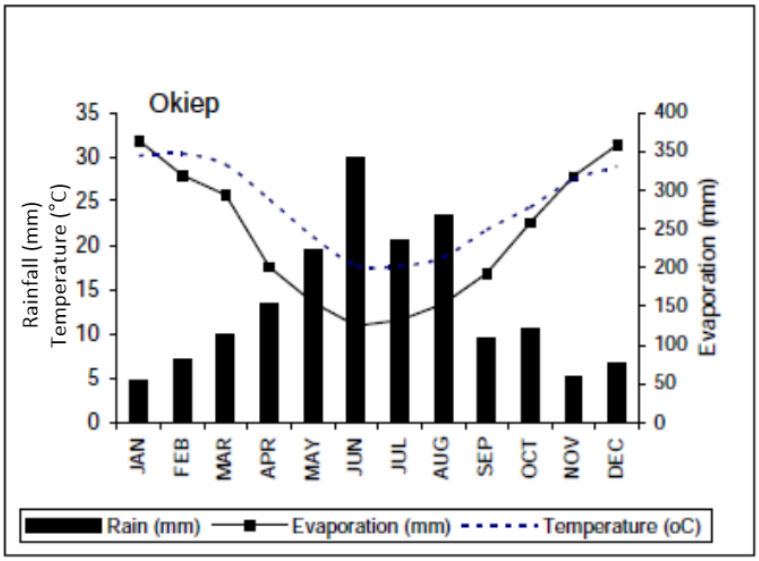

Figure 7: *Shows rainfall, evaporation, and temperature for Okiep* (Adams, et al., 2004)

1.8. Study Area Characterisation

The study area is a 4 km stretch of the Buffels River upstream from the coastal town of Kleinzee. The vegetation is sparse throughout the area, but there are sections where the vegetation is denser due to a higher groundwater supply (Figure 8). Water in this area is either surface or shallow groundwater which is being retained by an underground membrane put in place to dam underground flow in the river to supply additional water to the town of Kleinzee and the associated mining activities.

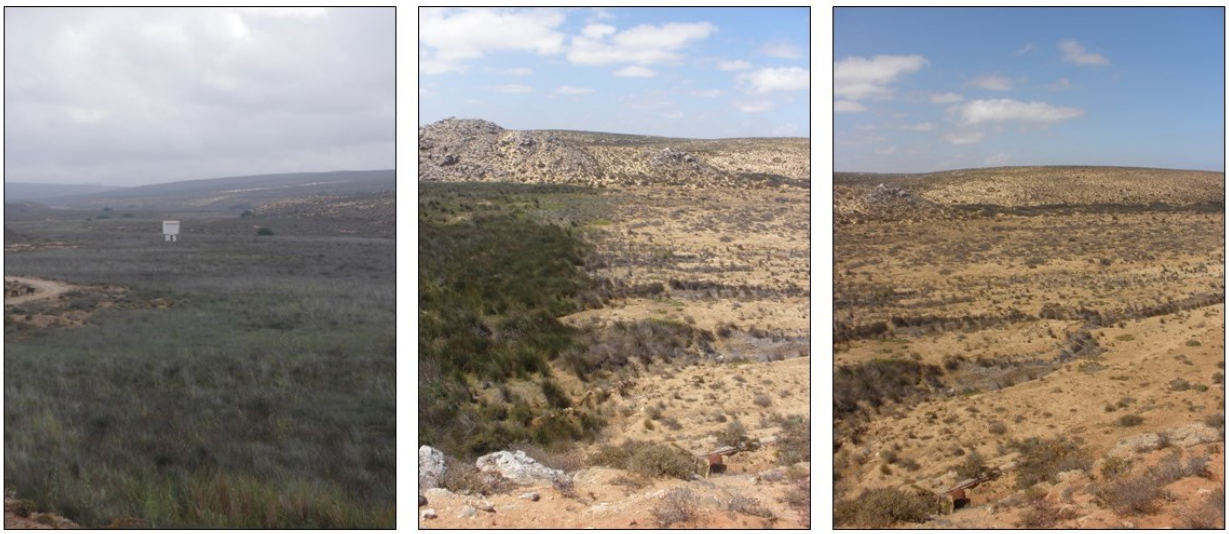

Looking east up river
Above membrane

At the membrane

Looking west down river
Below membrane

Figure 8: *The membrane study area. Looking east upstream from the membrane, and looking west downstream from the membrane. The vegetation growth is seen upstream from the membrane due to the higher groundwater levels. Downstream of the membrane there is no vegetation due to an absence of groundwater.*

1.8.1. Location Description

The research site is approximately 5km upstream from Kleinzee (Figure 10). The dry river bed has cut into the surrounding geology and is 15-20 meters lower than the surrounding plateau (Figure 11). The river bed is predominantly sandy with anastomosing streams intermingling within the main riverbed. The river bed is currently being used by farmers to abstract groundwater for livestock. Windmills and hand or excavator dug wells have been put in place by the farmers to access the groundwater found within the river bed. A membrane has been put in place to dam up groundwater, and the town of Kleinzee has a pump station to utilise this groundwater source. The samples were collected throughout the study area in an attempt to get an overview of the geochemistry. Within the riverbed there are various different channels (Figure 9). The interpreted surface flow was used to help in determining where shallow groundwater would be more likely to be found. Two samples were also taken 23km further upstream from the membrane.

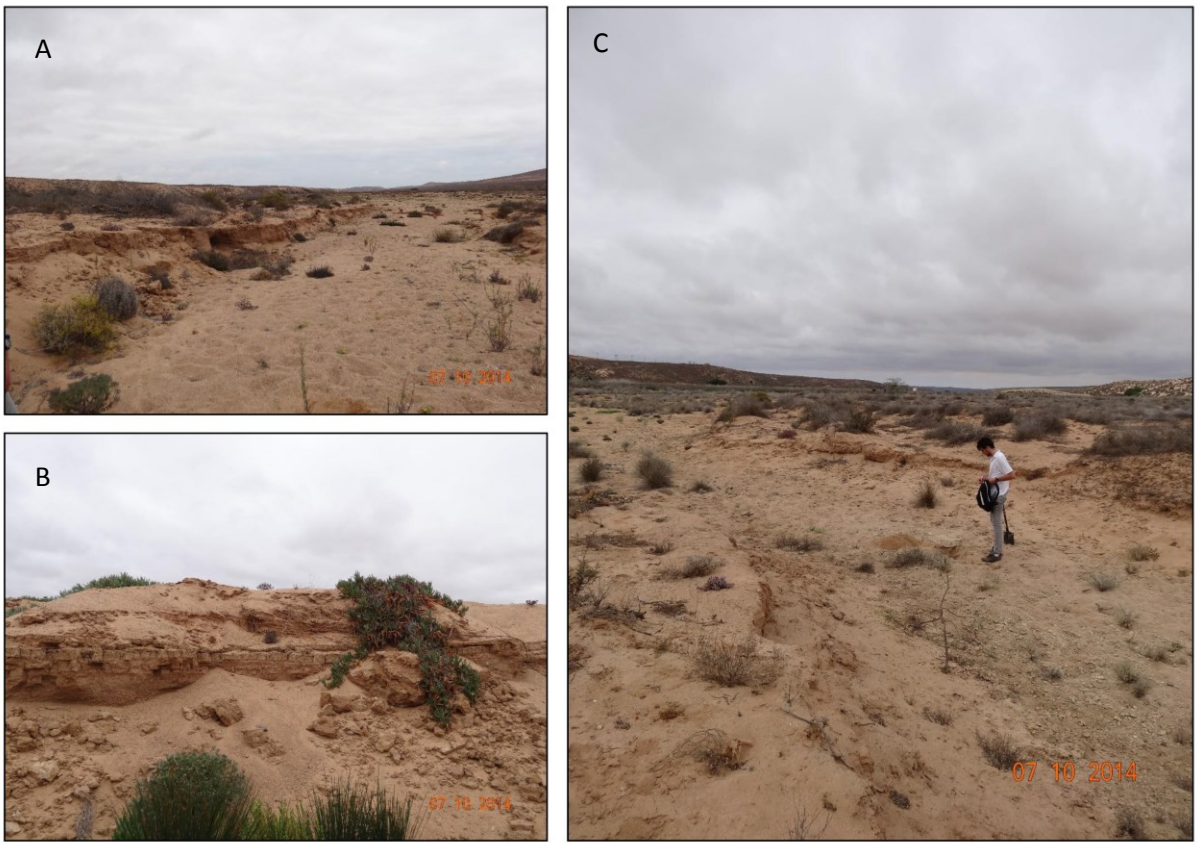

Figure 9: The anastomosing river cuttings found within the main Buffels River cutting. A) Shows one of the larger river cuttings found within the main Buffels River. B) The sediments found on the edge of the river cuttings. These highlight historical flooding events found in the region. C) One of the main river cuttings found upstream from the membrane.

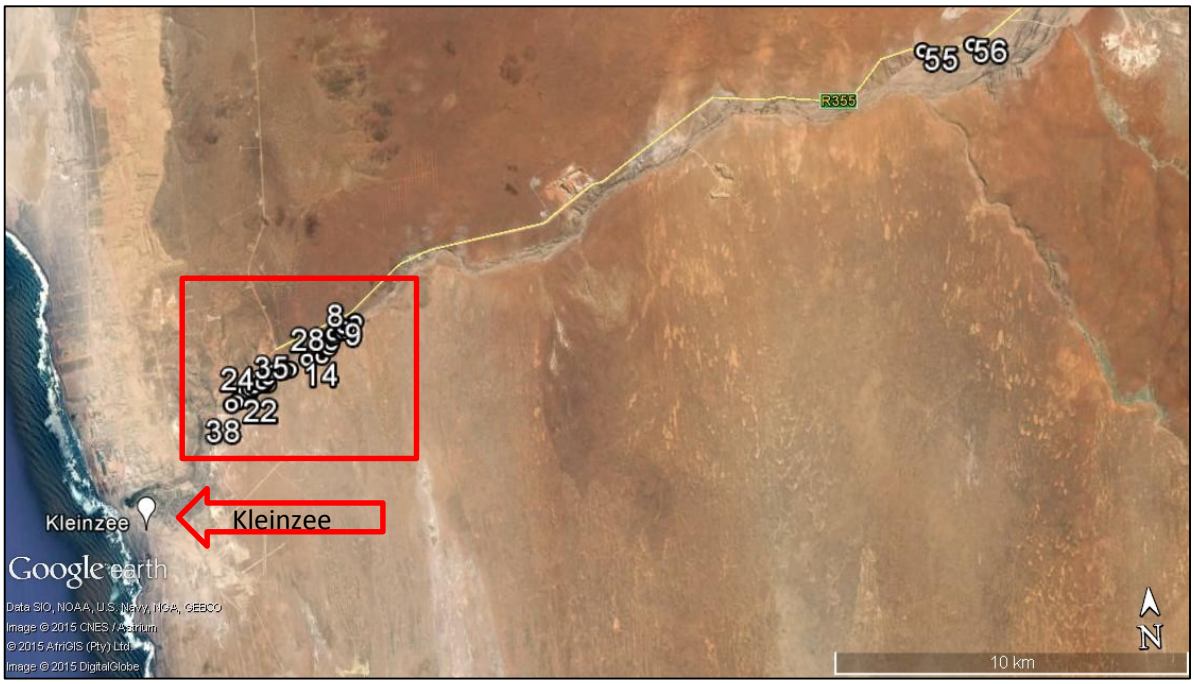

Figure 10: *Google image showing the location of the study area in reference to Kleinzee and the Buffels River.*

Figure 11: *A photograph showing the Buffels River cutting into the surrounding plateau. This photograph was taken from inside the Buffels River bed.*

1.8.2. Membrane

In 1995-1996 a membrane was installed across the Buffels River to help in damming up groundwater to be used by the town of Kleinzee. To install the membrane, the river bed was dewatered and excavated to a depth of 250m and then a concrete foundation was cast against the bedrock (O Smith 2015, pers. comm. 28 May). A non UV protected, non-permeable plastic membrane with a thickness of 1.5-2mm was then connected to the foundation using a "T" bar connection (Figure 12) (O Smith 2015, pers. comm. 28 May). The dam wall was then profiled into two steps. A gravel filter bed and four stand pipes were installed for future use before backfilling (O Smith 2015, pers. comm. 28 May).

In 1997 a severe flood happened in the area causing the river bed to rise by approximately 1m. After the flood the water table had risen by approximately 750mm from the pre-flood water table (O Smith 2015, pers. comm. 28 May). Boreholes both above and below the membrane were monitored before and after the installation of the membrane and showed an initial drop, but after a year the water table throughout the area had risen. Due to the shallow water gradient in the area the push back effect of the membrane extends 1.5km upstream. The Fehlmann Well was constructed in the 1960's and has supplied the town of Kleinzee with water (Figure 13). The water being used in Kleinzee is a made up of a mixture of 60% coming from Namaqua Water, which is piped from the Orange River, and the other 40% from the membrane source (O Smith 2015, pers. comm. 28 May).

The effects of the membrane can be seen from aerial photographs and Google Earth images. Behind the membrane, upstream, there is shallow groundwater which has aided growth of long grasses and reeds. This growth stands out from the sparse and arid region surrounding the river valley and downstream of the membrane. Shallow pools can also be found behind the membrane.

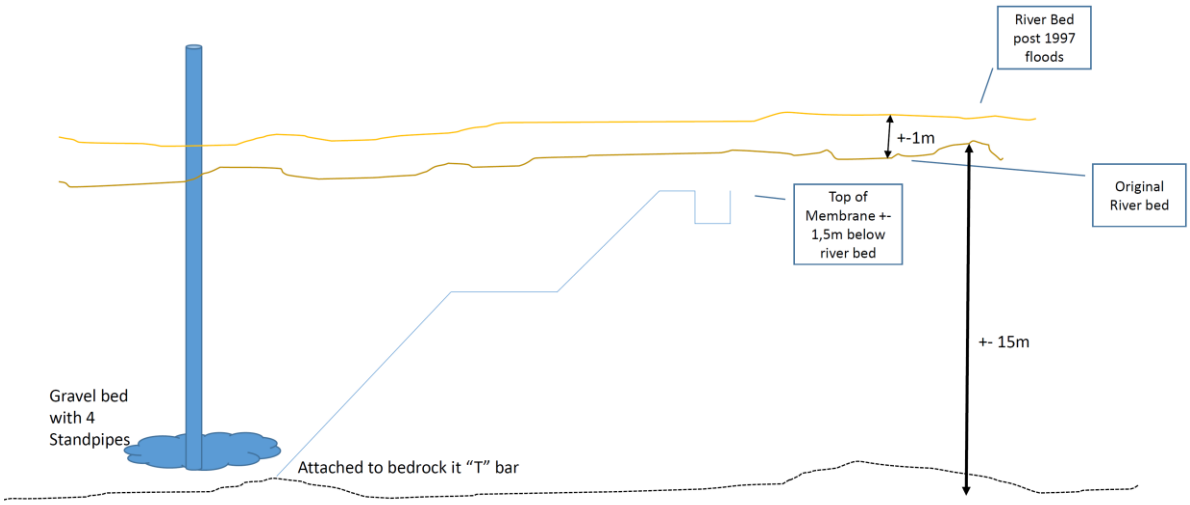

Figure 12: *Image drawn up by O. Smith on how the membrane was installed in the Buffels River.*

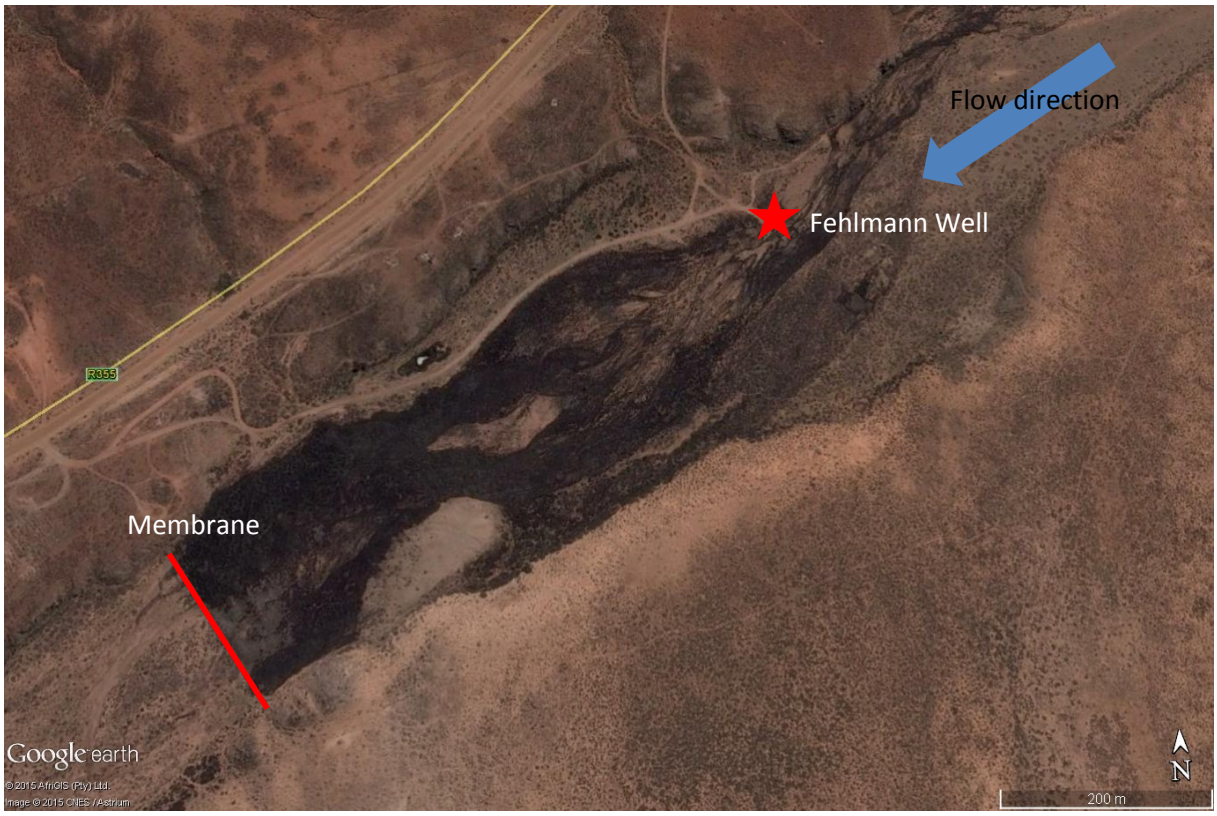

Figure 13: *Google earth image of the study area showing the membrane and Fehlmann Well. There is a clear line of vegetation growth behind the membrane due to the higher groundwater levels. The Fehlmann well is the site where the pump station is that pumps the water to the town of Kleinzee.*

2. METHODS AND MATERIALS

Below is an explanation of the sampling methods in addition to the methods used in various lab experiments and analysis. The following methods were all used to help in understanding the questions outlined in the aims and objectives.

2.1. Selection of Sampling Sites

Two sampling trips took place during 2014, one at the end of February during the summer season, and one in October at the end of winter. The summer trip yielded no water samples, but 14 sites were selected for sediment samples. The winter field trip yielded better results, with 46 sites selected for sediment samples and of those, 14 samples had groundwater. The sample sites were selected along the Buffels River both upstream and downstream of the membrane near Kleinzee (Figure 14). The entire study area extended over a 4 km section of river bed. It was important to get a transect of sample sites above and below the membrane while trying to keep within the flow patterns of where the surface waters would have moved. The areas where surface water had eroded deeper into the river bed was more likely to be a good yield for groundwater close to the surface. Samples were collected within the anastomosing river cuttings found within the river valley near the membrane. Further away from the membrane the samples were collected from within the main river cutting. It was important to collect sediment and groundwater samples during both winter and summer to help in the understanding of the mobility and accumulation properties of the sediments with regard to salinity and trace metals. Unfortunately groundwater samples were only able to be collected after the winter rains.

Figure 14: *All the samples collected near the membrane in the Buffels River. The samples were mostly sediment samples. The samples were differentiated in figure 15 and 16.*

Figure 15: *A) Sediment and groundwater sample. B) Sediment sample collected from the side wall of the hole used for sampling. C) Open water body being sampled. D) Sediment sample collected in highly saline area. Salt precipitation on the surface. E) Sediment and groundwater sampling method. F) Windmill used for groundwater collecting away from the membrane.*

2.2. Field Sampling

Sediment samples collected from the study area on the two field trips in 2014 were kept at Stellenbosch University. Approximately 1 kg of sediment was collected in clear plastic sample bags and labelled according to the site location and depth of the sample. GPS locations were also recorded along with detailed photographs of the sample and sample location. A brief description was taken in the field and a more in depth description was done once back at Stellenbosch University. Water samples were processed in the field and given the same sample labels according to the recorded GPS location.

2.2.1. Sediment Samples

The sediment samples were collected using an auger or garden spade and were collected from approximate surface (0 cm) to approximately 30 cm to 50 cm and the final sample as deep as possible. In some cases this was to a depth of 30 cm while others were to a depth of 90 cm. The sample depths became more difficult in some of the areas where there was a lot of sand which kept collapsing on the

sides of the hole and falling back into the sampling hole. This made collecting a representative sample difficult, and a cross section was taken from the side wall of the hole in this case (Figure 15 B). The sample depths were chosen dependant on morphological changes as opposed to a fixed depth method. If a morphological difference was noted in the field, then two samples were taken at that site corresponding to the differing depths. The samples collected in clay areas were also difficult to collect because the ground was hard and both the spade and the auger struggled to dig into the ground. The samples collected were then placed into thick plastic bags, sealed and labelled accordingly. Differing sediment samples were also collected where there was a noticeable difference in the sediment morphology. Such as grain size variation, texture and colour. A GPS location was also recorded, and these sampling holes were then able to be used for water sampling where they filled up with groundwater (Figure 15 A and D). It was important to keep the ground surface as clean as possible as there were animals in the area and surface organic matter needed to be kept to a minimum as faecal matter would affect the processing and results of the sediment samples. In these cases the surface debris was removed to reveal a clean sediment surface to start sampling.

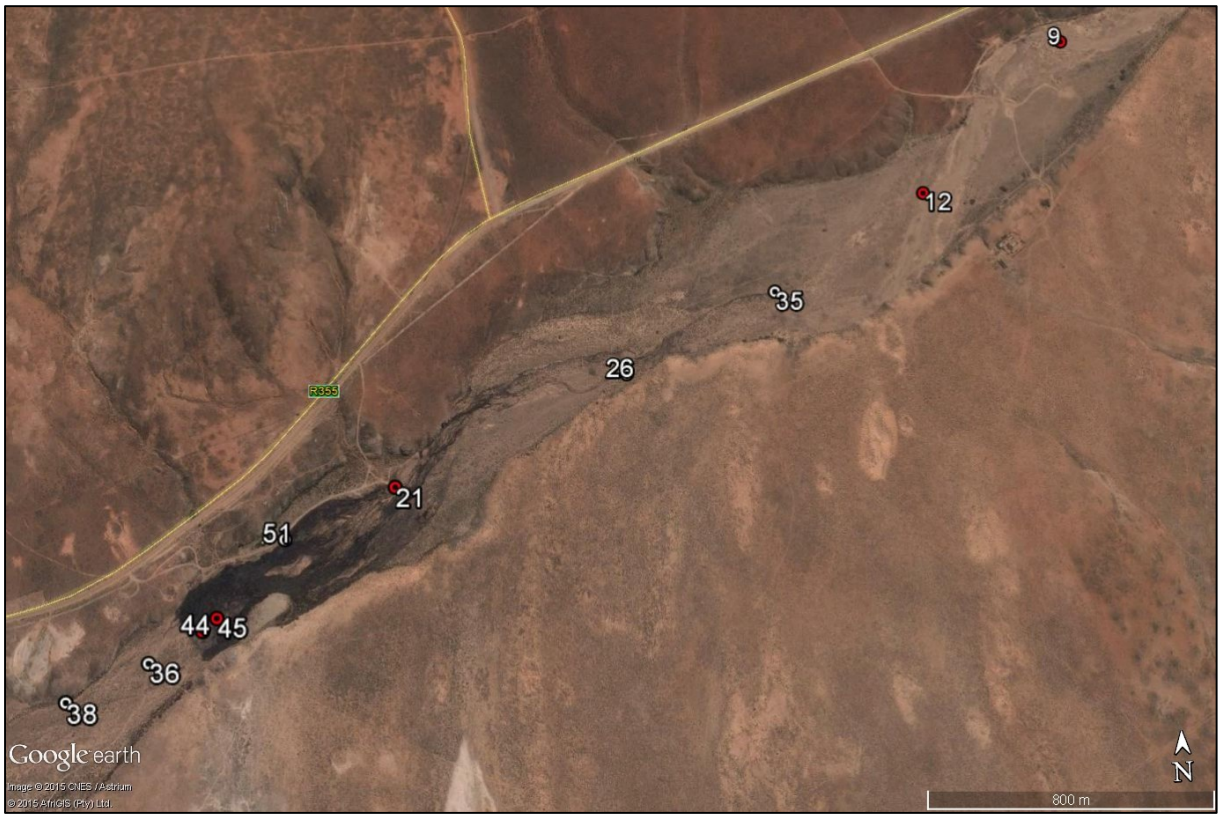

Figure 16: *Sediment samples collected. White locations single sediment sample at varying depths. Red samples are two samples taken at different depths.*

2.2.2. Water Samples

The water samples were collected from the hole dug with a standard garden spade or auger used for collecting the sediment sample. The water sample sites were often chosen because of surface water nearby, or a higher chance of finding groundwater due to a depression or river cutting (Figure 15 E and C). Some water samples were also taken from windmill pumps, which pumped water from the river bed (Figure 15 F).

All the water samples were collected in the same manner. The EC, pH and temperature were measured using an Extech EC500. All the probes were calibrated on a daily basis. The pH and Electrical Conductivity (EC) readings were recorded once the probe showed stabilization in the measurements. Field alkalinity was determined using a Hach Digital Titrator with Green-Methyl Red and Phenolphthalein indicators. Samples were titrated to a pH of 4.5 using 1.6M sulphuric acid. In all samples total alkalinity was equal to the bicarbonate alkalinity. Cations and anions were collected in PP acid washed 50 ml conical tubes. All water samples were filtered on site with 0.45µm cellulose acetate syringe filters. Cation samples were acidified to a pH less than 2 using ultrapure concentrated nitric acid. All samples were kept at less than 4°C in the field and transferred to fridges in the laboratory.

Figure 17: *Groundwater samples taken. All samples collected were above the membrane as there was no easily accessible groundwater below the membrane. Site 27 was taken from a hole dug into the ground by a farmer, approximately 2 meters deep. Site 28 and 29 were both sampled from windmills. Site 54 was taken from an open water body. Site 56 has been excluded from the google image as it was 23km further upstream.*

2.3. Sediment Sample Field Descriptions

As sediment samples were collected, field notes were taken on the sediment characteristics. Comparing these various sediment samples collected, they could be divided into two main categories. The first was relatively clean sands, which were found further away from the membrane and vegetation. The second was finer sediments with a higher organic content which was found closer to the membrane in the highly vegetated area. These categories are discussed further in the following section. These categories are based on morphological differences and not grainsize differences as grainsize differences could not be easily determined in the field. The differences noted were the presence of clay, colour differences, and amount of organic material.

2.3.1. Sand

The clean sands consisted of brown to light brown sands with mostly angular grains with some slightly rounded. The grain sizes were predominantly larger than the sediments found near the membrane. The grains mostly consisted of quartz, which could be seen with the use of a hand lens. The clean sands also contained less organic matter due to being in contact with less vegetation. They were also drier which made sampling at depth difficult because the hole kept collapsing. The clean sands did not have a smell associated to them, and in areas where finer gained sediments were at the surface faint mud cracks were present. The clean sands were found both upstream and downstream of the membrane but were clearly not affected by the presence of the membrane.

2.3.2. Sand and Silt

The sand and silt sediments were generally found as surface sediments. The sand and silt samples were a darker colour, and had more moisture than the clean sands. These sediments were clearly affected by the membrane being in place. The sediments also had a stronger smell to them, which was mostly due to the organic content and higher amount of moisture. The finer grains were also more rounded. The field samples where a top sediment and bottom sediment were taken also showed the bottom sediments to contain a higher sand percentage grains.

2.4. Preparation and Processing of Sediment Samples

Sediment samples were air dried in a drying room for two days to be ensured the samples were completely dry before further processing. The dry samples were then sieved through a 2 mm sieve to remove organic matter (roots, sticks etc.) as well as the coarse grains found at each sampling site. Coarse grains were made up of clumped together sand, clay or silt samples. These coarser pieces were broken down using a pestle and mortar in order for the samples to be sieved. The larger sediment pieces unable to be broken down were then placed in a different sample bag. The samples were then weighed to keep track of the amount of <2 mm fraction and >2 mm fraction. Further analysis was done on the <2 mm fraction.

2.4.1. Saturated Paste Extract

To collect cation, anion, pH and EC data from the sediment samples the methods used by the National Soil Survey Centre (NSSC) were followed to create a saturated paste. 125 g of the <2 mm fraction for each sample was weighed out and placed into a beaker. DI water was added to create a saturated paste and all the samples were left for 24 hours. After 24 hours the samples were placed into a Buchner funnel already prepared with Whatman number 50 filter paper. The Buchner funnel then filtered the water that was saturating the sediment samples. The water extracted using the Buchner funnel was then filtered once again using a syringe and a 0.45 μm cellulose acetate filter. The EC and pH were recorded for each of the samples before being sent off for further cation and anion analysis.

Electrical conductivity of the saturated extract is indicative of the total dissolved salts in the sediment sample. The EC values are used to classify the salt hazard of brackish soils and estimate the leaching requirements of brackish sediment for reclamation purposes (Chharbra, 1996). The conductivity cell was calibrated with 0.01mol dm-3 KCl solution. This solution has a known conductivity of 141.18 mS m^{-1} at 25°C. The conductivity cell was then rinsed with saturation extract. The conductivity of the saturation extract was then able to be determined and the electrical resistance was able to be calculated from this value. A Metrohm 827 pH Lab probe was calibrated before each use to calculate pH. The pH probe was only used if the calibration reading was above 98%. Anything below was recalibrated before being used. The calibration solutions of pH 7.0 and 4.0 were used.

2.4.2. Grain Size Analysis

To help in understanding sediment accumulation of salinity and trace metals it was important to do a grain size analysis on the sediment samples. The procedure used was from the NSSC (1995). This allowed for the separation of the sediments into three basic categories (sand, silt and clay). Various research done by (Ujevic, et al., 2000) shows accumulation to be higher in finer grained sediments where the surface areas are greater. Clays are also well known for their accumulating properties.

Dried sediment samples were sieved through a 2 mm sieve to remove the coarse grain fraction. The finer particles that passed through the sieve were then analysed further. 40 g of the air dried fine sediment (<2 mm) was added into a 600 ml glass beaker. De-ionised water was then added to wet the soil and peroxide was slowly added to remove the organic material. When the frothing from the organic material had ceased several days later the soil was dried on a steam bath to remove all the liquid.

10 cm^3 Calgon and de-ionised water was used to remove all the sediment from the beaker and into a 1 litre cylinder. The sample was filtered through a 0.053 mm sieve before going into the 1 litre measuring cylinder. The coarse fraction (>0.053 mm) was rinsed thoroughly allowing the fine matter into the measuring cylinder before being air dried and sieved further in 0.5 mm, 0.25 mm, 0.106 mm

and 0.053 mm sieves. Each of the sieved samples was then weighed to determine the particle size distribution according to weight.

The fine fraction (<0.053 mm) was then used for extraction. The samples were stirred up and allowed to settle. A 25 ml sample was drawn (using a pipette) from the 1 litre measuring cylinder from a depth of 10 cm from the surface at 4 minutes and 32 seconds. This drawn sample was then dried and weighed. It made up the representative amount of silt and clay in the sample. The 1 litre measuring cylinder was then used to draw a second sample at a depth of 7 cm from the surface. The second sample was taken at 5 hours and 30 minutes from when the samples were stirred up. This extraction was used to determine the amount representative of clay in the sample.

The 25 ml samples extracted were then placed in pre-weighed porcelain dishes and allowed to dry. The porcelain dishes were then weighed and the following equations were used to determine the sand, clay and silt fractions.

Table 1: *Equations used to determine the grain size percentages from the weighed out proportions* (Klute, 1986).

A = mass (g) of sand fraction in sieve **B = mass (g) of pipetted fine silt plus clay** **C = mass (g) of pipetted clay** **D = mass (g) of pre-treated over dry sample** **E = mass correction of dispersing agent (0.01g)**	**Percentage of sieved sand fractions** $= \frac{A\,X\,100}{D}$ **Percentage of fine silt** $= \frac{(B-C)X\,1000\,X\,100}{D\,X\,25}$ **Percentage of clay** $= \frac{(C-E)X\,1000\,X\,100}{D\,X\,25}$

The final results could then be calculated to 100% with a representative amount for sand, silt and clay. These percentages could then be plotted on a ternary diagram allowing for the results to be easily interpreted. **Figure 18** highlights the method and processing of the sediments.

Further analysis on the 40 g samples placed in the 1 Litre cylinders was also used for the clay separation for XRD analysis. The sample contained only clay and silt <0.053 mm. These were stirred and poured into two beakers. One for the addition of 18.5 g of $MgCl_2$, and the other beaker had 30 g of KCl added. These samples were all stirred for 2-10 minutes until the $MgCl_2$ and KCl had dissolved and allowed a flocculate to form. The samples were then left to settle for 3 days and the water above the slurry was removed. The slurry was then moved into 50 ml centrifuge tubes where they were centrifuged and the solution was removed leaving the clay and silt in the tube. All the samples were washed and centrifuged twice with DI water. They were then filled with a 1:1 Methanol solution and centrifuged again.

The samples were then tested with $AgNO_3$ by pouring out the methanol solution and dropping a small amount of $AgNO_3$ into the solution. This was used to determine whether salts were present in the clay and silt samples still. If the methanol solution water turned milky they were washed again with DI water and the process was repeated until the addition of $AgNO_3$ didn't affect the Methanol solution. The samples were then dried and sent to iThemba LABS for XRD analysis.

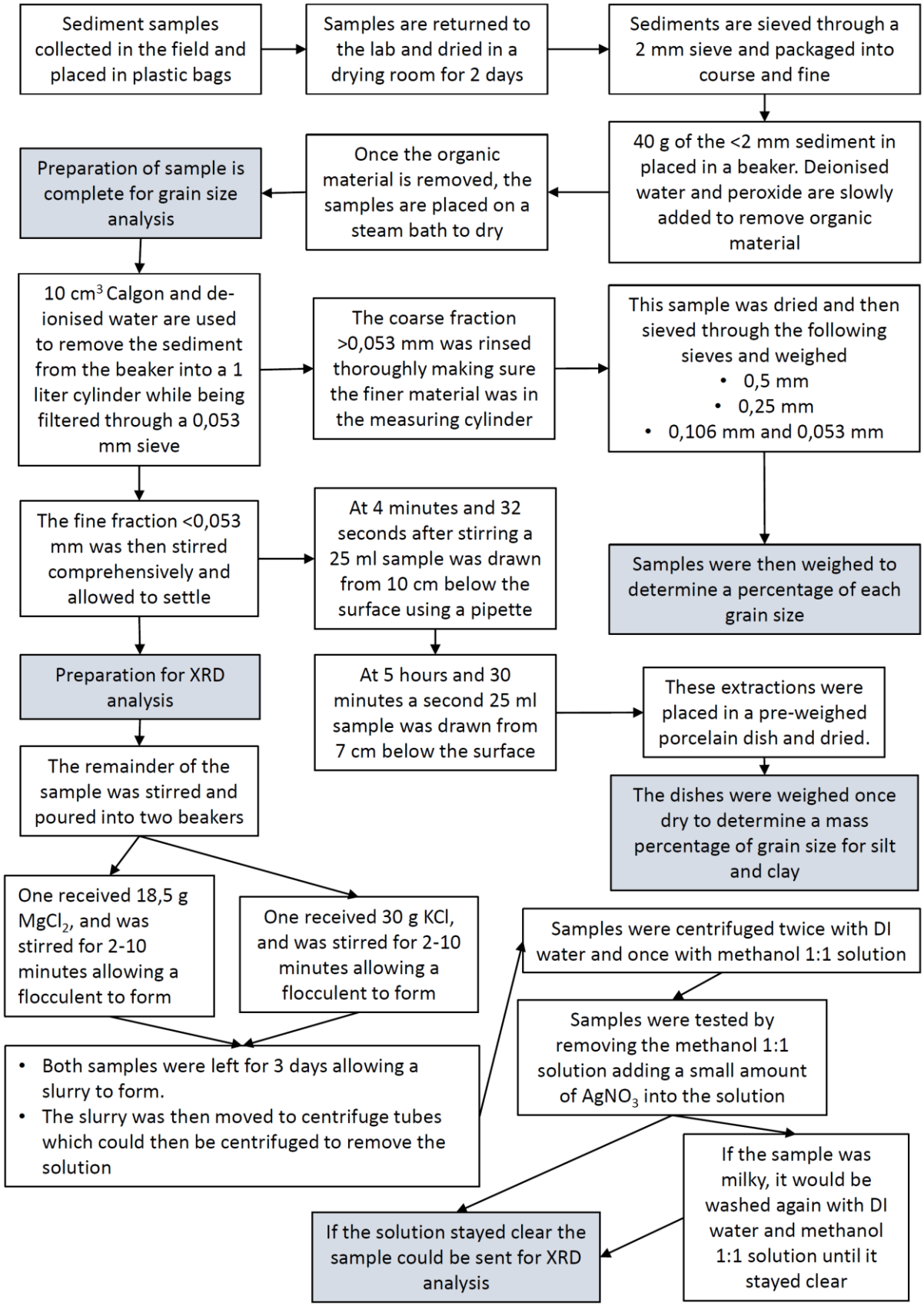

Figure 18: *Flow chart showing the process of grain size analysis and XRD preparation*

2.5. Analysis Techniques

The following analytical techniques were used on the sediment and groundwater samples collected in the Buffels River study area. The samples were collected and prepared before the following analyses.

2.5.1. Clay Mineralogy Determination (XRD)

Prepared sediment samples were sent to iThemba LABS in Cape Town for XRD analysis using a BRUKER AXS (Germany) with a D8 Advance diffractometer and measurement of ϑ-ϑ scan in locked coupled mode. The tube used Cu-Kα radiation at (λKα1=1.5406Å) with a 1600 Channel PSD Vantec-1, Gas detector. Measurements were conducted at a tube voltage of 40kV, tube current of 40mA with variable slits at V20 and a measurement time of 1 sec/step which is statistically satisfactory. The analysis does not indicate the presence of specific mineral orientations but measures the bulk abundance of all the minerals present, regardless of orientation. It should be kept in mind that XRD analysis is not strictly a quantitative technique and that the results are only semi-quantitative at best. The results are able to determine the minerals present but are not able to give the researcher the abundance or weight percent of the mineral.

2.5.2. Sediment Composition (XRF)

In order to understand the presence and distribution of trace metals within the sediments of the Buffels River, 22 sediment samples were selected for bulk compositional analysis by XRF. Sites were selected based on distribution with respect to the membrane as well as sediment type and through a preliminary screening using a hand held XRF gun. Approximately 20 g of each sample were ball milled into a fine powder for two minutes which was then placed into small sealable plastic bags. The ball mill was cleaned with acetone and then with pure quartz chips prior to each sample being milled. The resultant powders were analysed with a Thermo Niton XL3t XRF gun to determine the chemical characteristics of the sediments. Samples were analysed by placing them into the gun container while allowing them to be in contact with the gun window. The samples were tested through the thin plastic sample bags they were placed in. This was done to minimise contamination and to make sediment handling easier.

The results gathered from the XRF analysis with the XRF gun were then used to further narrow down to 15 sites where anomalies were found. These samples were then sent off for further analysis through the Central Analytical Facility at Stellenbosch University. X-ray Fluorescence (XRF) analysis was conducted using an Axios from PANalytical with a 2.4kW Rh X-ray Tube. The international (NIST) and national (SARM) standards were used in the calibration procedures and quality control (precision and accuracy) for both major and trace element analyses of the XRF. Detection limits for the elements

quoted, depending on the matrix (combination of elements present), are approximately 0.5 ppm for trace elements on a pressed pellet and approximately 0.001 wt% for major elements on a fused bead.

2.5.3. Cations and Anions

Major cation and trace element analysis on field acidified water samples was performed using an Agilent 7700 ICP-MS in the ICP-MS/AES Laboratory of the Central Analytical Facility at Stellenbosch University. Calibration was done according to NIST traceable standards. Anion analysis was performed using a Waters IC-Pak 717 Autosample conductivity detector-Agillent 1120 pump in the Mass Spectrometry laboratory also of the Central Analytical Facility at Stellenbosch University. Samples were run either as undiluted, volumetrically diluted x10 or volumetrically diluted x100 depending on EC values to bring the anion concentration to within range of the standards. Calibration was done using Spectrascan SS-028555 standards and analytical errors did not exceed 10%.

2.6. Atacamite Samples

Atacamite samples were also analysed to determine the mobility and stability of the copper in the soil. This was important in understanding the effects of groundwater moving through copper polluted soil. The atacamite samples were collected from the Spektakel mine by Stephan Le Roux. This soil sample was then used for the leaching experiment, while a synthetic atacmite was made to be used in the titration experiment.

2.6.1. Atacamite Preparation

Synthetic atacamite crystals were prepared by Stephan Le Roux according to the method proposed by Sharkey and Lewin (1972). This method produces a 3 g atacamite yield by adding 1 g of powdered calcite to a 0.1M $CuCl_2$ solution. To increase the yield Le Roux multiplied by a factor of ten. One litre of 1.0M $CuCl_2$ solution was prepared and set to stir on a magnetic stirrer while 10 g of calcite power was added to the stirring solution in 2 g increments. This was done to prevent the solution from bubbling over due to the CO_2 gas which is released during the reaction. Once all the calcite had been added the solution was left to stir for 24 hours until the reaction was complete.

After 24 hours of stirring the reaction had completed and the atacamite minerals remained in suspension. Centrifuge tubes were then filled with 40 ml of the solution and 10 ml of 0.5M $Mg(NO_3)_2$. The 0.5M $Mg(NO_3)_2$ solution was added to aid in flocculating the atacamite minerals and rinse them of any Cu2+ and Cl ions which may have been on the surface. The tubes were then vortexed to remove as much of the Cl^- and Cu^{2+} ions as possible. Once rinsed the tubes were centrifuged again for 15 minutes at 3500 rpm to flocculate the atacamite crystals. The atacamite crystals could then be collected and washed using a 0.2M Mg(NO3)2 solution until the most of the remaining Cl^- and Cu^{2+} was removed from the crystals. The solution was checked for any excess Cl^- and $AgNo_3$ after each wash. The crystals were then able to be dried over night at 50 °C and milled into a powder using an agate

mortar and pestle. Le Roux sent the samples for XRD mineral analysis to determine the purity which confirmed the mineral to be atacamite (Le Roux, et al., 2015).

2.6.2. Leaching Experiment Using Synthetic Atacamite

A leaching experiment was performed by using six separatory funnels that were previously acid washed and rinsed using DI water. A filter made from glass fibers and broken up filter paper was placed in the bottom of the funnels. 80 g of atacamite soil collected from Spektakel was then placed in each separatory funnel. A 0.5M NaCl solution was made up and used on three of the separatory funnels. The other three funnels received normal de-ionised water. An amount of 45 ml was added to each funnel respectively. The samples were then left for 24 hours before the leached through water was removed by suction. The leachate collected was weighed, filtered using 0.2 µm GVS Cellulose Acetate Membrane Syringe Filter and the pH was measured. The sample then received a few drops of nitric acid. 25 ml of solution was added to each of the drained funnels, three receiving 0.5M NaCl solution while the other three receiving de-ionised water. The experiment was repeated every 24 hours for 18 days and the samples collected were used to determine the amount of copper released from the atacamite soil into the solution. The Cu^{2+} concentrations were determined by Ion Chromatograph (IC) in the Soil Science Department at the University of Stellenbosch. The IC used was a Metrohm 761 Compact Ion Chromatograph (IC) with a Metrohm Metrosep A Supp 5 - 250/4.0mm Anion Column. To quantify the results each time new eluent was prepared the IC was calibrated with the Fluka range of IC calibration standards.

2.6.3. Titration Experiment

A Metrohm 905 Titrano autotitrator was used in the Earth Science Department at Stellenbosch University. A measured amount of 0.4g of pure synthetic atacamite was added to 40 ml of 0.5M NaCl solution in a 50 ml glass beaker. The pH was recorded at the start and 0.5M H_2SO_4 was added to drop the pH to 4.5. Once at a pH of 4.5 a 0.7 ml aliquot was drawn and the time was recorded. At 0 minutes, 1 minute, 2 minutes, 3 minutes, 4 minutes, 5 minutes, 10 minutes and 20 minutes from the pH reaching 4.5 a 0.7 ml aliquot was drawn each time. Once the full experiment was complete the samples were then filtered using a 0.2 µm GVS Cellulose Acetate Membrane Syringe Filter and diluted by adding 10 ml of MilliQ water. The diluted samples were then able to be submitted for Cu concentrations by means of IC. Three replications for 0.5M NaCl solution and three replications for DI water were used.

This experiment was then repeated again using 1M HNO_3 as the titrant and DI water for three replications and then 1M NaCl solution for the following three replications. This was done using 1.8 g of atacamite soil instead of the synthetic atacamite previously used. Care was taken to ensure that there was the same amount of atacamite in the soil sample as there was in the synthetic sample. This was calculated from the total Cu concentration of the soil. The same parameters for pH and sampling

were used. The 0.7 ml aliquot was drawn and collected at 0 minutes, 1 minute, 2 minutes, 3 minutes, 4 minutes, 5 minutes, 10 minutes and 20 minutes from the pH reaching 4.5.

3. RESULTS

The following section outlines the geochemical and sediment analysis as part of this study. The full data set is given in Appendix 1 whilst the summarised tables are provided in the section where relevant. This section is broken down into sediment samples, water chemistry and atacamite experiments.

3.1. Sediment Samples

Sixty-seven sediment samples were collected throughout the study area from 46 selected sites. Of these 46 sample sites, selected sediment samples were then further analysed for grain size variation and the composition of the sediments themselves. Some samples were sampled at two depths due to noticeable differences in morphology in the field. The varied depths were determined in the field and determined by the percentage of noticeable clay and sand percentage, colour and amount of organic material. Leachable cations and anions were determined through the saturated paste extracts. The results for each of these sets of analyses are discussed below. Since the grain size analysis was performed prior to the saturated paste extract, this data is presented first.

3.1.1. Grain Size Analysis

Grain size analysis was undertaken on all 64 sediment samples collected and the results are given in Appendix 1. The process used to determine grain size percentages separates the percentage of sand into 0.5 mm, 0.25 mm, 0.106 mm and <0.053 mm. The samples collected above 0.053 mm got added together as the sand percentage. The samples <0.053 mm and >0.02 mm are silt, and those <0.02 mm are clay. The results show all 64 soil samples were 98.83% sand, 0.64% clay and 0.53% silt. With a standard deviation of 4.36% for sand, 2.24% for silt and 2.18% for clay. From these 64 sediment samples, 15 were analysed in more detail for geochemistry and hence the detailed sediment grain size analysis of these samples is shown in Table 2. These samples show the percentage of sand, silt and clay found in each sediment sample collected. The results for 15 selected sample sites were also plotted on a ternary diagram (Figure 19).

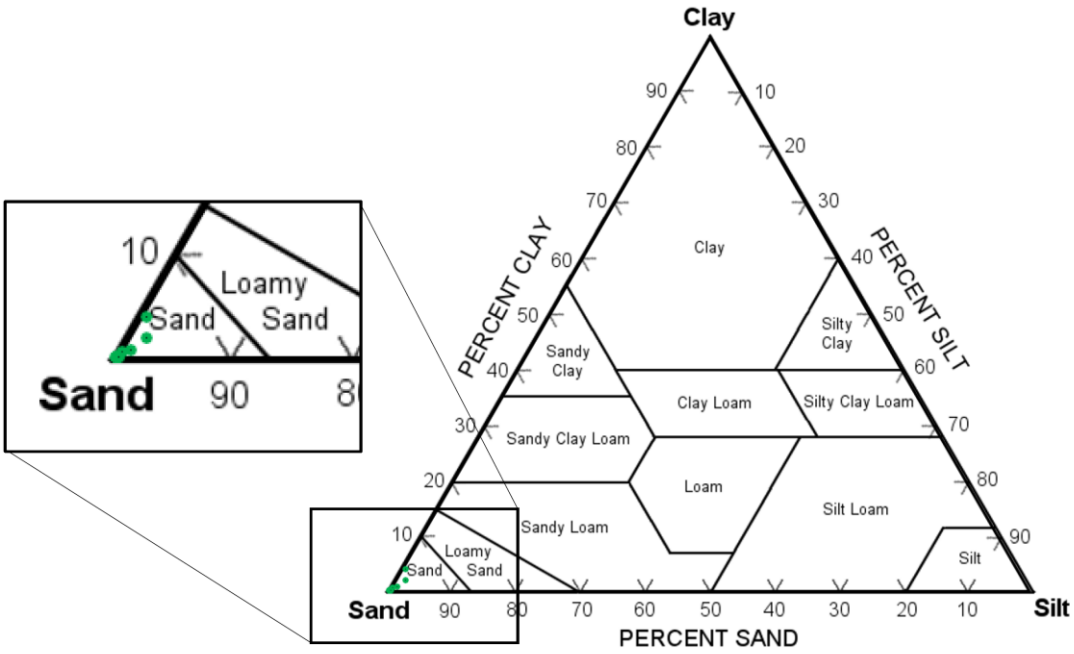

Figure 19: *Classification of grainsize.*

Table 2: *The grain size percentages for the 15 selected sample sites.*

Sample Site	Depth of Sample	Sand (%)	Silt (%)	Clay (%)	Total (%)
Site 9	0-20cm	99.697	0.114	0.189	100
Site 9	20-40cm	99.892	0.055	0.053	100
Site 12	0-50cm	99.907	0.035	0.058	100
Site 12	50-90cm	99.931	0.000	0.069	100
Site 21	0-30cm	99.132	0.522	0.347	100
Site 21	30-50cm	99.928	0.035	0.037	100
Site 26	0-30cm	99.903	0.052	0.045	100
Site 35	0-30cm	99.890	0.046	0.063	100
Site 36	0-40cm	99.970	0.005	0.025	100
Site 38	0-30cm	98.313	0.749	0.938	100
Site 44	0-15cm	95.491	3.879	0.630	100
Site 44	15-30cm	99.774	0.066	0.160	100
Site 45	0-15cm	96.461	1.795	1.744	100
Site 45	15-30cm	99.884	0.037	0.079	100
Site 51	0-50cm	99.662	0.095	0.243	100

3.1.2. Saturated Paste Extracts

Cations and anions analyses of the saturated paste leachate are given in Table 3. The results are shown in Figure 20, 21, and 22 in terms of distance from the membrane. Sites 38 and 36 were downstream from the membrane, while the rest were upstream from the membrane. Some of the sites have double samples which indicate that they were taken at two different depths at the same location. The first sample is the sample taken at the surface, and the second sample indicated is the one from deeper in the sediment column. The exact height profile of each sample is given in Table 3. Site 44 and 45 showed different sediment morphologies at different depths. At shallow levels these two samples were classified as sand and silt, whereas at depth and along with all the other samples they were classified as sand as indicated in section 2.3 above. As they contained a higher percentage of silt and clay in comparison to the other sediment samples. The rest of the samples were categorised as sand only.

Table 3: *Field measuremnets, cation and anion results from the saturated extract performed on the sediments collected.*

		Field measurements		Anions		Cations								
Sample Site	Depth of Sample	EC	pH	mg/l Chloride	mg/l Sulphate	mg/l Ca	mg/l Cu	mg/l Fe	mg/l K	mg/l Mg	mg/l Mn	mg/l Na	mg/l Pb	mg/l Zn
Site 38	0-30cm	9.30 mS/cm	7.20	2167.2	1003.4	480.20	0.12	< 0.01	45.52	231.90	0.09	1103.0	< 0.05	< 0.05
Site 36	0-40cm	0.50 mS/cm	7.83	88.7	70.1	29.98	0.08	0.23	8.17	11.01	0.03	68.2	< 0.05	< 0.05
Site 44	0-15cm	26.40 mS/cm	7.35	7849.2	1933.0	1341.00	0.30	< 0.01	50.11	678.80	6.72	5255.0	< 0.05	0.13
Site 44	15-30cm	7.42 mS/cm	7.15	7727.2	2673.7	199.20	< 0.05	< 0.01	34.44	108.40	3.59	730.7	< 0.05	0.15
Site 45	0-15cm	37.70 mS/cm	7.16	16275.3	5490.1	1235.00	0.11	< 0.01	98.68	910.20	3.29	5119.0	< 0.05	< 0.05
Site 45	15-30cm	6.36 mS/cm	7.05	6163.1	1736.6	992.90	< 0.05	< 0.01	85.05	551.50	6.97	3609.0	< 0.05	< 0.05
Site 51	0-50cm	20.00 mS/cm	7.70	1202.4	253.2	188.50	< 0.05	< 0.01	17.84	103.90	0.55	602.1	< 0.05	< 0.05
Site 21	0-30cm	22.90 mS/cm	7.01	7050.6	2208.1	1424.00	< 0.05	< 0.01	149.90	625.00	2.32	4367.0	< 0.05	< 0.05
Site 21	30-50cm	5.08 mS/cm	7.67	1026.8	741.1	262.00	< 0.05	< 0.01	28.06	81.05	0.41	649.9	< 0.05	< 0.05
Site 26	0-30cm	1.09 mS/cm	7.26	209.2	154.3	61.45	0.14	0.16	11.27	27.07	0.11	135.6	< 0.05	< 0.05
Site 35	0-30cm	0.29 mS/cm	6.90	59.9	17.1	14.34	0.12	1.18	16.30	8.55	0.03	38.4	< 0.05	< 0.05
Site 12	0-50cm	0.01 mS/cm	7.66	2.2	-	1.46	< 0.05	0.90	1.93	1.25	0.01	4.0	0.04	< 0.05
Site 12	50-90cm	0.07 mS/cm	7.68	10.2	-	2.17	0.02	2.87	2.99	1.85	0.02	17.8	< 0.05	0.01
Site 9	0-20cm	0.08 mS/cm	7.85	15.8	-	5.49	0.10	0.93	4.16	2.97	0.03	18.5	< 0.05	< 0.05
Site 9	20-40cm	0.05 mS/cm	7.67	5.0	-	2.18	0.02	1.27	3.02	1.58	0.02	9.6	< 0.05	< 0.05
Mean		9.15 mS/cm	7.41	3323.5	1480.1	415.99	0.11	1.08	37.16	223.00	1.61	1448.5	0.04	0.10
Standard Deviation		11.54 mS/cm	0.31	4586.0	1551.2	524.14	0.08	0.84	41.71	296.86	2.37	1949.4	0.00	0.06

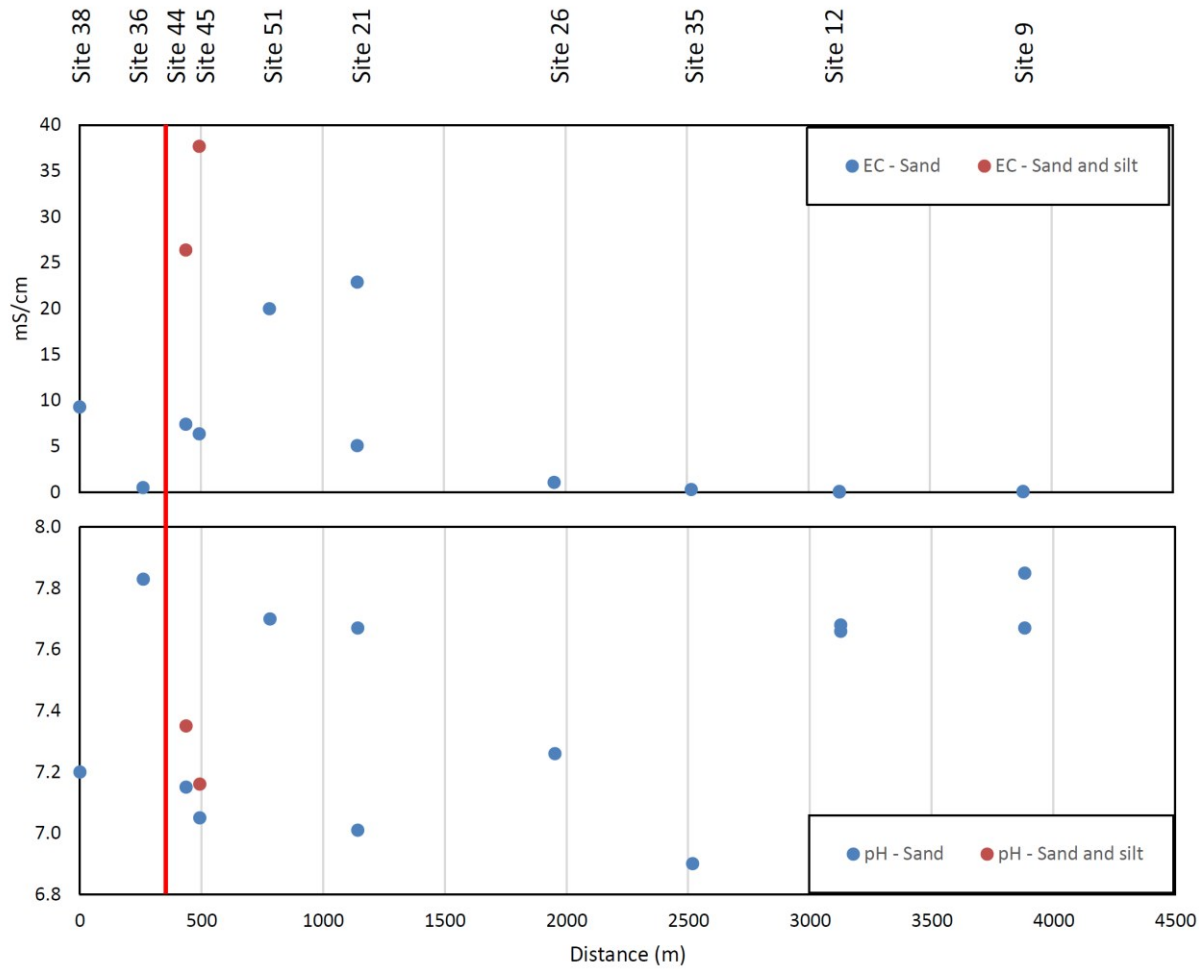

Figure 20: *pH and EC from saturated paste extract*.

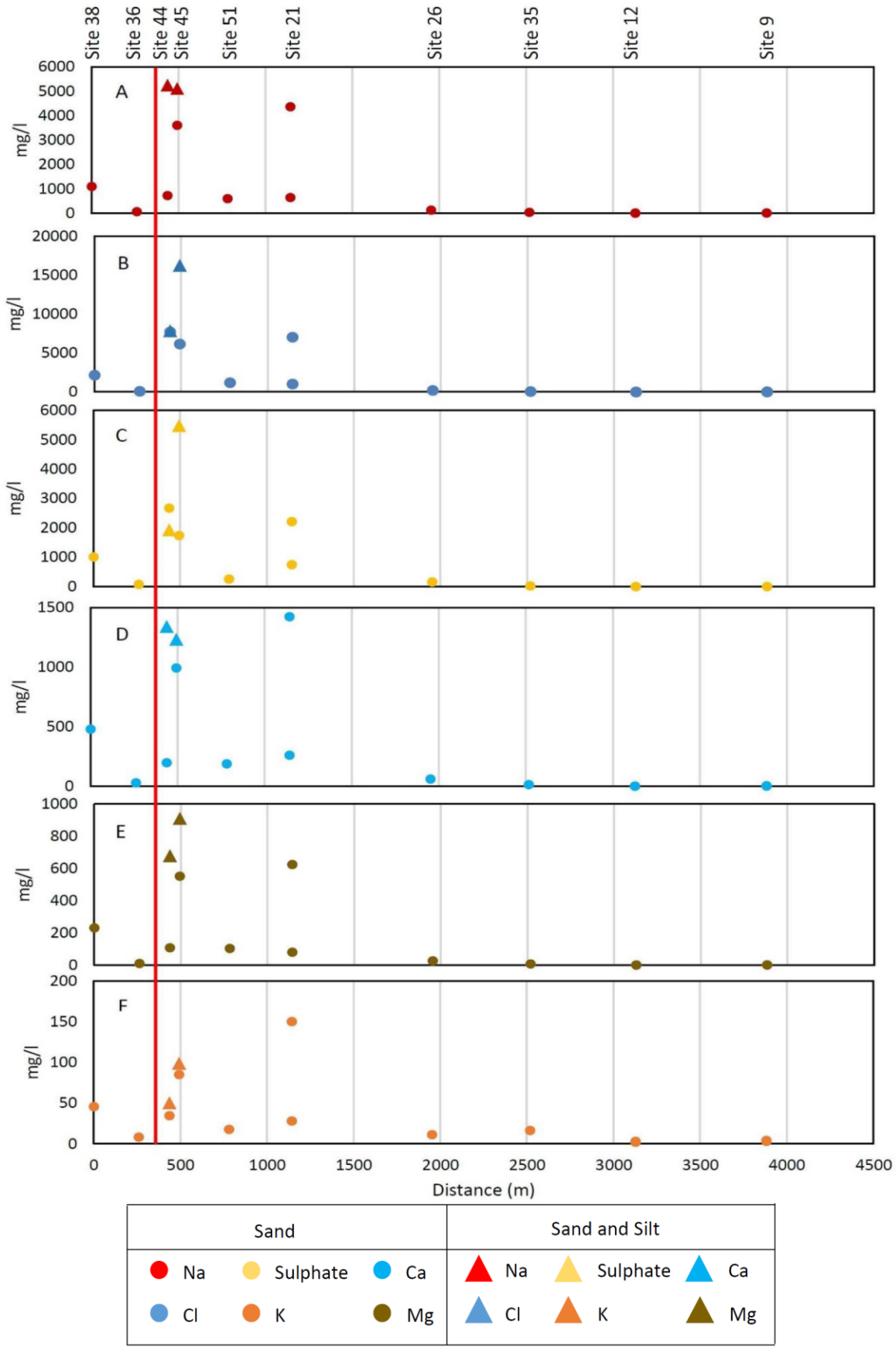

Figure 21: *Saturated paste extract results for A) Na, B) Cl, C) Sulphate, D) Ca, E) Mg, F) K. The triangles represent sand and silt sediments, while the circles represent sediment sample with predominantly sand.*

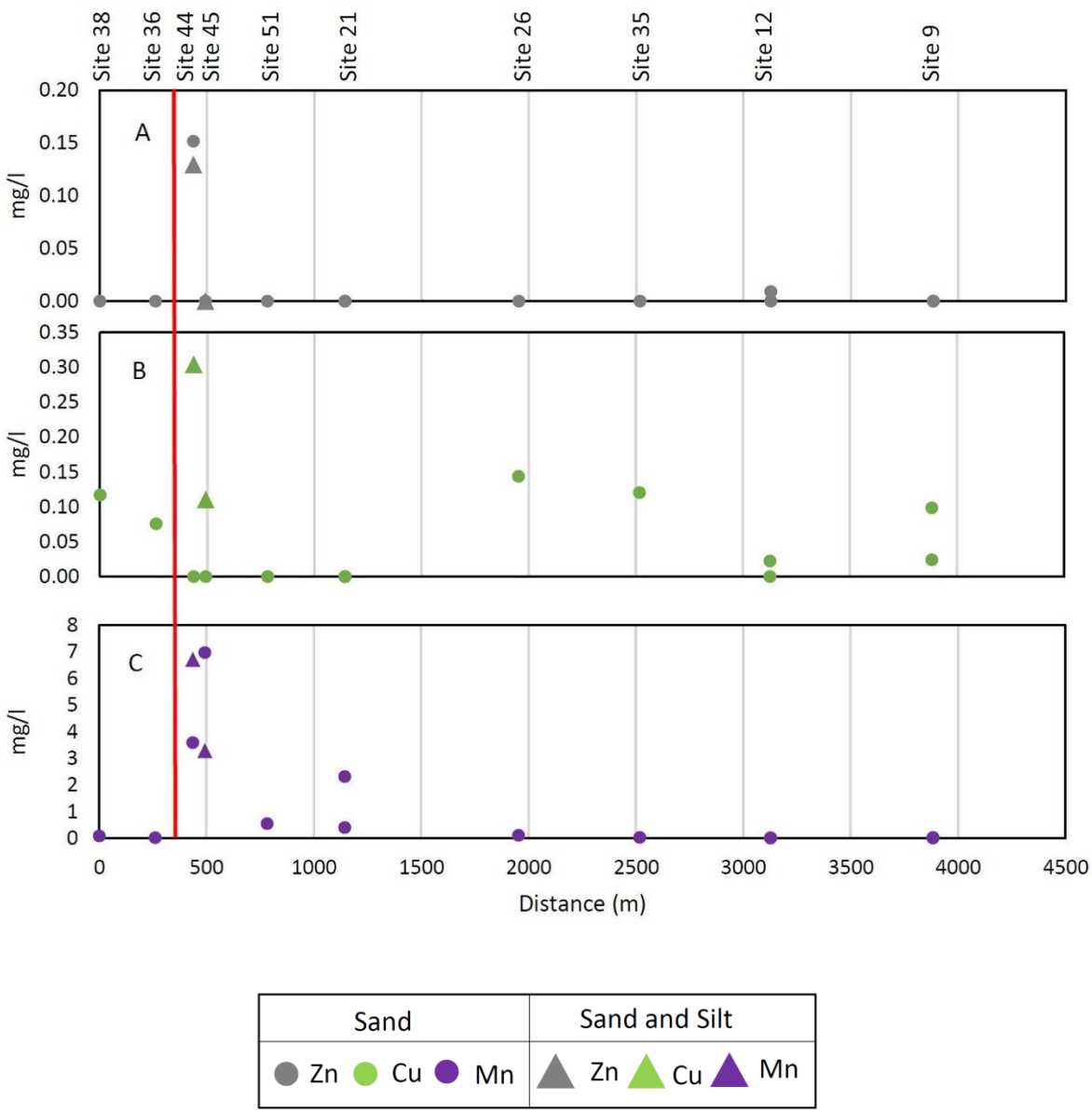

Figure 22: *Saturated paste cations for A) Zn, B) Cu, C) Mn. The triangles represent the sand and silt sediments, while the circles represent predominantly sand sediments.*

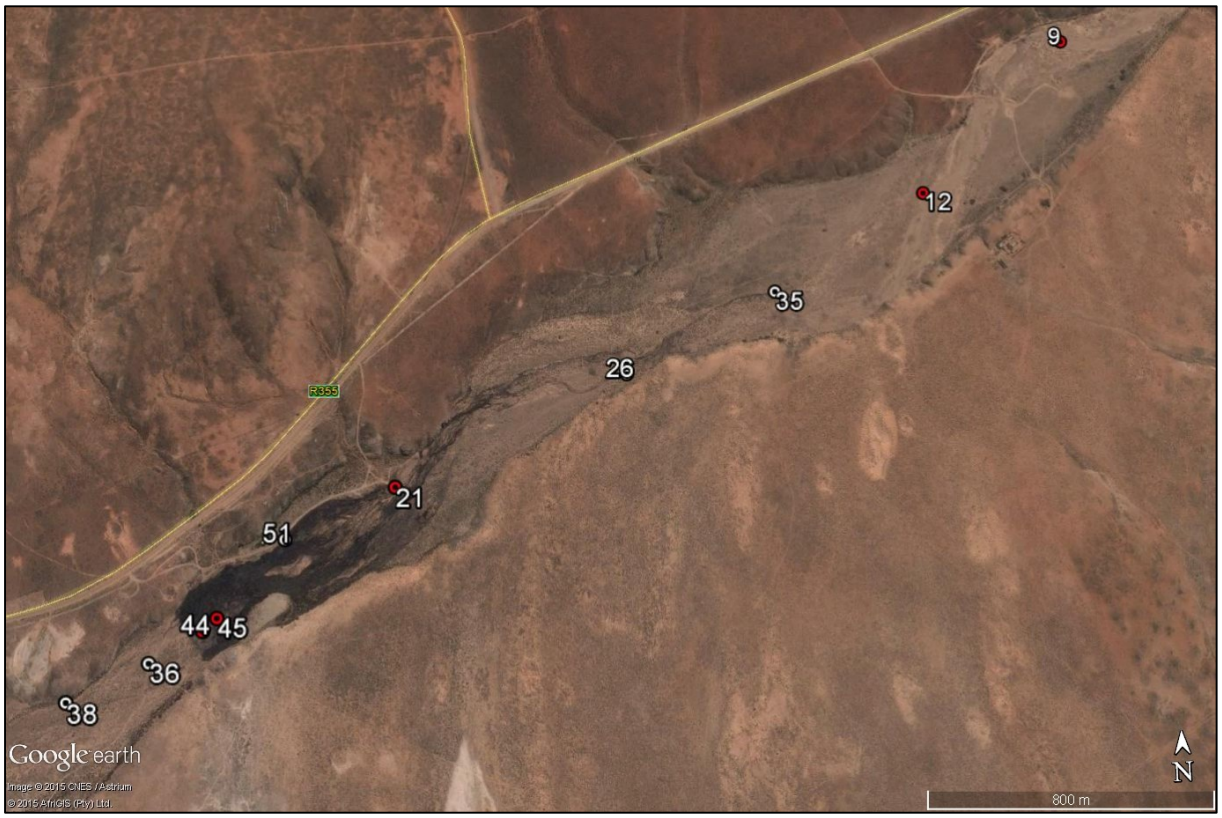

Figure 23: *Google Earth image showing study area and sediment sample sites collected and used for further analysis. The red locations had two samples taken, one upper sediment sample and one lower sediment sample. The white locations had one single sediment sample taken. Site 44 and 45 had different morphologies and contained higher silt percentage than the rest. These have been illustrated differently on the other plots.*

Electrical conductivity and pH collected from the saturated paste extract showed the results seen in Figure 20. The pH had an average of 7.41 with a high of 7.85 from sample 9 (0-20 cm) and a low of 6.90 from sample 35 (0-30 cm) (Figure 20). The standard deviation for the pH was 0.32, which illustrates that the pH of the study area was stable throughout all of the sediments sampled.

The EC for the study area shown in Figure 20 had a maximum value for the upper sample from site 45 (0-15 cm) of 37.7 mS/cm, and minimum value for the upper sample from site 12 (0-50cm) of 0.0125 mS/cm. The average EC recorded from the saturated paste extract was 9.15 mS/cm. The sample closer to the membrane generally showed a higher EC value than those situated further upstream from the membrane. The sites where two samples were taken illustrated lower sediments generally having a lower concentration that the sediment samples taken deeper in the soil column.

Figure 21 A and B show the variation in Na^+ and Cl^- concentration with respect to distance from the membrane. The average Na^+ sodium concentration from the saturated paste extract was 1448.5 mg/l. The Na^+ is predominantly spread between site 44 to site 21, where there is an average of 2904.7 mg/l. The Cl^- showed a similar trend with regard to the spikes found in the study area. The average Cl^- throughout the study area was 3323.5 mg/l, with an average of 6756.4 mg/l found between site 44 and site 21. This average drops off drastically after site 21 upstream from the membrane for both Na^+

and Cl^-. The lowest values were recorded further upstream and from the membrane at sites 12 and 9. The highest values were at site 44 for Cl^- and at site 45 for Na^+. These values were 16275.3 mg/l and 5119 mg/l respectively. Sodium and Cl^- are shown together as they can be related to the salinity caused by NaCl salts in the area.

The K^+ found in the sediment showed higher concentrations in the upper sediments where two samples were taken (Figure 21 F). The highest concentration was found at site 21 (0-30 cm) with a concentration of 149.90 mg/l. The concentration drops off further away from the membrane. The lowest recorded concentration was found at site 12 (0-50 cm) with 1.93 mg/l. There was spike found below the membrane at site 38 (0-30cm) of 45.52 mg/l. The Ca^{2+} concentrations had a maximum concentration of 1424 mg/l, and a minimum concentration of 1.46mg/l (Figure 21 D). The average concentration was 415.99 mg/l. There were higher concentrations found in the upper sand and silt sediments compared to the lower sand sediments for sites 44 and 45.

Mg^{2+} and SO_4^{2-} shown in Figure 21 C and E displays a similar relationship regarding accumulation behind the membrane. These spikes were at site 44, site 45 and site 21. The average Mg^{2+} value was 223 mg/l with the highest value at site 45 (0-15 cm) with a concentration of 910.20 mg/l. The lowest value was at site 12 (0-50 cm) where the concentration was 1.25 mg/l. The sites furthest away from the membrane upstream (sites 12 and 9) had an average of 1.91 mg/l. Once again the high concentrations were found between site 44 and 21 with a substantial drop in concentration moving upstream from the membrane.

The highest Cu^{2+} concentration found in the study area (Figure 22), was found at site 44 (0-15 cm), with a concentration of 0.30 mg/l. The average Cu^{2+} concentration from the saturated paste extract was 0.11 mg/l. Sites 51, 21, 12 and the lower samples from site 44 (15-30 cm) and 45 (15-30 cm) had Cu^{2+} concentrations below the detection limit of 0.05 mg/l. Zinc was also found in the area, at site 44 and the lower sample collected from site 12 (50-90 cm). The Zn^{2+} results can be seen in Figure 22 A. The Zn^{2+} had a high of 0.15 mg/l for the lower sample at site 44 (15-30 cm). The lowest recorded concentration was found at site 12 (15-90 cm). The rest of the samples were below the detection limit.

Mn^{2+} results seen in Figure 22 C show a maximum concentration of 6.67 mg/l in the lower sand sediments at site 45 (15-30 cm). The concentration quickly decreases as the sediments move away from the membrane. The average concentration below the membrane was 0.06 mg/l. The four sites right after the membrane showed an average of 3.41 mg/l. The upper sand and silt sentiment for site 44 showed a higher concentration than the lower sand sediments. This was however not consistent with site 45 where the sand sediment showed a higher concentration in the lower sand sediment.

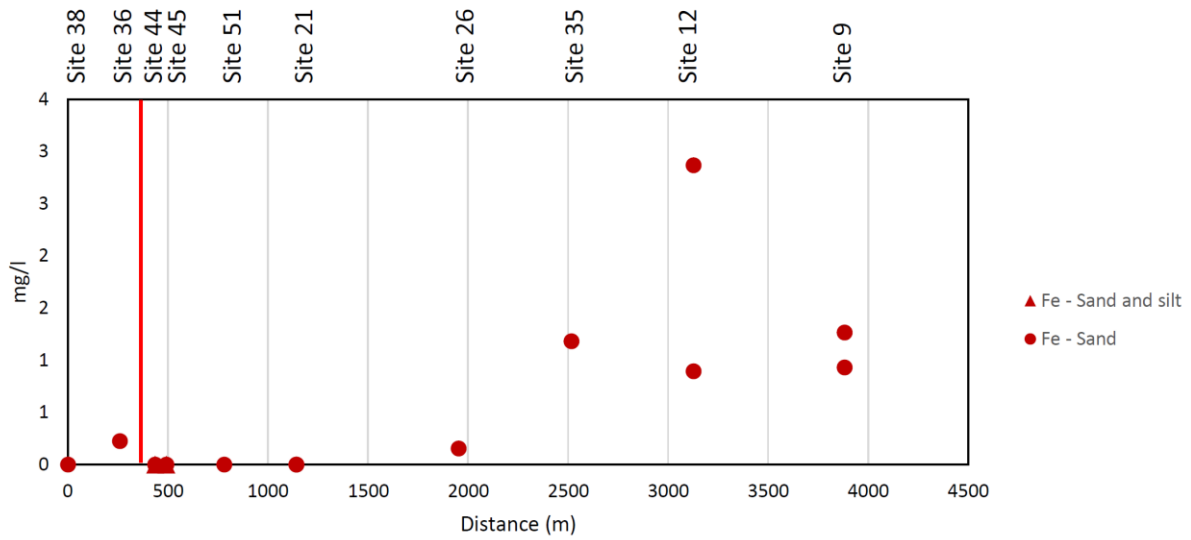

Figure 24: *The Fe^{2+} concentration derived from the saturated paste extracted samples collected. The triangles are sand and silt samples. The circles are sand only.*

The maximum concentration for Fe^{2+} was found at site 12 in the lower sediment (50-90 cm) at 2.87 mg/l (Figure 24). The sand and silt sediments were both below detection limits. Several sand sites had values below detection limit.

3.1.3. Sediment Mineralogy

Sediment mineralogy was determined via semi-qualitative XRD analysis of the clay fraction of each sediment sample. All 14 samples contained quartz, albite, kaolinite, illite, and orthoclase. Site 21 (0-30 cm) was the only site to contain calcite. Both sediment samples for 12 contained vermiculite in addition to the upper sample for site 9 (0-20 cm). Smectite or chlorite was found in the following sites: Site 21 (15-30 cm), 26, 35, 36, 38, and both samples for site 44 and 45. Site 9 (0-20 cm) was unfortunately lost in the preparation for XRD analysis, and was therefore unable to be analysed.

Table 4: *XRD results showing the minerals present in the selected sediment samples. Site locations can be seen in Figure 16.*

Site	Depth	Quartz	Albite	Kaolinite	Illite	Orthoclase	Calcite	Smectite/chlorite	Vermiculite
Site 12	0-50cm	X	X	X	X	X			X
Site 12	50-90cm	X	X	X	X	X			X
Site 21	0-30cm	X	X	X	X	X	X		
Site 21	30-50cm	X	X	X	X	X		X	
Site 26	0-30cm	X	X	X	X	X		X	
Site 35	0-30cm	X	X	X	X	X		X	
Site 36	0-40cm	X	X	X	X	X		X	
Site 38	0-30cm	X	X	X	X	X		X	
Site 44	0-15cm	X	X	X	X	X		X	
Site 44	15-30cm	X	X	X	X	X		X	
Site 45	0-15cm	X	X	X	X	X		X	
Site 45	15-30cm	X	X	X	X	X		X	
Site 51	0-50cm	X	X	X	X	X			
Site 9	0-20cm	X	X	X	X	X			X
Site 9	20-40cm								

3.1.4. Sediment Composition

Fifteen sediment samples were chosen for further XRF analysis based on anomalies and spatial distribution in relation to the membrane. As expected SiO_2 was the dominant component in the river sediments. The results are shown in Figure 25, and tabulated in appendix 1. An average of 75.64 wt% SiO_2 was found in the samples analysed. The highest SiO_2 percentage was found at site 36 (0-40 cm), while the lowest was found at site 44 (0-15 cm). This was as expected, because site 44 and 45 were slightly upstream from the membrane by a few meters. The samples found in this area had a clay and silt consistency for the top sediments (0-15 cm) and a more sandy consistency below (15-30 cm). Sample 44 (0-15 cm) and Sample 45 (0-15 cm) have 59.42 wt% and 60.84 wt% SiO_2 respectively. The lower sections for these samples have a SiO_2 percentage of 76.60 wt% and 77.96 wt%, which is close to the average found for all 15 samples.

Al_2O_3 has an average of 11 wt% for all 15 sediment samples; this percentage is however higher for the samples that contain more clay and silt compared to those sediments that have a more sandy consistency. An examples is site 35 (0-30 cm), site 44 (0-15 cm) and site 45 (0-15 cm). The Al_2O_3 percentages are 14.34 wt%, 16.32 wt% and 15.57 wt% respectively. Removing those spikes from the average percentage calculation for Al_2O_3 drops the average to 9.90 wt%. Figure 26 shows a linear relationship between the clay percentage and the wt% Al_2O_3 as would be expected.

Fe_2O_3 is another chemical component that increases in the more clay rich samples, this can be seen in Figure 26. An average of 2 wt% for all 15 samples is seen, with a spike at samples 38 (0-30 cm), 44 (0-15 cm) and 45 (0-15 cm). These spikes are 4.07 wt%, 5.80 wt% and 5.50 wt% which are more than double the average for the whole sample studied. The rest of the samples were all fairly consistent for the mineral percentages.

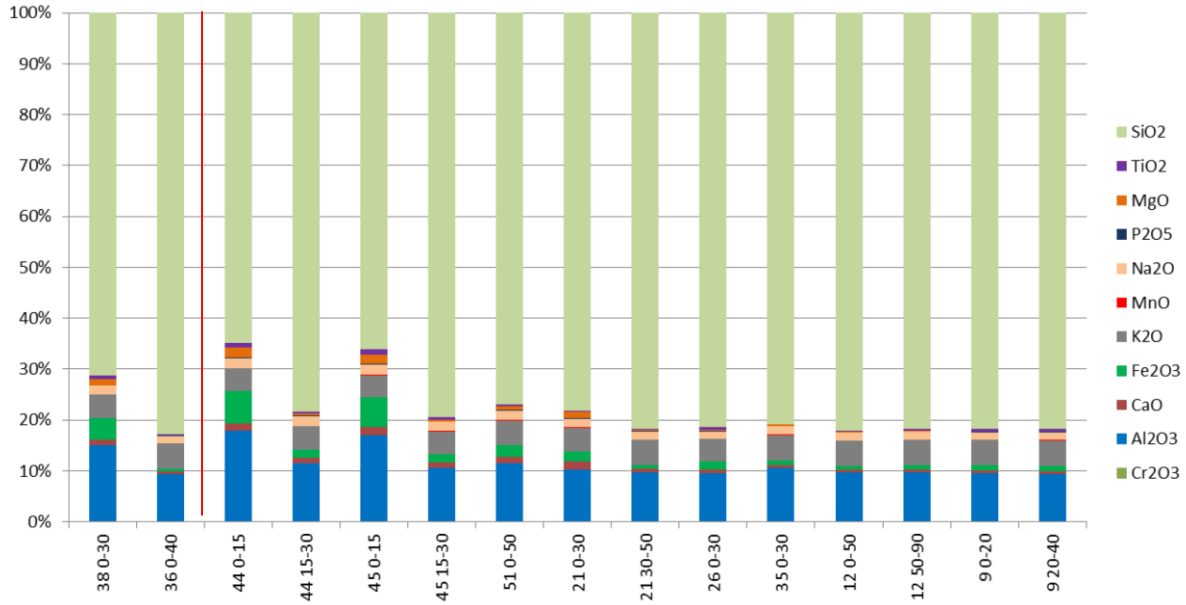

Figure 25: *The XRF results from the sediment samples taken in the Buffels River study area. Sites locations can be seen in Figure 16.*

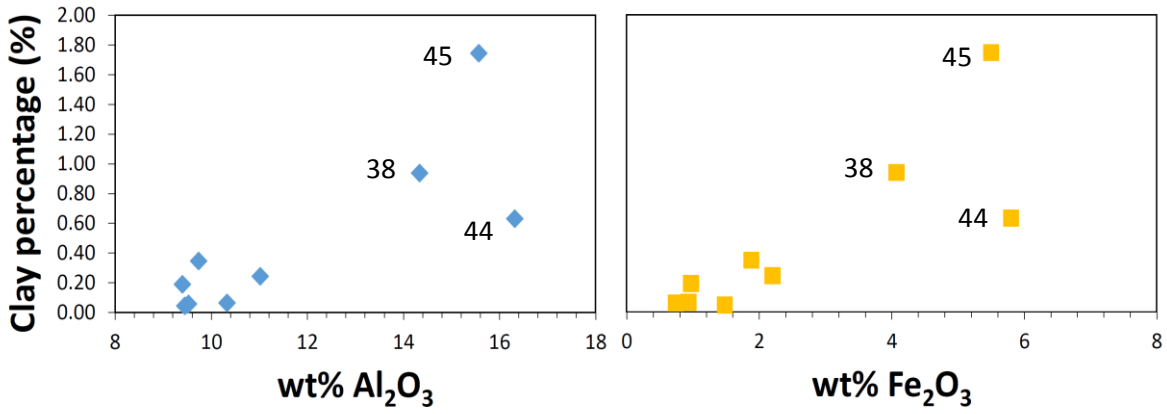

Figure 26: *Clay percentage compared to the wt% of Al_2O_3 and Fe_2O_3.*

3.2. Water Chemistry

Fourteen groundwater samples were collected during the second field season (October 2014) (Figure 27). The groundwater samples were collected from a hole dug from surface, and analysed for cations and anions at Stellenbosch University. No groundwater samples were collected from below the membrane due to a lack of accessible groundwater. Selected results for the water chemistry are shown below in Table 5, with all the sample results found in Appendix 1.

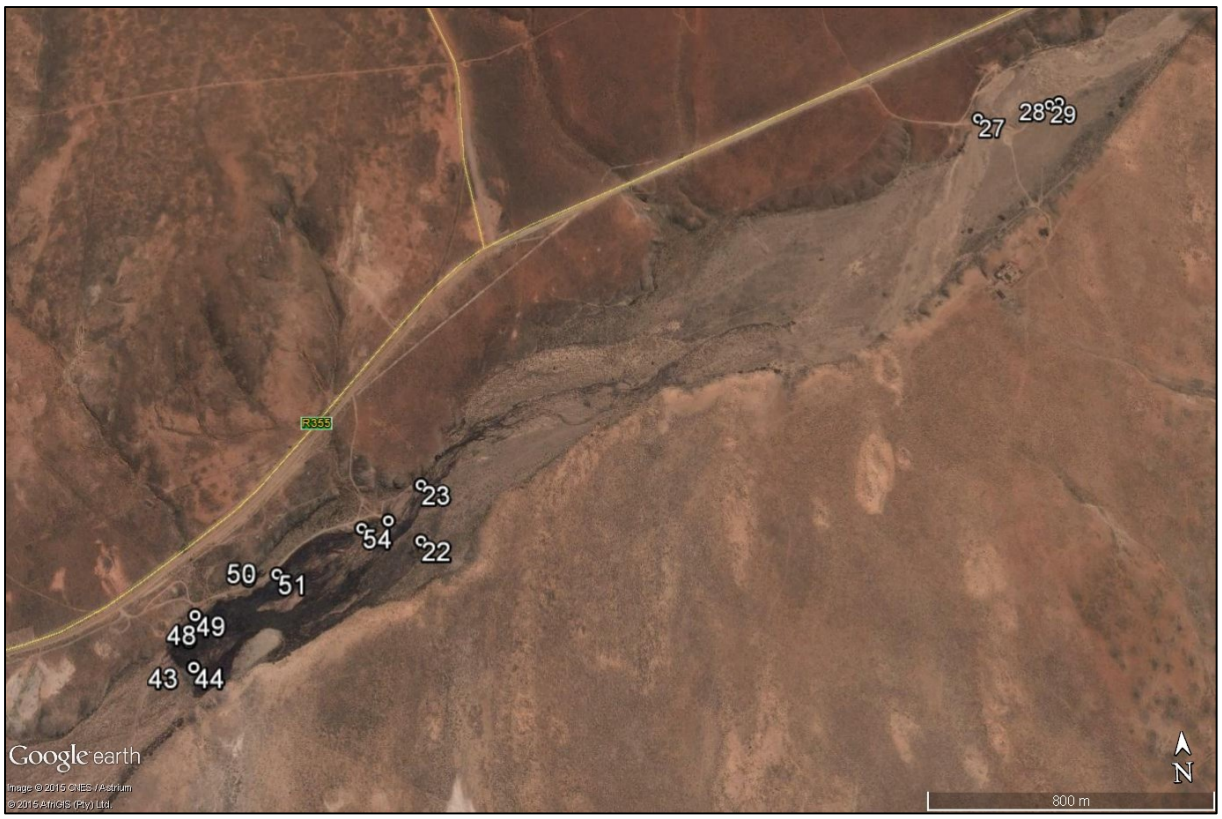

Figure 27: *Google earth image showing the groundwater samples collected and locations. No groundwater samples were collected below the membrane due to an absence of groundwater available. Groundwater was also difficult to access between site 23 and site 27. Site 56 was at a mine dam situated 23km upstream from the membrane.*

Table 5: *Groundwater cation and anions.*

Sample Site	Field Measurements		Anions		Cations							
	EC	pH	ppm Chloride	ppm Sulphate	ppm Ca	ppm K	ppm Mg	ppm Na	ppm P	ppb Cu	ppb Zn	ppb Mn
Site 43	3.88 mS/cm	7.39	2200.64	464.59	275.00	19.20	141.70	804.10	0.04	6.72	2.87	112.79
Site 44	5.67 mS/cm	6.75	3587.51	484.71	328.70	24.31	223.00	1196.00	0.04	9.60	105.22	11659.53
Site 48	4.37 mS/cm	6.62	2414.71	356.00	281.90	13.84	139.10	864.90	0.04	0.31	7.34	6140.05
Site 49	3.56 mS/cm	6.65	2091.54	445.16	211.90	24.06	119.10	783.00	0.03	0.34	5.01	836.42
Site 50	2.85 mS/cm	7.26	1788.86	441.42	161.70	18.58	103.60	628.80	0.14	1.58	2.51	83.10
Site 51	8.99 mS/cm	7.34	5375.13	1364.63	545.80	28.44	343.40	2176.00	0.14	26.81	4.49	4.38
Site 54	15.79 mS/cm	7.15	10308.93	4306.01	2034.00	44.02	957.20	3796.00	0.03	9.63	9.02	15110.20
Site 21	2.73 mS/cm	7.19	970.30	345.89	157.20	14.96	79.36	503.60	0.23	8.13	1.94	14.62
Site 22	2.44 mS/cm	6.72	1231.52	358.17	158.60	14.67	85.81	467.80	0.02	24.89	7.50	2154.58
Site 23	5.18 mS/cm	6.96	3015.56	985.44	352.50	24.43	176.70	1234.00	1.01	29.39	3.26	1817.68
Site 27	5.05 mS/cm	6.81	2549.56	770.53	326.30	37.59	153.80	1056.00	0.08	11.86	5.92	2332.39
Site 29	3.31 mS/cm	7.44	1525.02	330.40	218.50	18.46	117.90	655.00	0.04	5.48	53.11	10.21
Site 28	3.06 mS/cm	7.41	1965.30	413.99	181.50	15.75	100.00	547.20	0.08	10.43	172.84	2.80
Site 56	15.21 mS/cm	7.21	10008.32	2969.07	866.80	95.20	467.20	3966.00	0.02	1.28	5.81	91.89
Mean	5.864 mS/cm	7.1	3502.35	1002.571	435.74	28.1	229.1	1334.2	0.14	10.5	27.63	2883.62
Standard Deviation	4.254 mS/cm	0.3	2914.994	1140.52	479.86	20.5	227.4	1122	0.25	9.45	48.85	4626.51

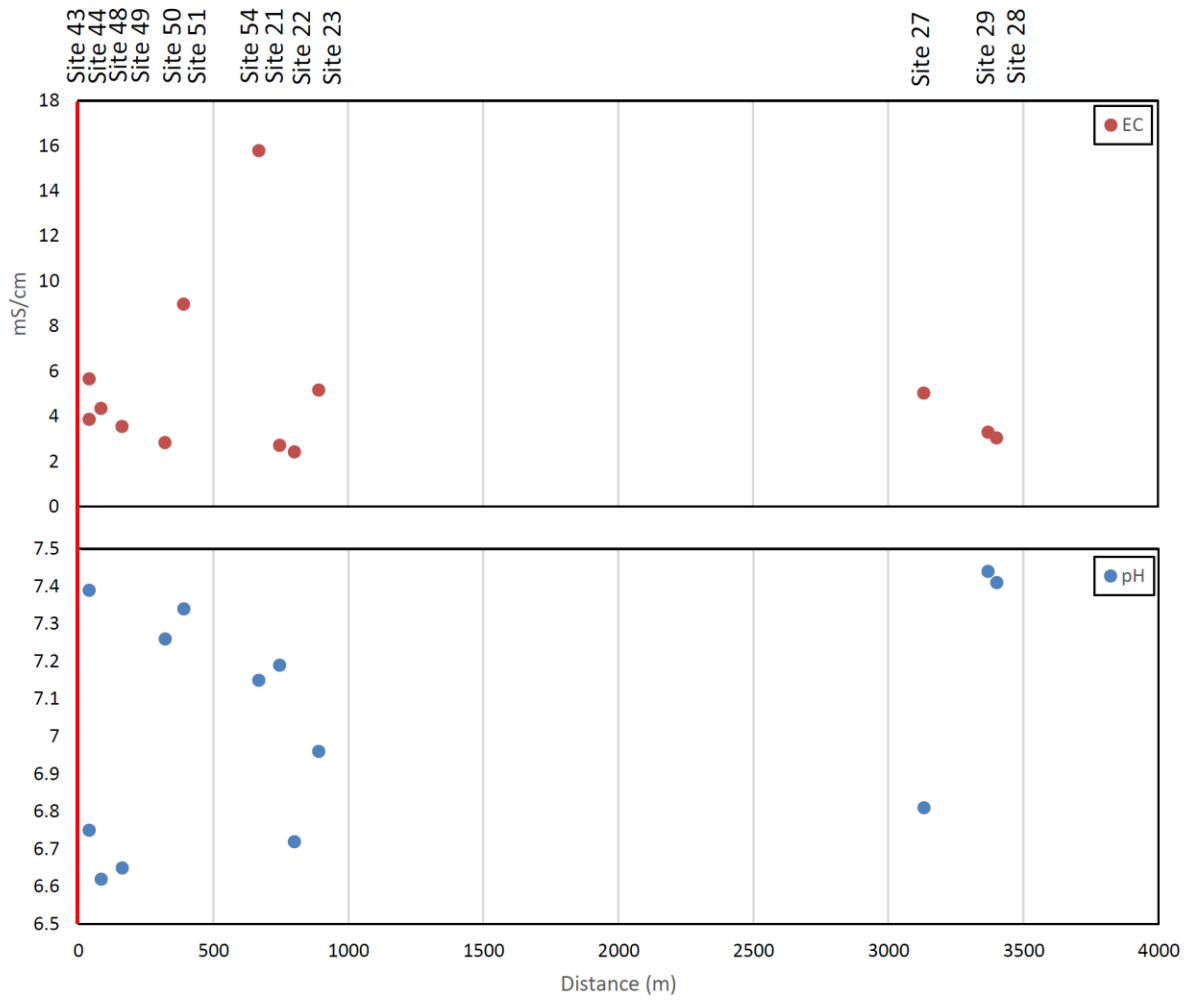

Figure 28: *pH and EC data collected from groundwater samples in relation to the membrane. The red line denotes the location of the membrane. No samples were able to be collected below the membrane due to a lack of groundwater. Site 56 has been removed from the above results because it is located 23km further upstream from the membrane.*

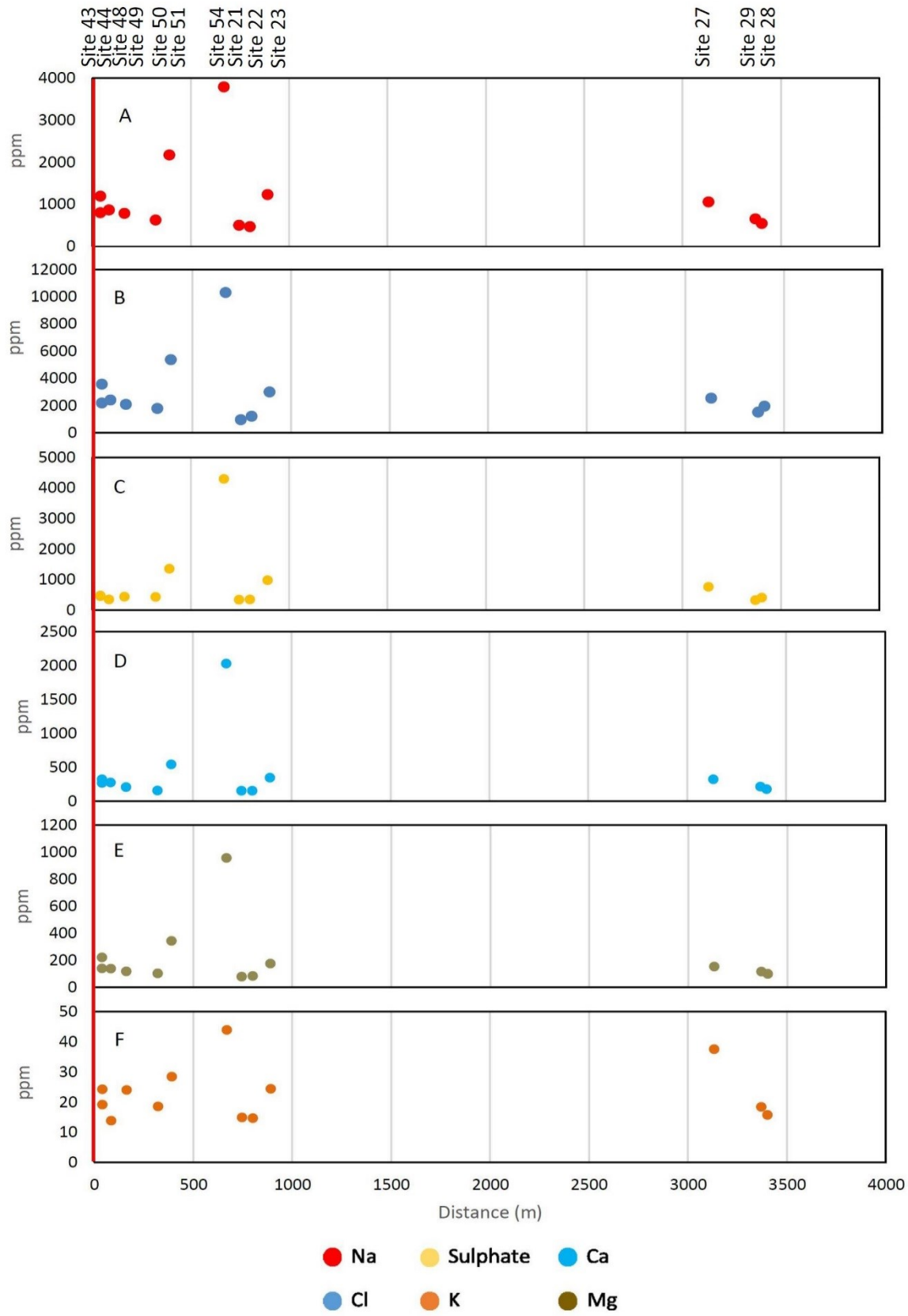

Figure 29: *Groundwater cations and anions in relation to distance upstream from the membrane. A) Na, B) Cl, C) Sulphate, D) Ca, E) Mg, F) K. Site 56 was excluded due to the distance from the membrane.*

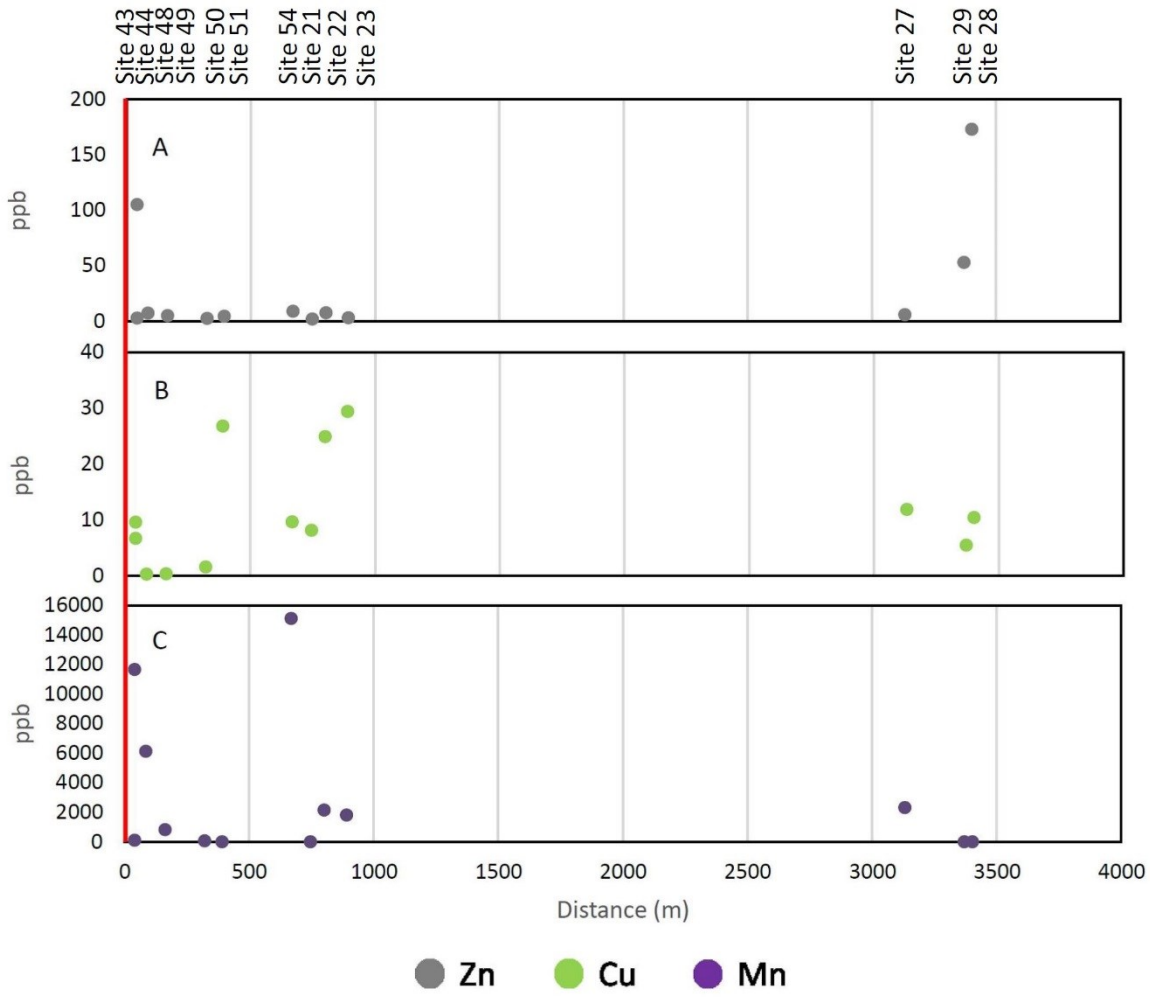

Figure 30: *Groundwater cations with regard to the distance upstream from the membrane. A) Zn, B) Cu, C) Mn. Site 56 was excluded due to the distance from the membrane.*

Electrical conductivity collected from the field (Table 5 and Figure 28) showed spikes at site 51, 54 and 56. Sites 54 and 56 were open water bodies while the remainders were all groundwater samples. The EC readings had a high of 15.79 mS/cm at site 54 and a low of 2.44 mS/cm at site 22. The average including these two high spikes was 5.86 mS/cm and excluding them was 4.26 mS/cm. The EC readings were plotted in Figure 28 but site 56 was removed to make the data more easily legible. Site 56 was located at a mine waste dam 23 km away from the membrane. The reason for the inclusion of site 56 in the data is that it has similar results to those seen in the open water body at site 54 close to the membrane.

The pH seen in Figure 28 was relatively consistent, with an average of 7.06. The highest pH was recorded at site 29 with a pH of 7.44. The lowest recorded pH was 6.62 found at site 48. The standard deviation for the pH was 0.29. Alkalinity was collected in the field on the groundwater samples using a titration method, and checked in the lab using an autotitrator. The results see in Figure 31 showed a trend similar to those seen in the EC readings collected. The lab alkalinity readings were used further, as they were likely to be more accurate than the field measurements. A high of 897.2 mg/l was found at site 51. A low of 97 mg/l was found at site 50. The average alkalinity including the three spikes at site 51, 54 and 56 was 350.5 mg/l, while excluding them the average dropped to 234.17 mg/l.

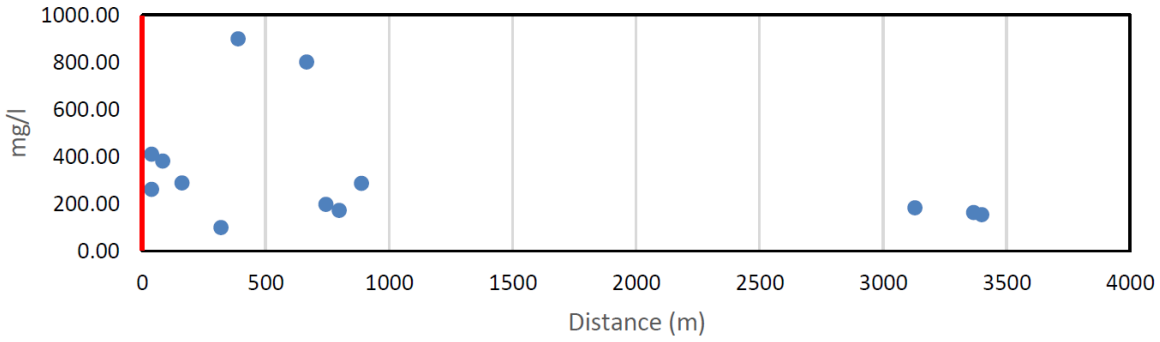

Figure 31: *Lab alkalinity with the red line denoting the location of the membrane upstream samples are to the right in the diagram.*

Cl^- and Na^+ were plotted against one another again (Figure 29). The highest Cl^- groundwater concentration found at site 54 where the Cl^- was 10308.93 ppm, the second highest was found at site 56 which is situated further away from the study area. Site 56 had a Cl^- concentration of 10008.32 ppm. The average Cl^- concentration for the groundwater found in the study area was 3001.89 ppm, including site 56 the average increase to 3502.35 ppm. The lowest concentration was found at site 21 which was 970.30 ppm. The Na^+ found in the groundwater in the study area had an average of 1131.72 ppm excluding site 56. Including site 56 the average increases to 1334.17 ppm. The lowest recorded Na^+ was found at site 22 at 467.8 ppm, while the highest sodium concentration was 3796 ppm found at site 54.

SO_4^{2-} was plotted with magnesium as before (Figure 29). The Sulphate had spike values of 4306 ppm at site 54 and 2969.07 ppm at site 56. Including site 54 and 56 the average SO_4^{2-} is 1002.57 ppm, excluding site 56 and 54 the average drops to 563.41 ppm. The lowest sulphate concentration was at site 29 with 330.40 ppm. Mg^{2+} also had a spike at site 54 and 56 of 957.2 ppm and 467.2 ppm respectively. The average concentration of Mg^{2+} in the groundwater was 229.13 ppm, this includes site 56. Excluding site 54 the average drops to 210.82 ppm.

K^+ results from the groundwater showed spikes at sites 54 and 27 of 44.02 ppm and 37.59 ppm. Including these spikes the average was 22.94ppm. Excluding these spikes the average concentration dropped to 19.70 ppm. Site 56 which was removed from the plots due its distance from the membrane had an anomalously high concentration of 95.20ppm. The lowest concentration was found at site 22 with a concentration of 14.67 ppm. Ca^{2+} was plotted in Figure 29 and had a maximum concentration of 2034 ppm at site 54. The lowest concentration was 157.2 ppm found at site 21. The average concentration excluding the two spikes found at sites 54 and 56, which were open water bodies was 266.63 ppm. Including these spikes the Ca^{2+}concentration increases to 435.74 ppm.

Cu^{2+} found in the groundwater was less than expected (Figure 30). These were measured in ppb as opposed to ppm or mg/l. Site 51, 22, and 23 were higher than the rest, with the highest concentration being 29.39 ppb found at site 23. The average Cu^{2+} concentration for the study area was 10.46 ppb with the lowest concentration found at site 48 with 0.31 ppb. Mn^{2+} showed three spikes also, this time at sites 44, 48 and 54 (Figure 30). The highest concentration was found at site 54 with 15110.20 ppb, and the lowest was found at site 28 with 2.80 ppb. The average concentration for Mn^{2+} was 2883.62 ppb. All of the sample sites were able to be determined, and none of them fell below detection limits.

Zn^{2+} results showed two large spikes of 105.22 ppb and 172.84 ppb for sites 44 and 28 respectively (Figure 30). The groundwater average concentration for Zn^{2+} was 27.63 ppb including the two spikes, but the average drops significantly if these anomalously high values are removed to an average of 9.07 ppb. The lowest concentration was found at site 21 where a concentration of 1.94 ppb was recorded. Site 56 which was removed from the plot had a concentration of 5.81 ppb. Iron had spikes behind the membrane, with a maximum concentration at site 48 of 992.1 ppb (Figure 32). The minimum recorded concentration was found at site 21 at 4 ppb. The average concentration of iron was 146.2 ppb. That is excluding site 56. Site 56 recorded a concentration of 5.1 ppb. The groundwater TDS was calculated using the equation found in section 1.3 and had a maximum value at site 54 of 10263.5 mg/l, with a minimum at site 22 of 1586 mg/l. The average calculated TDS was 3811.3, which included site 56 that had a value of 9886.5 mg/l. However, excluding site 56 dropped the average calculated value to 3344 mg/l. These results have been plotted in Figure 33, and can be found in Appendix 1.

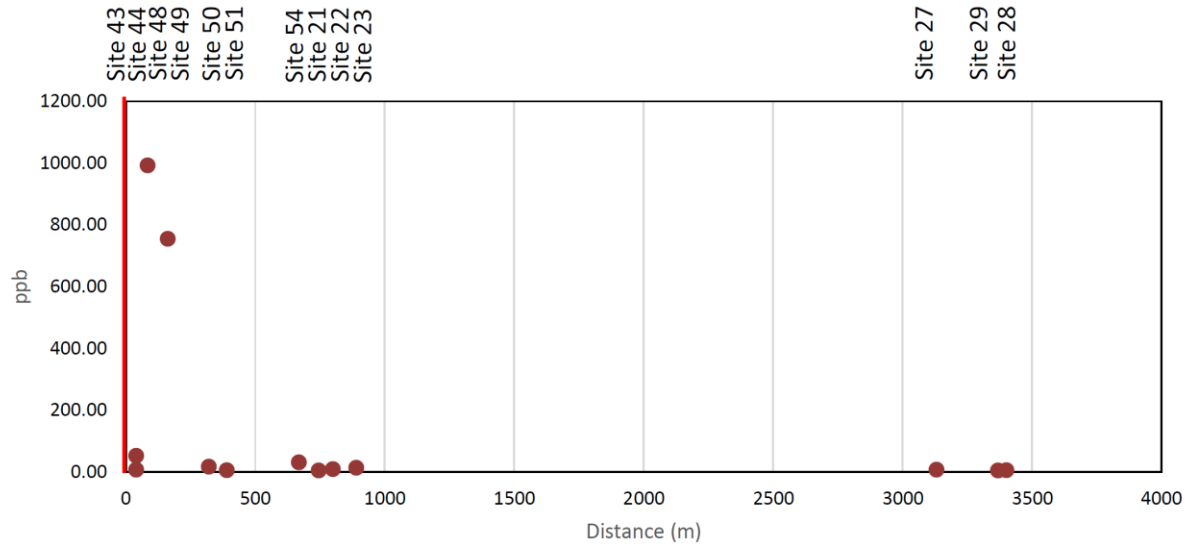

Figure 32: *The Fe concentrations in groundwater samples. The red line denotes the location of the membrane.*

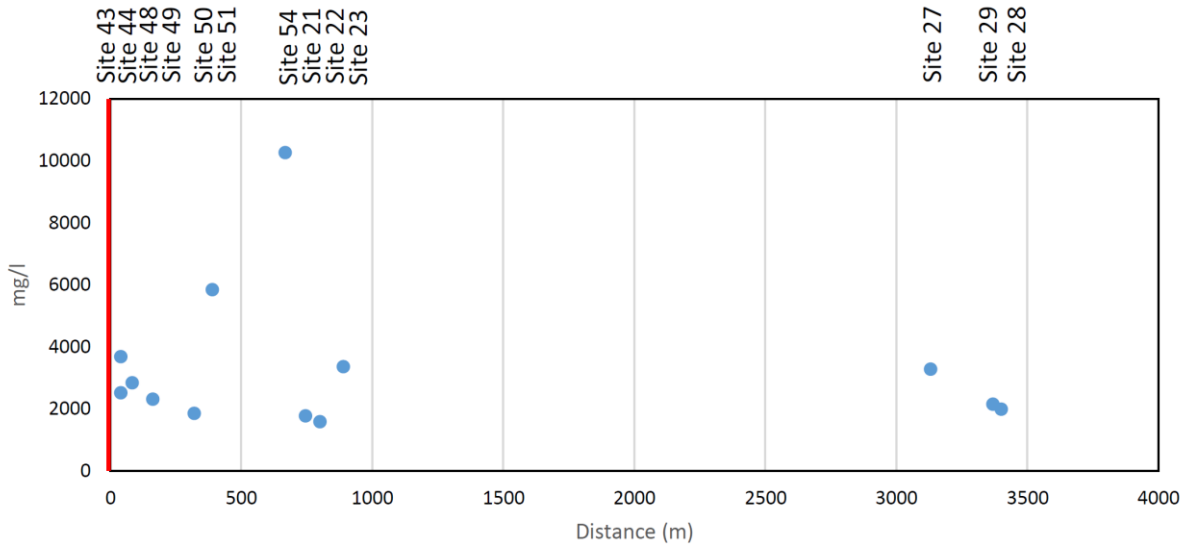

Figure 33: *TDS calculated for the groundwater from the EC results. The red line denotes the location of the membrane.*

3.3. Atacamite Experiments

The below results were obtained from experiments performed using atacamite soils collected from the Spektakel mine and synthetic atacamite. The leaching and titration experiments were done to help in understanding the mobility of Cu^{2+}. The results gathered from the field show a very low concentration of Cu^{2+} found in the sediments and groundwater at the membrane. The use of the atacamite experiments would be to help in understanding a worst case scenario for Cu^{2+} leaching out of sediments and into groundwater. The reaction rates were calculated using the results from the titration experiment.

3.3.1. Leaching Experiment

Using DI water as a leaching solution through atacamite soil gave the following pH results. The three replications using DI water as a solution were labelled A, B and C (Figure 34). The average pH over the 18 day period was 5.54. A dip in the pH at days 7 and 8 should also be noted, and could potentially be related to an issue in calibration of the pH probe on those two days. The pH showed a gradual increase in pH over time, with a minimum average of pH of 5.16 on day one and a maximum average pH of 5.78 on day 17. Using atacamite soil and leaching through 0.5M NaCl solution over a 24 hour period gave the following pH results seen in Figure 35. These results show the pH for the three replications (D, E and F) changing over time. The average pH was 5.38 over the 18 days of sampling. The minimum average pH recorded from the three replications was 4.99, with the maximum average pH recorded being 5.74 on day 17. The pH probes were correctly calibrated at the start of each day, and rinsed thoroughly between readings.

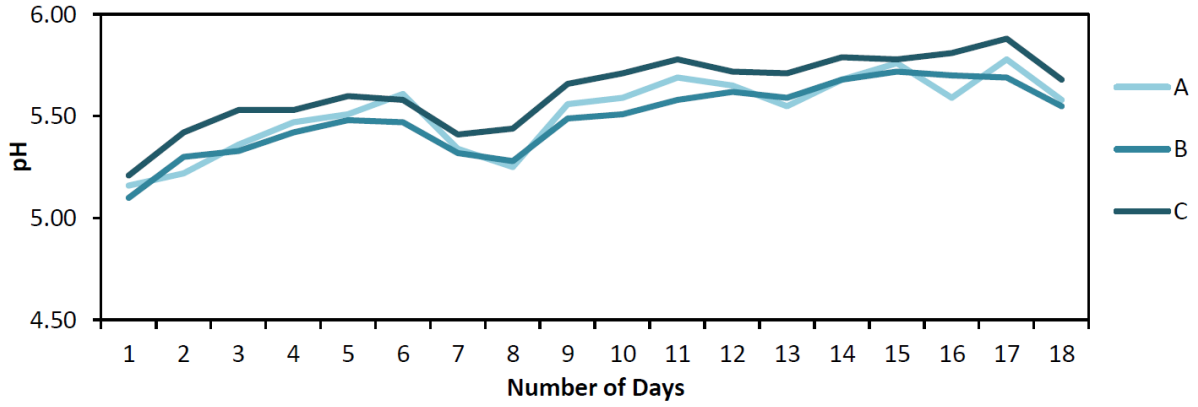

Figure 34: *The results from the leaching experiment using DI water and atacamite soil. A, B and C are replications of the same experiment.*

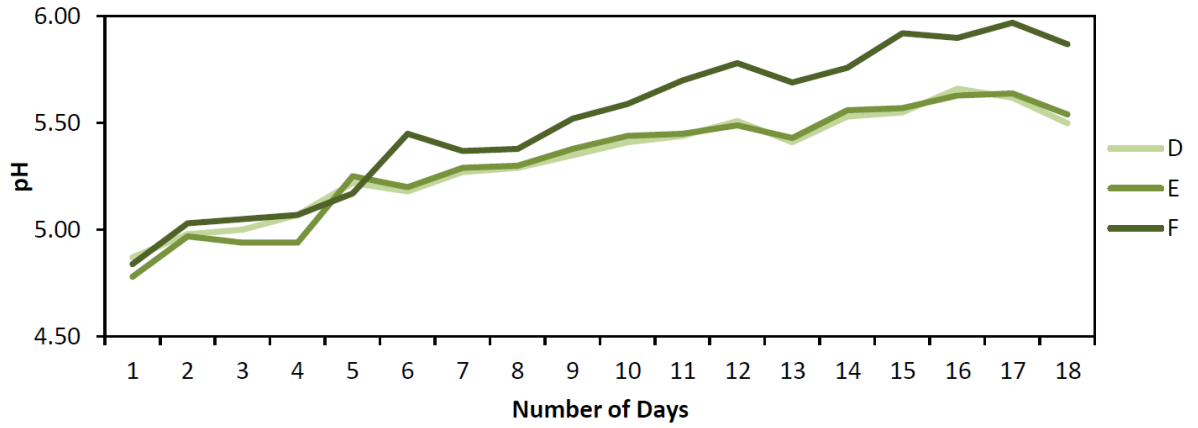

Figure 35: *pH of 0.5M NaCl over time. These are three replication of the same experiment.*

The Cu^{2+} concentration over time (Figure 36) for the leaching experiment using DI water (A, B, and C) shows a linear decrease in Cu^{2+} concentration over time. The concentration on day 1 was on average 95.46 mg/l and on day 17 the average concentration was 40.26 mg/l. That equates to an average decline of 3.24 mg/l over 17 days. The leaching rate decline for the first four days was 6.37 mg/l per day. The last four days (day 13 to day 17) had a leaching rate decline of 2.06 mg/l per day. The experiment using 0.5M NaCl solution to leach through the atacamite soil (D, E, and F) had a different graph. The rate of Cu^{2+} leaching decline was higher at the start and gradually slowed down to average the experiment using DI water. The amount of Cu^{2+} leached into solution on day 1 was higher at 153.76 mg/l as an average, and by day 17 the average was down to 12.76 mg/l.

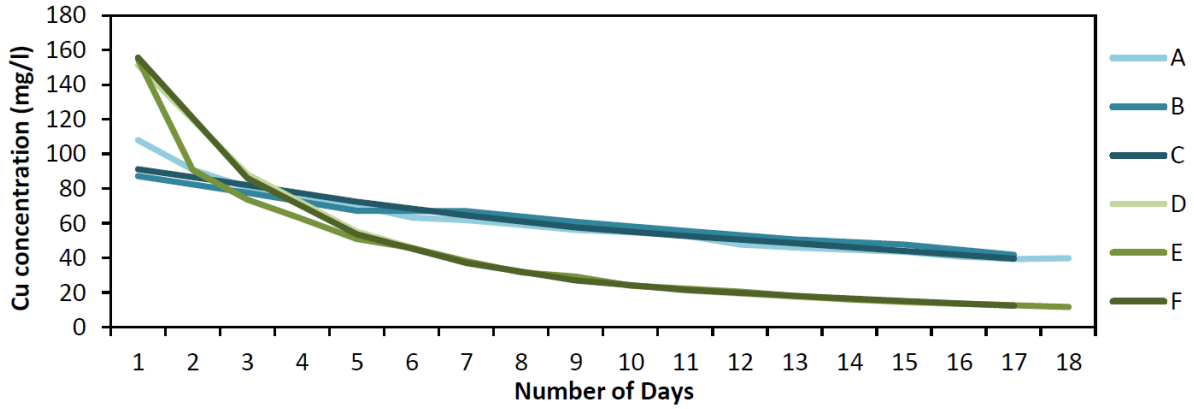

Figure 36: *Copper concentration results for the leaching experiment using DI Water (A, B, C) and 0.5M NaCl solution (D, E, F).*

3.3.2. Titration Experiment

A titration experiment was performed to understand the mobility of copper under various conditions. The first experiment used synthetic atacamite with a 0.5M NaCl solution, and a DI water solution. Three replications for each condition were used. The solutions were dropped to a pH of 4.5 for all the experiments.

The first experiment shows a high leaching rate of Cu^{2+} in the beginning, which then slows down as time continues. Run 1 has a slight dip in the graph, but the general trend is still noticeable. The reason for using the 0.5M NaCl solution was to help in recreating the highly saline conditions found in the area. The second experiment tends to plot a more linear line with a fairly constant rate of Cu^{2+} dissolution over the 1200 second time period. The reason for using DI water was to recreate flooding events, where the soil is flushed with high volumes of rain water. Plotting both the data sets against each other (Figure 37) shows how much higher the dissolution of Cu^{2+} is in DI water as opposed to 0.5M NaCl solution.

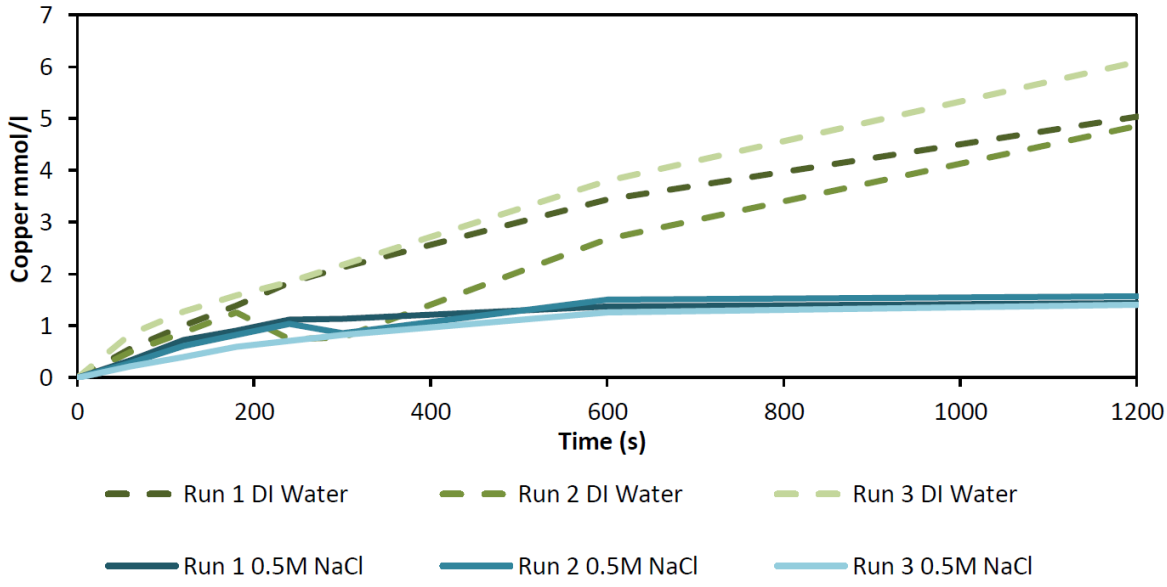

Figure 37: *The results of the titration experiment using DI water and 0.5M NaCl as the analyte at a pH of 4.5. The runs using DI water are dashed, while the runs using 0.5M NaCl are solid lines. The titrant used was 0.5M H_2SO_4.*

This experiment was repeated once again using atacamite soil in place of synthetic atacamite. The soil was found close to the Spektakel mine in the study area. The acid used in the titration experiment using atacamite soil was 1M HNO_3, with the pH remaining 4.5. Three replications were done once again using DI water, 0.5M NaCl and 1M NaCl. These results can be seen in Figure 38. Once again the DI water solution (Run 1-3) leached out more $Cu^{2+}$from the soil than both the 0.5M (Run 7-9) and 1M (Run 4-6) NaCl solutions. The rate of these reactions was also higher at the start.

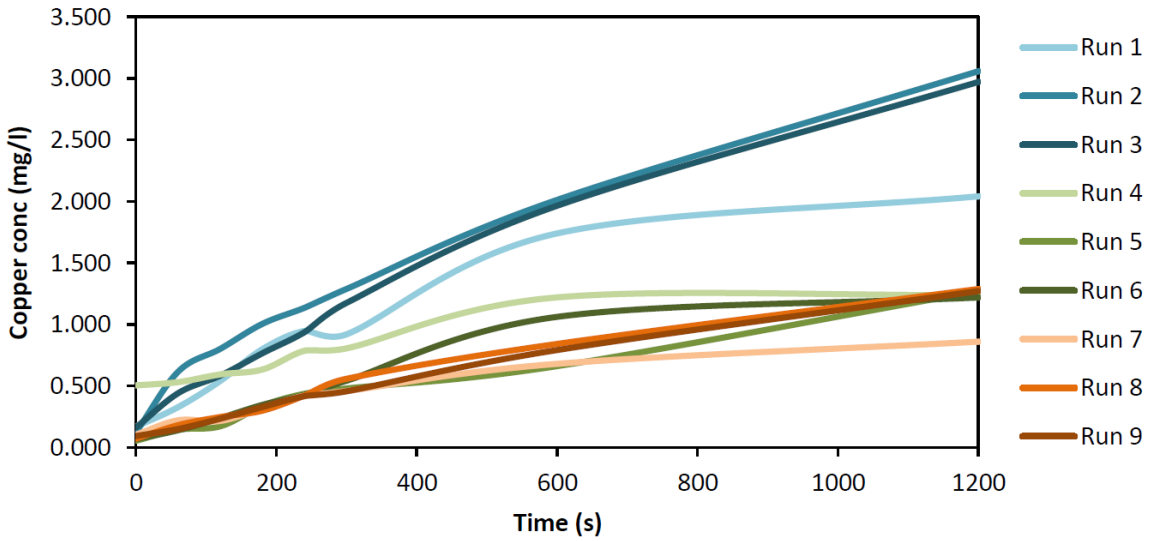

Figure 38: *Graph showing the results from the atacamite soil titration at a pH of 4.5, and an acid solution of 1M HNO_3. Using DI water, 0.5M NaCl and 1M NaCl solutions. Run 1-3 was done using DI Water. Run 4-5 was done using 1M NaCl. Run 7-9 was done using 1M NaCl.*

3.3.3. Atacamite Reaction Rate

Reaction rates were calculated using the graphs plotted from the titration experiments using synthetic atacamite (Figure 39 and Figure 40). The first couple of sample points for each run were used to determine an average gradient (reaction rate) which was then used further. The gradients calculated for each of the synthetic samples was then converted mol.m^{-2}.s^{-1}. This was done using the Brunauer-Emmett-Teller (BET) surface area of 18 m^{2}g^{-1}. Figure 39 highlights the reaction rates of the synthetic atacamite in DI Water. Figure 40 illustrates the reaction rates of the synthetic atacamite in 0.5M NaCl.

The runs done with DI water showed an average reaction rate of 2.43X10^{-08} mol.m^{-2}.s^{-1} (Table 6). The samples run using 0.5M NaCl had an average reaction rate of 1.34X10^{-08} mol.m^{-2}.s^{-1}. This means the initial reaction rates were faster for the samples using DI water as the solution. The reason for calculating the reaction rates was to recreate a flooding event where the sediments would be leached with rain water allowing for $Cu^{2+}$to leach out of the atacamite sediments.

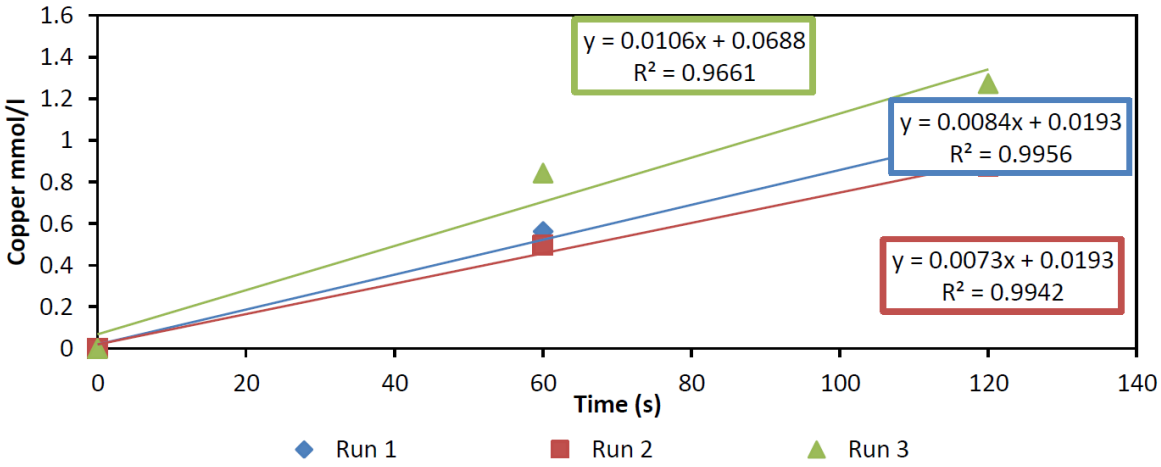

Figure 39: *Calculation of the reaction rate took the first 120 seconds of copper mobility at a pH of 4.5. This experiment was done using synthetic atacamite and DI water. The acid used was 0.5M H_2SO_4*

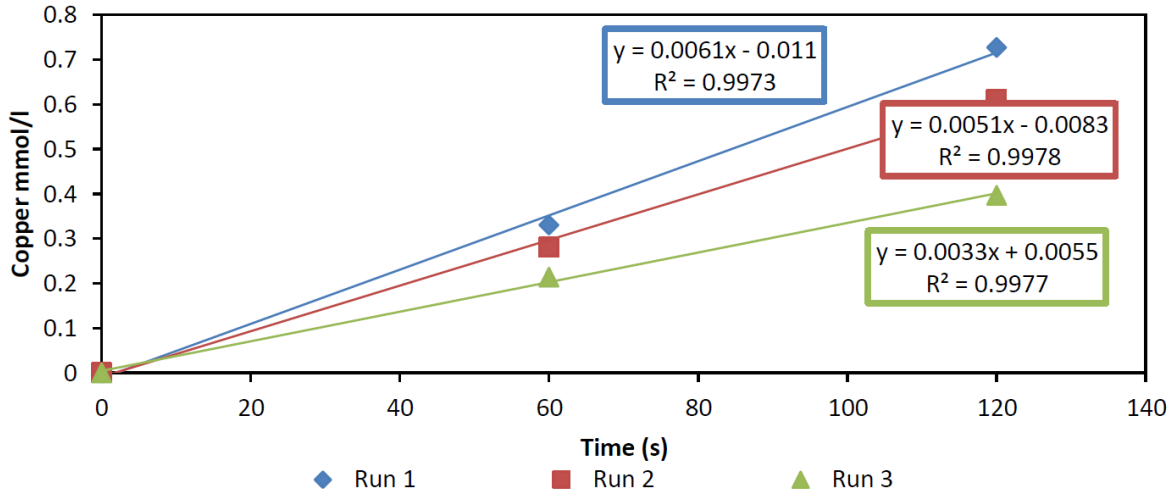

Figure 40: *Calculation of the reaction rate took the first 120 seconds of copper mobility at a pH of 4.5. This experiment was done using synthetic atacamite and 0.5M NaCl solution. The acid used was 0.5M H_2SO_4.*

Table 6: *Calculated reaction rates for synthetic atacamite. These reaction rates were calculated using the rates calculated in figure 38 and 39.*

Synthetic DI Water	mol per m^2 per s
Run 1	2.33333E-08
Run 2	2.02778E-08
Run 3	2.94444E-08
Average	2.43519E-08
Synthetic 0.5M NaCl	
Run 1	1.69444E-08
Run 2	1.41667E-08
Run 3	9.16667E-09
Average	1.34259E-08

4. DISCUSSION

4.1. System Characterisation

4.1.1. Sediments

Grain size analysis on selected sediment samples indicates that the sediments are dominantly sand with only one or two containing a small amount of silt and clay. The mineralogical composition of the sediments is dominated by quartz as well as minor amounts of albite, kaolinite, illite, orthoclase and smectite or chlorite. This mineralogy is consistent with the surrounding geology. As expected, the geochemistry of the sediments is consistent with the mineralogy being dominated by quartz.

The pH of the sediment sample saturated paste extract was relatively neutral, with an average pH of 7.41 (Figure 20).The EC of the sediment samples was however highly variable (Figure 20). In the samples composed of silt and sand, the EC was higher at shallow levels, whereas the opposite was seen in the samples classified as sand where deeper sediment had a higher EC. This is clearly illustrated at Site 45. Clarke et al. (2014) also highlight that EC values found in the Spektakel mine topsoils are high (21-29 mS/cm) and decrease with depth. They suggest that this is due to concentration of salts in the soil surface through near-surface evaporation of pore water.

The $Mg^{2+}$and SO_4^{2-} results also showed an accumulation behind the membrane (Figure 21). Clarke et al (2014) postulate that the source of the Mg^{2+} is the mafic nature of the Spektakel ore body suggesting that elevated Mg^{2+} levels are a mining signature. There was a general trend of elevated Mg^{2+} concentrations in upper sediment samples, and lower concentrations in deeper sediment samples. The same could be said for SO_4^{2-} which is most likely derived from the mining leachate (Clarke et al., 2014). Cu^{2+} and Zn^{2+} concentrations were much lower than expected (Figure 22). The highest Cu^{2+} concentration of 0.30 mg/l was found directly above the membrane. The same site also recorded the highest Zn^{2+} concentrations in the study (Figure 22). The Cu^{2+} concentrations were also only found in surface sediments while Cu^{2+} in the deeper sediments was generally at or below detection limits.

4.1.2. Groundwater

Groundwater samples collected in the field do not exhibit a trend of increasing trace metal and salt concentrations with proximity to the membrane and generally, the pH and EC of the groundwater is similar throughout the study area (Figure 28). However, open bodies of water showed spikes in both trace metal and salt concentrations and particularly in Na^{+} and Cl^{-} (Figure 29). This is not what was originally hypothesised as an accumulation in the groundwater behind the membrane was expected. Likewise, the groundwater samples also did not show concentration spikes in SO_4^{2-} and Mg^{2+} in the way that the sediments did. It was expected that the groundwater would mimic the sediment trace metal and salt accumulation as groundwater may have been the medium by which the trace metals

and salts were transported from the mining areas downstream to the membrane. In particular, Cu^{2+}, Mn^{2+}, and Zn^{2+} in groundwater did not show a systematic accumulation trend with distance from the membrane, but instead had various spikes (Figure 30), but these spikes were not at the same sites each time, and not found consistently in open water bodies. Fe^{2+} had a very interesting trend in the groundwater (Figure 32) as the elevated Fe^{2+} values were recorded close to the membrane, whereas elevated Fe^{2+} in the sediment was found further upstream (Figure 24).

4.2. Source of Trace Metals and Salts

Previous studies have indicated that salinization along the Buffels River is from both dissolution of rock mass and concentration by evaporation (Nakwafila, 2015; Adams, et al., 2004). These studies suggested that there may have also been a contribution of salts derived from mining activities along the river. Salt accumulation in sediments and groundwater is noticeable throughout the valley, and even more so at open water bodies. Figure 41 is a mine waste dam situated 23 km from the membrane and illustrates the salt precipitation surrounding the open water body. The accumulation is through evaporation of the open water source, which is thought to have a higher salt concentration due to the mine in the area.

The trace metals found in the area are thought to be from mining activity in the area, this includes the high SO_4^{2-} and Mg^{2+}. Removing the outlier found at site 54 the average SO_4^{2-} concentration for the area is 563.5 mg/l. The high SO_4^{2-} found in the groundwater could be as a result of the sulphuric acid that is used in the heap leach mining method throughout the Buffels River Valley. The acid used in this process is often recycled rather than treated. The recycled acid is stored in liner dams which are prone to leakage into the surrounding groundwater and sediments over time. The ore being mined also has high SO_4^{2-} as a by-product of leaching pyrite out of mining dumps and into the groundwater.

The high Mg^{2+} levels found in the groundwater are from the Cu^{2+} mining waste waters and materials. Clarke et al. (2014) also highlight the high concentrations of Mg^{2+}, Ni^{2+}, Zn^{2+}, and sulphate found in sediments near the Spektakel mine and are linked to waste products from mining. Al^{3+}, Mg^{2+}, and other gangue minerals are known to be mobilised by the acidic leaching solution (Smith, 2002). Mg^{2+} does not precipitate out of this leaching solution and therefore accumulates over time. Mg^{2+} is therefore a mining signature that is clearly seen in both the sediments and the groundwater at the membrane.

Considering the high amount of Cu^{2+} mined in the area, the Cu^{2+} concentrations were lower than expected. An average of 10.46 ppb was collected for the study area, with a high of 29.39 ppb found at site 23, which is well below the World Health Organisation standard of 2 mg/l Cu^{2+} in drinking water. The low Cu^{2+} concentrations is thought to be due to the pH of the groundwater in the area not allowing the Cu^{2+} to mobilize into the groundwater. Therefore the only way for the Cu^{2+} to mobilise and move downstream to the membrane would be through particulate matter being flushed down river.

Figure 41: *Site 56 was what looked to be a mine waste dam approximately 23 km upstream from the membrane. A high amount of precipitated salt was found surrounding the open water body. The area also had a strong smell to it.*

4.3. Mobilization and Accumulation

The mobility and accumulation of salts and trace metals in the Buffels River Valley was one of the main objectives of this study. Synthetic atacamite and atacamite sediments were used to further understand the mobility of Cu^{2+} into groundwater through solubility experiments. Samples were also gathered near the Kleinzee membrane and analysed for any accumulation and mobility trends. This is discussed further in the section below:

4.3.1. Salinity

The groundwater samples contained consistently less Cl^- and Na^+ than the sediment samples (Figure 42). This appears to be a general case throughout the study are but can be directly compared at sites 44 and 21, where both groundwater and two sediment samples were taken. The sediment samples showed a higher accumulation of salts in the surface sediments compared to the deeper sediments. Unfortunately these were the only two sites that could be studied like this, as samples were collected on morphological differences and not on a fixed depth method.

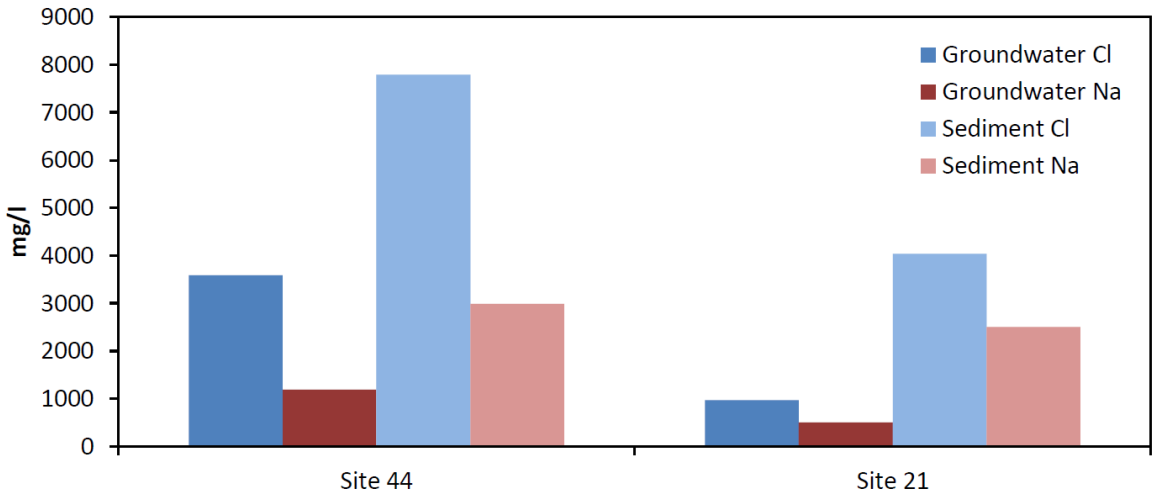

Figure 42: *Graph representing the difference between the groundwater and sediment Na and Cl concentrations from the same sites (44 and 21).*

The results from this show that there is a higher accumulation of NaCl salt in sediments than in the groundwater. The accumulation is expected to be due to evaporative concentration. The upper sediments once saturated with saline groundwater form salt layers which coat the grains as evaporation takes place. When more water is added through groundwater rising or precipitation percolating through, the salt crystals are dissolved. This would be added to the groundwater, increasing the groundwater salinity. Repeated cycles of evaporation and recharge result in concentration of salts in these sediments over time. An additional source of the salts could also be off the ocean which is approximately 5 kilometres from the study area. This would be a small addition to the predominant salinity source from the dissolution of the geology in the area. The study area also experiences very low rainfall which would usually flush the salinity out of the top soil into the lower soils and groundwater, this however does not happen often in the Namaqualand. The low rainfall recorded in the area is mostly light rainfall, which does not penetrate deep into the soil and accentuates the accumulation found in the top soils. Capillary action is also a likely answer to salt moving up the through the sediment column and depositing in the upper sediments. Capillary action allows groundwater to move vertically upwards in sediments with the use of surface tension and adhesive forces. Due to the higher concentrations of salt in the sediments, and the low amount of rainfall, the source of the salts is more likely to be from saline groundwater as opposed to precipitation.

Generally there is no NaCl salt accumulation trend noticeable in the groundwater chemistry behind the membrane. This is interesting, as the sediment samples point to a clear and noticeable accumulation trend. All the sediment samples collected within 800 meters of the membrane have an average Cl^- concentration of 4634 mg/l. The average Na^+ concentration for those sediment samples are 1991.7 mg/l. The samples collected from 1500 meters or further from the membrane have an average concentration of 50.4 mg/l for Cl^- and 37.3 mg/l for Na^+. This could be due to the groundwater

being linked throughout the aquifer, with no noticeable outliers found in the river bed. The salinity is therefore evenly distributed throughout the aquifer with outliers found at site 54 and 56 due to higher evaporative accumulation of the open water bodies.

4.3.2. Trace Metals

a. Groundwater

As previously discussed by Acosta et al. (2011) saline groundwater aids in the mobilisation of trace metals and this can be seen in the Buffels River Valley where the salts have aided in the mobilization and accumulation of trace metals. The membrane found upstream form Kleinzee was thought to be accumulating trace metals in the form of Mg^{2+}, Mn^{2+}, Fe^{2+}, Cr^{2+}, Cu^{2+} and Zn^{2+} in the sediments and groundwater. All are known contributors from mining processing and waste (Smith, 2002; Clarke, et al., 2014).

The idea of accumulation of trace metals behind the membrane was not seen in the groundwater results. The results showed a consistent concentration of trace metals in the groundwater within the river bed. This was excluding the two spikes at site 54 and 56 which were open water bodies with high concentrations of trace metals. Pb^{2+} concentrations were stable throughout the study area with an average of 0.2 ppb. Cr^{2+} and Se were not found throughout the study area as some were below detection limits, but the concentrations that were found were low. Fe^{2+} found in the groundwater within the river bed showed a possible accumulation trend. When plotted against the position of the membrane, the following results were found (Figure 32). A spike at site 48 and 49 could possibly be seen as an accumulation of Fe^{2+} in the groundwater. Whether or not this is linked to the membrane, is not certain. The source of Fe^{2+} in this location only could be due to contamination or pollution within this location.

Co^{2+}, V, and As^{3+} in the groundwater samples showed no accumulation trend. The concentrations were low, with no spikes throughout all the samples taken. Ni^{2+} was also very consistent, but showed a spike at site 23. Cu^{2+} was also very consistent, and the concentrations found in the groundwater were far less than expected. The Cu^{2+} did display higher concentrations at site 22 and site 23, but due to the generally low concentrations these recorded values are not seen as a true accumulation of trace metals in the groundwater. Generally the Mg^{2+} concentrations found for the groundwater were consistent and showed little to no correlation to an accumulation trend (Figure 29). The salinity curve for groundwater does however have a link to some of the trace metals found in the groundwater. Comparing the Mg^{2+} to Cl^- this can clearly be seen with a R^2 value of 0.81.

Unfortunately no groundwater samples were collected downstream of the membrane. It would have been an interesting comparison to do against the groundwater found upstream of the membrane. The

groundwater samples collected could have also been in the wrong location within the river bed. A variation across the river bed is highly likely as the groundwater could be flowing in a different manner to that seen on the surface water.

b. Sediments

The results from the saturated paste extract which were done on the sediment samples show an accumulation trend which the groundwater was lacking. The sediment samples generally showed a higher concentration in trace metals, with an accumulation trend (Figure 42). Site 38 and site 36 were both sediment samples taken below the membrane. An accumulation trend can be seen for both Mg^{2+} (Figure 29) and Mn^{2+}, with concentrations gradually decreasing as the samples are further away from the membrane. The high concentrations found downstream from the membrane could be due to over flow and movement of sediment and groundwater in flooding events. The sediment could possibly be moving downstream of the membrane due to flooding events moving the surface sediments but this would require flowing surface water. Alternately possible overflow of the membrane dam would allow for the groundwater to move over the top of the membrane and reach the top sediments downstream of the membrane. This over time could allow for the movement of trace metals to below the membrane. The highest concentrations would be found at the surface sediments. The membrane could also potentially be perished in certain areas allowing for a flow of groundwater to move below the membrane and deposit trace metals.

Sediment Fe^{2+} concentrations are not consistent with those in the groundwater (Figure 24). Appreciable Fe^{2+} was only found approximately 2 km upstream from the membrane, from site 26 to site 9, with a spike at site 12. The water chemistry did not show a spike of Fe^{2+} at site 12 and the only appreciable Fe^{2+} in the groundwater was close to the membrane (Figure 32). Farming equipment, or any other possible iron source left in the river bed would be a reasonable explanation for the Fe^{2+} found in the sediments. The possibility of localised contamination of the sediments being linked to the groundwater accumulation of Fe^{2+} in the groundwater would be a great result, however Fe^{2+} does not mobilise as it prefers to precipitate and oxidise. The source of these spikes is therefore unknown and beyond the scope of this study.

Cu^{2+} and Zn^{2+} concentrations in the sediments did not show any accumulation trend, and the Cu^{2+} concentration was much lower than originally hypothesised (Figure 22). Higher concentrations of Cu^{2+} were expected for the sediments and groundwater due to the current and historical Cu^{2+} mining activity in the drainage basin. The historical mining was expected to play a role in the Cu^{2+} concentrations due to the old mining practices and the lack of environmental awareness at the time. Low Cu^{2+} concentrations could be due to the stable pH of the groundwater, a possible drop in pH could potentially allow for more Cu^{2+} mobility in groundwater. The source of the Cu^{2+} would be from mined

ore, such as that found at Spektakel mine. The Zn^{2+} concentrations in the sediment samples were mostly below detection limits; only three sites had recorded values (Figure 22). This was not enough to establish any true findings.

Grain size is known to play an important role in the adsorption of metals and in particular finer-grained clays are more likely to contain heavy metals (Minkina et. al., 2011). Higher concentrations found in this study also correspond to the finer grained sediments closer to the membrane. The sites that were separated into different samples due to morphological differences had higher concentrations of trace metals in the upper clay and silt fraction than the lower sand sediments.

4.3.3. Copper Mobilization

The experiments using atacamite in both its natural sediment form, and a synthetic form gave some interesting results. The reason for doing these experiments was due to the low concentration of Cu^{2+} in the groundwater and sediments close to the membrane. Knowing that there was a source of Cu^{2+} contamination up river in the form of copper mines, made the lack of Cu^{2+} at the membrane a concern. The atacamite experiments were used to help determine the worst case scenario for Cu^{2+} to be mobilised from an upstream source down the drainage basin. The leaching experiment used atacamite sediment collected from the Spektakel mine, which had various solutions leached through a column of soil over 18 days. The titration experiment used both the atacamite sediment from the Buffels River Valley and synthetic atacamite.

The leaching results using DI Water (A, B and C) showed a relatively consistent release of copper over time (Figure 36). The Cu^{2+} release over the first four days was higher from the 0.5M NaCl, but the Cu^{2+} release from DI water exceeded the Cu^{2+} release from the salt solution from the fourth day onwards. The experiment using 0.5M NaCl had a high rate of Cu^{2+} release for the first four days, but that subsequently slowed down to be below the Cu^{2+} release of the DI water experiment. This suggests that the initial Cu^{2+} released in the NaCl solution could represent an exchangeable Cu^{2+} phase, which releases large amounts of Cu^{2+} in the first few leaching cycles. After the first few leaching cycles the rate returns to something similar to the experiment done using DI water. This therefore suggests that after the removal of the labile exchangeable phase, the atacamite equilibrium starts to control the amount of Cu^{2+} released. A study done by Woods and Garrels (1986) shows that equilibrium reaction involving Cu^{2+} hydroxyl minerals happen quickly. The initial Cu^{2+} release from exchangeable phase could possibly explain the lower pH we see in the equilibrium experiment as a result of Cu^{2+} hydrolysis reactions.

The idea behind the leaching experiments was to recreate conditions of Cu^{2+} release found in the area during a large rainfall event. The added solutions only saturated the soils, and the high concentration of Cu^{2+} release initially in the NaCl solution indicates that if a spike of laden water is likely to move

through the soil profile at the onset of a rainfall event, Cu^{2+} mobilisation is likely to decrease as a rain event continues. However a sustained release of Cu^{2+} will happen as atacamite dissolves and the more the soil solution is diluted the higher the sustained release of Cu^{2+} will be. The Cu^{2+} released over the 18 day period was 732.5 mg/l for the 0.5M NaCl solution and 1073.9 mg/l for the DI water solution.

The atacamite titration experiment was done to calculate the dissolution kinetics. These kinetics would include the effects of pH, salt concentration and acid type. The following equation is the atacamite dissolution in an acid medium:

$$Cu_2(OH)_3Cl + 3H^+ \rightleftharpoons 2Cu^{2+} + Cl^- + 3H_2O$$

The results from the synthetic atacamite showed that atacamite has a higher dissolution rate in DI water in comparison to 0.5M NaCl solution at a pH of 4.5. The same can be seen with the results using atacamite soil.

It is thought that with a lower pH there would be a higher mobility of copper from the surrounding mines into the river bed. This drop in pH could be sourced through acid mine drainage in the area from surrounding mines. The Namaqualand region is well known for historic mining, which has left abandoned mines throughout the area which have not been correctly closed and rehabilitated. The acidic condition in the area could be sourced from sulphide minerals in the area interacting with the atmosphere and groundwater. Another source could be acid which is used to remove Cu^{2+} from the mined ore for further processing. This acid is usually kept in large dams, which could potentially leak into the groundwater causing a substantial drop in the pH of the groundwater. Currently mines use boreholes situated around these acid storage dams to help in determining if there is a leak into the surrounding groundwater. Accurate and frequent monitoring of these boreholes is uncertain though.

4.4. Environmental implications

The following section discusses the environmental implications the groundwater would have on farming and local inhabitants in the area. Water quality, climate change and the role of the membrane as a possible barrier to control pollution are discussed below.

4.4.1. Water Quality

Farming issues due to soil salinity include problems with growing crops, and water quality for livestock to list a few. The study area being looked at included a farm which had sheep and cattle. The animals were able to graze on the long grasses and reeds found near the membrane, but the sparse vegetation in other areas found in the Buffels River valley are an issue for farming. Farmers and locals are unable to use the groundwater as a source of clean drinking water due to the high salinity. Water is currently being pumped from the Orange River to help dilute the saline groundwater being pumped out of the aquifers in the basin.

The groundwater samples that were collected in the field had a pH that was in accordance to the World Health Organisation (WHO) standard of 6.5-8.5 for drinking water. All the samples collected fell within this bracket. Acid mine drainage is a way in which this pH value can change over time. Acid mine drainage is caused by groundwater coming into contact with sulphide rich minerals which then allow for sulphuric acid to form. This acid makes its way into surrounding groundwater and causes a drop in the pH. Leakage of acid from mining in the area, or abandoned mines with lack of rehabilitation is another way for acid to be added to the groundwater system.

The Environmental Protection Agency (EPA) which regulates public water supply allows for a maximum contamination level of 500 ppm, and considers anything above 1000 ppm to be unfit for human consumption. These are secondary standards that do not present an issue to human health, but are instead for aesthetic considerations such as taste, colour and odour. The groundwater sampled in the study area had an average TDS of 3811 mg/l, with the maximum being found at sample site 54 (10263 mg/l), and the minimum found at sample site 22 (1586 mg/l). This groundwater source would fail the EPA secondary standards for TDS content in suitable drinking water. TDS is the measure of dissolved substances in the groundwater source (Figure 33). As previously discussed the groundwater found in the study area contains high concentrations of various ions. Pristine lakes and freshwater rivers often have a TDS of 10 to 200 mg/l. The average TDS found in the lower reaches of the Buffels River are more than three times that of the drinking water limit for California according to the EPA (EPA, 2007). The alkalinity showed a similar trend to the TDS results (Figure 31). However one of the notable differences was the high alkalinity of site 51 over site 54. It was the opposite for the TDS results. The spikes at site 51, 54 and 56 are however similar to the TDS and salinity results for the groundwater.

Cl^- and Na^+ are indicators for salts in the groundwater, NaCl salt is derived from the evaporation and concentration of the already saline water found in the area. There was a high spike found at site 54, which was a dam alongside the actual river cutting. The dam was man made, which was 45 meters long, 15 meters wide, and approximately 1 meter deep in the deepest part. The high spike recorded could be due to a concentration effect caused by an evaporation of the surface water increasing the salt remaining in the water body found at site 54. The other spike recorded was at site 56 which was at a slimes dam 23km upstream from the study area (Figure 41). This dam was used to store what looked like mine waste water. The dam was surrounded by extremely salty soil, which had salt crystallising on the ground surface surrounding the dam. Unfortunately a groundwater sample was not taken in the area, however Nakwafila (2015) collected groundwater samples from the area and recorded values between (11216-14588 mg/l) Cl.

A guideline of 200mg/l for Na^+ was set by WHO; the sodium found in the study area is far higher than this standard. The average concentration for Na^+ in the area was 1131.72 mg/l, with the lowest being

467.8 mg/l found at site 22 and the highest being 3796 mg/l found at site 54 (Figure 29). These numbers are all above the acceptable standards set by WHO for drinking water. SO_4^{2-} and Mg^{2+} plots also showed and accumulation trend similar to the Na^+ and Cl^-. There were spikes for site 54 and site 56, which were not entirely part of the river system, but would have played a role in the water chemistry found in the study area. According the WHO, the maximum amount of SO_4^{2-} in clean drinking water should be 250 mg/l, and Mg^{2+} should be no more than 30 mg/l if there is 250 mg/l of sulphate. If there is less SO_4^{2-} , Mg^{2+} up to 125 mg/l may be allowed. For the groundwater samples collected the SO_4^{2-} had an average of 563.41 mg/l, this was excluding the two spikes at site 54 and 56. The Mg^{2+} concentration for the area had an average of 210.82 mg/l; this is once again excluding the spikes found at site 54 and 56. These are both well above the standards set by the WHO.

The Fe^{2+} amount found in the groundwater was also above the WHO standards for drinking water for sample sites 48 and 49. The WHO standard for drinking water 0.1 mg/l, this is predominantly due to the taste of the water. The groundwater samples at site 48 and site 49 recorded 0.9 mg/l and 0.7 mg/l respectively. The other sites sampled were below the standard of 0.1 mg/l.

Possible health implications due high salinity and trace metal contamination of the groundwater which is likely being used as drinking water would include high blood pressure, stomach cancer, and edema (fluid retention). Strokes and cardiovascular disease are also known health issues associated with high salt intake. Drinking water with a high concentration of trace metals is known to have adverse effects on health such as shortness in breath and several types of cancer. Cu^{2+} and Mn^{2+} in drinking water are known to cause mental health issues such as Alzheimers. High Mn^{2+} concentrations are also known to have adverse effects on children's intellectual functions at a young age. Ni-sulphate and Ni-Chloride as previously discussed is known for being linked to cardiac arrest.

4.4.2. Chemical Transport to Oceans

Rivers are one of the main mechanisms by which chemical components are transported to the ocean system and are a way of regulating the chemical composition of the ocean. Ocean pollution due to inland activities is currently a large global problem, especially for rapidly growing countries (Daoji & Daler, 2004). The annual river water discharge to the ocean system is estimated to be about 37400 km^3, which is $2.7X10^{-3}$% of the total volume of ocean water. It is estimated that river water carries approximately $4X10^{15}$ g of dissolved salts into the oceans each year (Martin & Whitfield, 1983).

Coastal waters receive a variety of land-based water pollutants, ranging from petroleum wastes to pesticides to excess sediments. Mining for materials such as copper and gold is a major source of contamination in the ocean (Martin & Whitfield, 1983). Copper is a major pollutant, which is toxic in the ocean and can interfere with the life cycles of numerous marine organisms and life. Excessive nutrients from fertilizers which contain nitrogen, phosphorus and trace elements also flow into oceans

from surface run off. Issues associated with fertilizers allow for algae to bloom. When they sink and die their decomposition uses oxygen in the lower ocean waters. This effects seagrass beds, coral, and other life forms in the deeper ocean water.

Currently the Buffels River has no system in place to monitor the quality of water flowing out into the ocean at Kleinzee. The membrane put in place has the potential to aid in monitoring and possibly controlling the water being discharged into the ocean. Contamination flowing downstream in the groundwater or as particulate could potentially be accumulated behind the membrane allowing for easier treatment and remediation. The groundwater within the valley is known for high salt content and possible animal waste from farming in the area could also be transported into the ocean at Kleinzee. Flooding events within the Buffels River could also be controlled by the vegetation growth found at the membrane. The vegetation plays a role in slowing down surface water to a speed where potentially polluted sediment is able to be deposited. This could then be remediated at a later stage.

4.4.3. Climate Change

Numerous climate change models (Figure 43) predict that precipitation will decline throughout large parts of south western Africa (Hulme, et al., 2001; Jury, 2013; Fauchereau, et al., 2003; Arblaster, et al., 2007). Lower rainfall and possibly increased temperatures would lead to higher evaporation rates (Fauchereau, et al., 2003). Higher evaporation rates would in turn lead to more accumulation of salinity and trace metals in the sediments above the membrane, as well as throughout the river bed. A model by Hulme et al. (2001) has highlighted possible temperature increases in Africa until 2080. This study has taken greenhouse gas induced climate change into account and modelled for four scenarios based on the severity of global mean temperature increases according to climate sensitivity. The predicted change in mean temperatures for the maximum scenario can be seen in Figure 44. The left panel shows a mean annual temperature change for the 2020s, 2050s and 2080s (with respect to 1961–90) for the highest scenario. These were modelled using a predicted temperature change and climate sensitivity. A high change in temperatures is noticeable in southern Africa, with climate change models also predicting an increase in extreme rainfall events which would lead to flooding conditions in places like the Buffels River Valley. Flooding events would allow for a higher mobilisation of trace metals and salinity down the Buffels River. This is what the atacamite experiments were looking at. The leaching of saline and DI water through atacamite soil showed that DI water leaching through copper-rich soil allowed for more copper mobilisation over a longer period of time in comparison to saline solution. The membrane would therefore allow for higher accumulation of trace metals and salinity in the top sediments as the salts and heavy metals are moved downstream in groundwater and sediment transportation. Extreme rainfall events would lead to an increase in the amount Cu being dissolved into the groundwater, the copper rich groundwater would then have the ability to move down stream and contaminate sediments and groundwater further downstream.

Continuous monitoring of rainfall and drought events would be needed to determine the absolute effects of climate change on the Buffels River Valley. Groundwater monitoring would also need to be put in place to monitor the groundwater being used by the town of Kleinzee to confirm that it is potable. Groundwater pH changes, as previously discussed, could allow for higher mobilisation of copper downstream. Flooding events would also need to be prepared for. Large volumes of water flowing down the Buffels River could cause damage to various infrastructure and collecting the possible future flood water could be looked into.

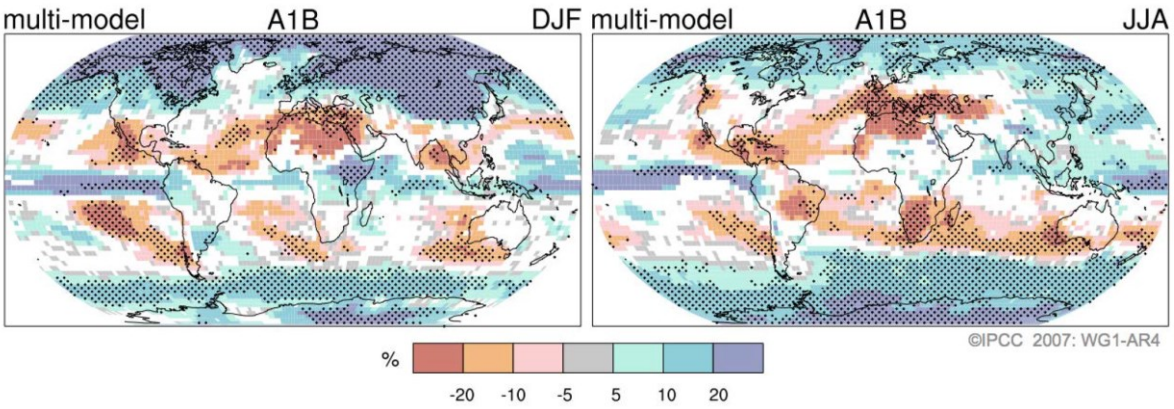

Figure 43: *Predicted global precipitation changes from current scenario to 2090* (Arblaster, et al., 2007)*. On the left is the model showing the predicted rainfall change over December, January, and February. The image on the right is the predicted change in rainfall over June, July and August.*

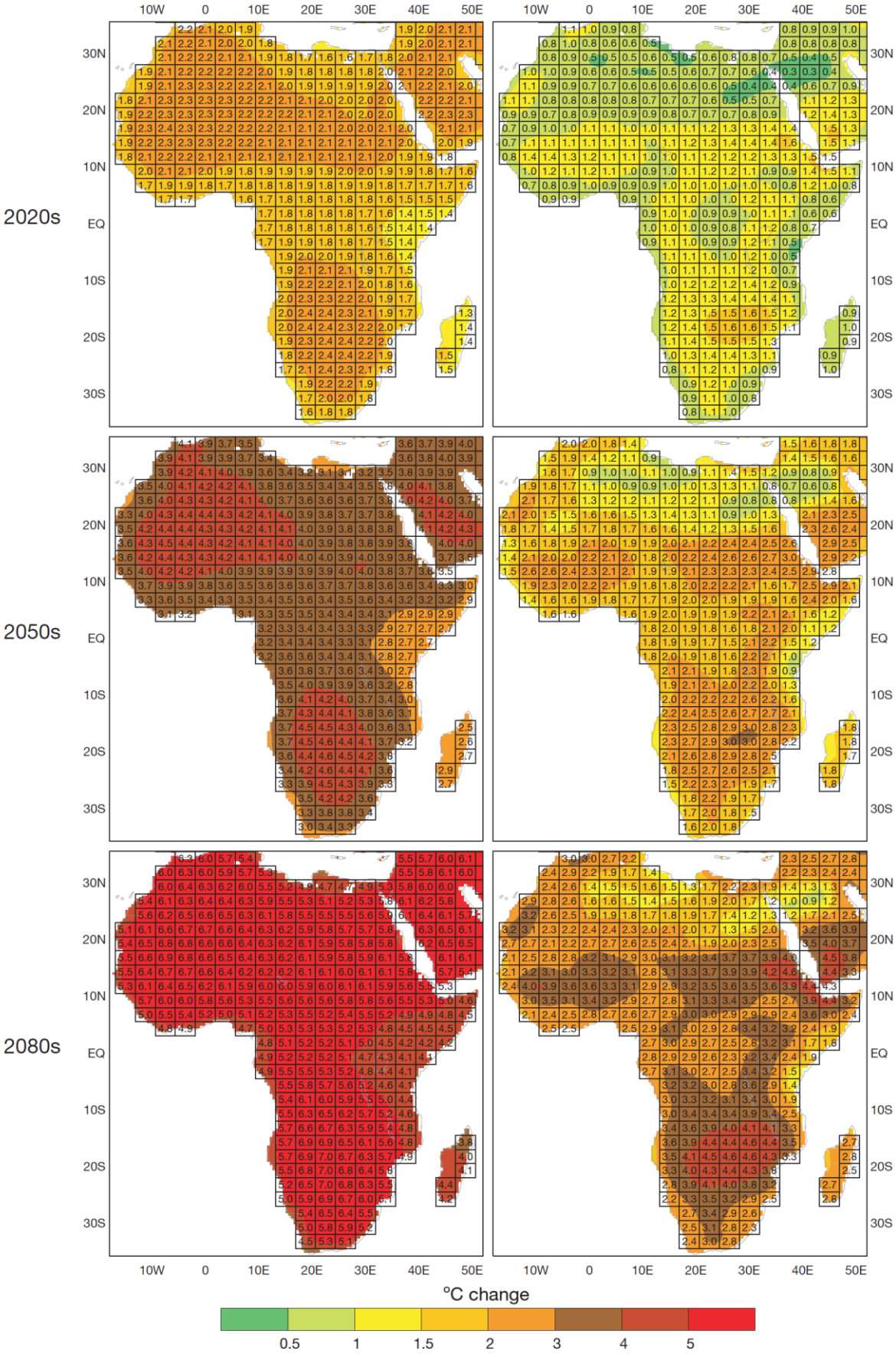

Figure 44: *Left panels: change in mean annual temperature for the 2020s, 2050s and 2080s (with respect to 1961–90) for the high scenario. Right panels: inter-model range in mean annual temperature change* (Hulme, et al., 2001).

4.5. The Way Forward

If left to continue in the current state, groundwater salinization within the Buffels River valley may continue to increase and as a consequence restrict the availability of potable water even further in the region. This is particularly a problem because the lack of access to potable water will depress development opportunities and these are needed to provide mechanism of social uplift. The three areas that need to be addressed in this respect are remediation, management and requirements for ongoing research.

4.5.1. Remediation

Groundwater remediation is a difficult process in arid environments. Usually a dilution method is used to dilute and flush the soils and aquifer of salts and other contaminants. However in an area with low rainfall and a small population most rehabilitation methods are too expensive to put in place. Reverse osmosis is a well-known water purification method that uses a semipermeable membrane to remove larger particles from water. For the process to work a high amount of pressure is used to overcome osmotic pressure. The practice can remove bacteria, and salinity from groundwater sources making them suitable for human consumption.

The issue with reverse osmosis is that it requires a large amount of electricity, which drives up the cost per litre of potable water produced. This is excluding the costs of building a plant and equipping it for the purification process. In poor and rural communities this is not a viable option; however it is currently being used further up the coast in Namibia, which experiences the same difficulties with water quality and quantities. The presence of certain compounds such as manganese, iron, nitrates and fluorides also need to be monitored as these can bump up production costs. Currently operating and capital costs of reverse osmosis are dropping as the technology becomes cheaper and more efficient. According to Swartz et al. (2006) reverse osmosis is becoming a more attractive option for coastal towns to supplement their drinking water. Groundwater standards would need to be maintained at their current level, or possibly flushed to try and remove the salinity from the soils and groundwater currently found in the drainage basin. This is also not a viable option.

Currently groundwater sourced in the Buffels River is being diluted by water piped from the Orange River. This is a solution to dilute the highly saline groundwater found in the area to make it potable. This is not a solution to the groundwater issues, but is a solution to availability of potable water. Over pumping of boreholes in the area will further hinder the availability of non-saline groundwater as ocean water intrusion is a highly probable event in the area.

4.5.2. Management

Groundwater management is an important factor for any groundwater source and this becomes more important when dealing with an arid to semi-arid region. The Buffels River Valley receives very little rainfall which is lower towards coastal towns like Kleinzee. Kleinzee needs to monitor the groundwater sourced from the membrane as often as possible for basic chemical signatures such as EC and pH. Chemical analysis should also be done on the groundwater source as often as possible. The high possibility of the accumulation of pollutants in the groundwater is something that needs to be considered and understood. The current situation behind the membrane is conducive to the accumulation of trace metals and salinity in sediments behind the membrane and this should be a worry for Kleinzee which use the groundwater as a potable water source.

Further pollution of the groundwater source would increase costs associated with cleaning the water. It would also increase the reliance on the Orange River water which is pumped to the town to dilute the membrane water. Monitoring and controlling the amount of groundwater being pumped out of boreholes by farmers in the area will aid in assessing the possibility of ocean water intrusion into the aquifer. Ocean water intrusion would hinder progress going forward in rehabilitating or maintaining the groundwater currently found in the area.

A possible management plan for the area would be to use the current Fehlmann well and additional shallow wells that would need to be put in place upstream and downstream of the membrane (Figure 45). The wells put in place downstream would need to be deep enough to interact with the groundwater. These wells will only be used as monitoring wells to assess the levels and chemical signatures of the groundwater. Simple chemical signatures such as pH and EC would be enough to determine whether further analysis would be needed. Further analysis would include cation and anion analysis to monitor the concentrations found in the groundwater source. Open water bodies should be covered to avoid further concentration through evaporation. This is a simple way to protect the water source as well as protect the surrounding groundwater which the dammed up underground water could have possible interaction with.

This proposed management plan would start off by monitoring the groundwater above and below the membrane but future data could be used to help with a remediation plan. Deterioration of the current groundwater would put stress on the supplied water from the Orange River pipeline. A larger amount of the Orange River water would need to be used to help in the dilution of the saline Buffels River water.

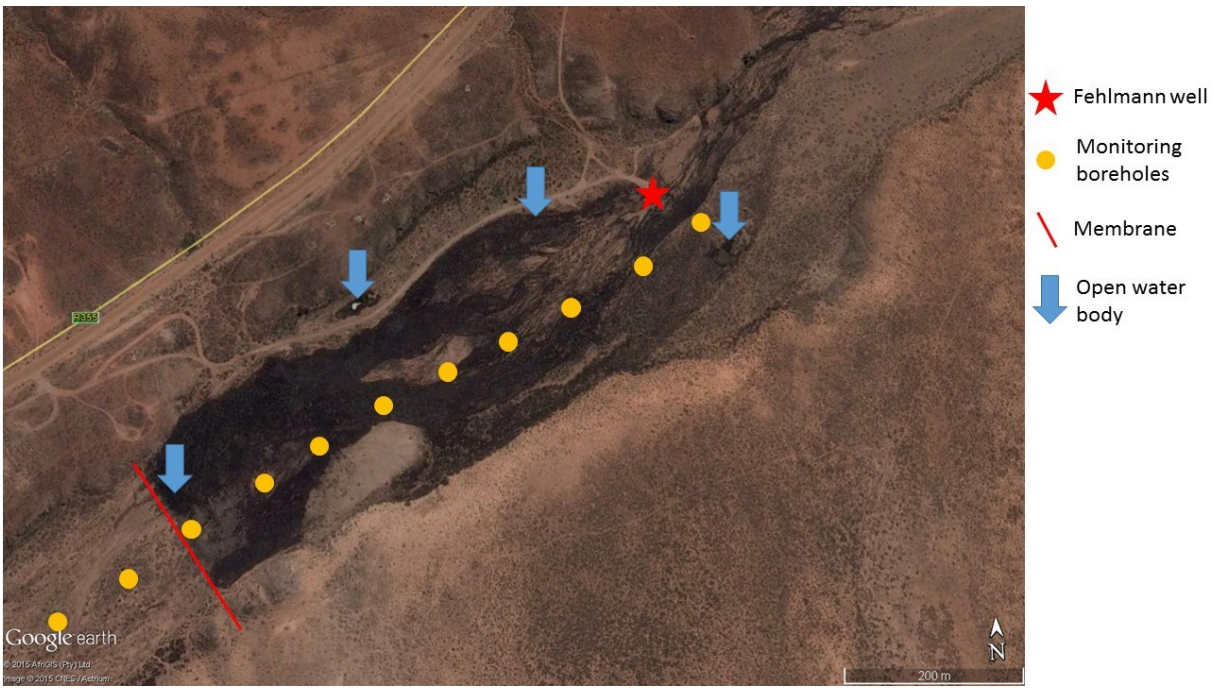

Figure 45: *Proposed management plan for the groundwater stored behind the membrane.*

5. CONCLUSION

5.1. General Conclusion

Groundwater quality is a major issue throughout Namaqualand, with high salt loads and trace metal accumulation being found within the Buffels River Valley groundwater and sediments. One of this studies aims was to characterize the nature and spatial distribution of the sediments above and below the membrane. The results showed that the grainsize was similar throughout the study area near the membrane installed outside of Kleinzee. Finer grained sediments in the form of silt and clay were found near the membrane and have most likely been deposited due to the vegetation found at the membrane. Grasses and reeds have grown due to the abundance of groundwater which is being dammed up by the underground membrane. The finer sediments were only found in the surface sediments while the deeper sediments consisted of predominantly sand.

The second aim of this research was to characterize the nature and distribution of salts in the Buffels River Valley looked at the distribution of the salinity in the sediments and groundwater. A salt accumulation trend was found in the sediments surrounding the membrane which could be linked to various concentration methods of salinity in sediments. High concentrations of Na^+ and Cl^- were found in dams in the Buffels River Valley. These dams have an ability to concentrate various salts and trace metals due to being more prone concentration via evaporation. The groundwater samples collected from the study area showed no true accumulation trend, but did show some smaller trends. The groundwater sampled was also compared to World Health Organization standards and failed due to various concentrations being over the prescribed standards for drinking water.

The third aim and objective was to characterize the nature and distribution of trace metals within the Buffels River upstream and downstream of the membrane. Unfortunately no groundwater was able to be sampled below the membrane, and only 6 sediment samples were taken. The groundwater and sediment data sampled, highlighted two varied results once again with the sediments showing an accumulation trend, and the groundwater only showing spikes at open water bodies. The trends were similar to the salinity trends for groundwater and sediments, which means the salinity concentrations and trace metal concentrations have a correlation. Generally the sediments showed a higher accumulation in the upper sediments near the membrane. The source of the trace metals are most likely due to mining in the area, as all the major trace metals found are linked to copper leach mining. This is confirmed by the work done by Clarke et al. (2014). The copper concentration in the groundwater and sediments was surprisingly lower than expected.

The last aim and objective looked at determining the mechanism(s) by which the trace metals are transported in the Buffels River Valley. Determining this is difficult, but the main transport mechanism

thought to be used was as dissolved ions within the groundwater. The study area does not experience much rain, and flooding happens too infrequently to be considered as the main transport mechanism of trace metal rich sediments. The membrane plays an important role in accumulation of salts and trace metals within the Buffels River, and there is a definite accumulation in the sediments which is most likely due to evaporation and concentration of trace metals and salinity from groundwater sources. Atacamite experiments were used to help determine the mobility of copper in groundwater. Two experiments were used, one being a leaching experiment and the other using the autotitrator. The results showed that copper is highly mobile in low pH conditions and the release of copper in DI water showed a larger amount of copper mobilization over time than that of saline solution. The copper is therefore stored further upstream as atacamite, which has not met the correct conditions for mobilizing through the groundwater.

To conclude, climate change would affect the area in a negative way. Climate predictions show a possible trend for higher temperatures, with lower rainfall. This would promote evaporation and evapotranspiration which in turn would increase the concentrating of trace metals and salinity found in the sediments. Extreme flooding events are also predicted to increase for the area, and this would flush sediments from areas of high trace metals contamination down the Buffels River, further polluting the groundwater source collected at the Kleinzee membrane. Rehabilitation is possible, but would be an expensive solution to the groundwater issues. Costs per litre of water would increase and the communities in the area would struggle to afford it. The current situation of bringing in water from the Orange River is the most cost effective and easiest solution. Groundwater monitoring would still need to be done in the area to maintain a good record and create a baseline for monitoring of possible further changes in groundwater and sediment concentrations of salinity and trace metals.

5.2. Recommendation for Future Work

Due to the results from this study, it can be seen that future work at the Buffels River membrane could include a more detailed geochemical map of the sediments and groundwater. This should potentially include samples moving across the river bed looking for possible changes in water and sediment chemistry. The groundwater variation in this study was predominantly done moving upstream from the membrane. After sampling, Owen Smith highlighted that while building the membrane two different veins of water were noticed. One very palatable, sweet water. And the other extremely saline. There is therefore a high probability that the groundwater would have different chemical signature on the northern bank and the southern bank near the membrane. Groundwater samples should also be taken downstream of the membrane to help in understanding the geochemistry of the groundwater flowing further downstream. This information could also help in understanding the uniformity of the groundwater that was sampled in this study. The groundwater sampled could be part

of a much larger aquifer which would explain the lack of accumulation of salinity and trace metals in the groundwater.

Sediment analysis in the form of doing a saturated paste could also be done across the river bed. The analysis could reveal a difference in the accumulation of the sediments. A larger scale study could be done in the future to look for more links and sources to possible accumulation within the catchment area. This would require collecting groundwater and sediment samples further up the Buffels River to confirm the results noted close to the membrane.

6. REFERENCES

Acosta, J. et al., 2011. Salinity increases mobility of heavy metals in soils. *Chemosphere,* Volume 85, pp. 1318-1324.

Adams, S., Titus, R. & Xu, Y., 2004. *Groundwater recharge assessment of the basement aquifer of central Namaqualand,* Cape Town: Water Research Commission.

Arblaster, J. et al., 2007. *Climate Change: The Physical Science Basis,* Geneva: Intergovernmental Panel on Climate Change.

Axtmann, E. & Luoma, S., 1991. Large-scale distribution of metal contamination in the fine grained sediments of the Clark Fork River, Montana. *Applied Geochemistry,* Volume 6, pp. 75-88.

Benito, G. et al., 2010. Management of alluvial aquifers in two Southern African Ephemeral Rivers: Implications for IWRM. *Water Research management,* pp. 641-667.

Bennett, S. & Hanor, J. S., 1987. *Dynamics of subsurface salt dissolution at the Welsh Dome, Louisiana Gulf Coast.* New York: Academic Press.

Borrok, D. M. & Engle, M. A., 2014. The role of climate in increasing salt loads in dryland rivers. *Arid Environments,* Volume 111, pp. 7-13.

Bridgman, H., Dragovish, D. & Dodson, J., 2008. *The Australian Physical Environment,* USA: Oxford University Press.

Cairncross, B., 2004. History of the Okiep Copper District, Namaqualand, Northern Cape Province, South Africa.. *Mineralogical Record,* pp. 289-317.

Campbell, E., Parker-Nance, T. & Bate, G., 1992. *A Compilation of the information on the magnitude, nature and importance of coastal aquifers in Southern Africa.,* s.l.: WRC Report No. 370/1/92.

Cantor, K., 1997. Drinking water and cancer. *Cancer causes control,* Volume 8, pp. 292-308.

Carpenter, A. B., Trout, M. L. & Pickett, E. E., 1974. Preliminary report on the origin and chemical evolution of lead-and zinc-rich oil field brines in central Mississippi. *Economic Geology,* Volume 69, pp. 1191-1206.

Carreira, P., Marques, J. & Nunes, D., 2014. Source of groundwater salinity in coastline aquifers based on environmental isotopes (Portugal): Natural vs human interference. A review and reinterpretation. *Applied Geochemistry,* Volume 41, pp. 163-175.

Chharbra, R., 1996. *Soil Salinity and Water Quality.* s.l.:s.n.

Clarke, C. E., Roux, S. G. l. & Roychoudhury, A. N., 2014. The role of evaporation on the formation of secondary Cu-hydroxy minerals in the arid Namaqualand soil system of South Africa. *Applied Geochemistry,* Volume 47, pp. 52-60.

Clifford, T. & Barton, E., 2012. The O'okiep Copper District, Namaqualand, South Africa: a review of the geology with emphasis on the petrogenesis of the cupriferous Koperberg Suite. *Mineral Deposits,* Volume 47, pp. 837-857.

Clifford, T., Barton, E., Stern, R. & Duchesne, J., 2004. U-Pb Zircon Calendar for Namaquan (Grenville) Crustal Events in the Granulite facies terrane of the Okiep Copper District of South Africa. *Journal of Petrology,* Issue 45, pp. 669-691.

Cowling, R., Esler, K. & Rundel, P., 1999. Namaqualand, South Africa—an overview of a unique winter-rainfall desert ecosystem. *Plant Ecology,* Volume 142, pp. 3-21.

Daoji, L. & Daler, D., 2004. Ocean Pollution from Land-based Sources: East China Sea, China. *Journal of the Human Environment,* Volume 33, pp. 107-113.

Desmet, P., 2007. Namaqualand - A brief overview of the physical and floristic environment. *Journal of Arid Environments,* Volume 70, pp. 570-587.

Deverel, S. & Gallanthine, S., 1989. Relation of salinity and selenium in shallow groundwater to hydrologic and geochemical processes, western San Joaquin Valley, California. *Journal of Hydrology,* Volume 109, pp. 125-149.

Dieter, H., Bayer, T. & Multhaup, G., 2005. Environmental copper and manganese in the pathophysiology of neurologic diseases (Alzheimer's disease and Manganism). *Acta Hydrochemistry,* Volume 33, pp. 72-78.

Du Laing, G. et al., 2008. Effect of salinity on heavy metal mobility and availability in intertidal sediments of the Scheldt estuary. *Estuarine, Coastal and Shelf Science,* Volume 77, pp. 589-602.

Eglington, B., 2006. Evolution of the Namaqua-Natal Belt, Southern Africa - A Geochronological and isotope geochemical review. *Journal of African Earth Science,* pp. 93-111.

EPA, 2007. *Drinking water standards,* San Francisco: United States Environmental Protection Agency.

Eriksson, N. & Destouni, G., 1997. *Combined effects of dissolution kinetics, secondary mineral precipitation, and preferential flow on copper leaching from mining waste rock,* s.l.: Water Resources Research.

Fauchereau, N., Trzaska, S., Rouault, M. & Richard, Y., 2003. Rainfall variability and changes in Southern Africa during the 20th century in the global warming context. *Natural Hazards,* Volume 29, pp. 139-154.

Freeze, R. A. & Cherry, J. A., 1979. *Groundwater.* Printice-Hall, New Jersey: s.n.

Gadd-Claxton, D., 1981. *The economic geology of the Okiep copper deposits, Namaqualand, South Africa.* Rhodes, South Africa: Unpublished Masters thesis.

Ghassemi, F., Jakeman, A. J. & and Nix, H. A., 1995. *Salinisation of land and water resources: human causes, extent, management and case studies,* s.l.: CAB international.

Gibson, R. & Kisters, A., 1996. The geology and mineralization of the Okiep Copper District: An overview. *South African Journal of Geology,* pp. 105-106.

Hahn, B. et al., 2005. A simulation model of long term climate, livestock and vegitation interactions on communal rangelands in the semi-arid succulant karoo, Namaqualand, South Africa.. *Ecological Modelling,* Volume 183, pp. 211-230.

Hanor, J. & Evans, W., 1988. Subsurface brines from rain water: the salinization of the Murray Basin, Australia. *Geological Sociaety of America,* Volume A364, p. 20.

Hartnady, C., Joubert, P. & Stowe, C., 1985. *Proterozoic crustal evolution in south-western Africa,* s.l.: s.n.

Herczeg, A., Dogramaci, S. & Leaney, F., 2001. Origin of dissolved salts in a large, semi-arid groundwater system: Murray Basin, Australia. *Marine Freshwater Research,* Volume 52, pp. 41-52.

Hoffman, M. & Cowling, R., 1987. *The physiognomy, phenology and demography of Karoo plants. In: Cowling, R.M., Roux, P.W. (Eds.), Karoo Ecology: A Preliminary Synthesis. Part II. South African National Scientific Programmes,* Pretoria: CSIR.

Hohne, S. & Hansen, R. N., 2008. *Preliminary conceptual geo-environmental model of the abandoned copper mines of the Okiep Copper District, Namaqualand, Northern Cape. Council for Geoscience,* s.l.: Sustainable Development through Mining. Council for Geoscience.

Hulme, M. et al., 2001. Africa climate change: 1900-2100. *Climate research,* Volume 17, pp. 145-168.

IARC, 1993. *Cadmium and cadmium compounds, Beryllium, Cadmium, Mercury and Exposure in the Glass Manufacturing Industry, IARC Monographs on the Evaluation of Carcinogenic Risks-Humans,* s.l.: International Agency for Research on Cancer.

Jarup, L., 2009. Hazards of heavy metal contamination. *British Medical Bulletin,* Volume 68, pp. 167-182.

Jury, M., 2013. Climate trends in Southern Africa. *South African Journal of Science,* 109(112), pp. 1-11.

Karim, Z., 2011. Risk Assessment of Dissolved Trace Metals in Drinking Water of Karachi, Pakistan. *Environmental Contamination and Toxicology,* Volume 86, pp. 676-678.

Kavcar, P., Sofuoglu, A. & Sofuoglu, S. C., 2009. A health risk assessment for exposure to trace metals via drinking water ingestion pathway. *International journal of hydrology and environmental health,* Volume 212, pp. 216-227.

Kim, Y. et al., 2003. Hydrogeochemical and isotopic evidence of groundwater salinization in a coastal aquifer— a case study in Jeju volcanic island, Korea. *Journal of Hydrology,* Volume 270, p. 282–294.

Klute, A., 1986. *Methods of Soil Analysis: Part 1 - Physical and Mineralogical Methods,* s.l.: American Society of Agronomy.

Knight, C., Kaiser, G., Robothum, L. H. & Witter, J., 1997. Heavy metals in surface water and stream sediments in Jamaica. *Environmental Geochemistry,* Volume 19, pp. 63-66.

Lau, S., Mohamed, M., Yen, A. & Su'ut, S., 1998. Accumulation of heavy metals in freshwater mollusks. *Science of the total environment,* Volume 214, pp. 113-121.

Le Roux, S. G., 2013. *Physiochemical controls on the formation and stability of atacamite in the soil surrounding the Spektakel mine, Northern Cape Province, South Africa,* Stellenbosch: Stellenbosch University.

Le Roux, S., Miller, J., Dunford, A. & Clarke, C., 2015. The dissolution kinetics of atacamite in the acid range and the stability of atacamite containing soils from Namaqualand, South Africa. *Applied Geochemistry,* pp. 1-8.

Leshomo, J., 2011. *Investigation of hydrochemistry and uranium radioactivity in groundwater of Namaqualand, Northern Cape, South Africa.,* Johannesburg: MSc thesis, University of Witwatersrand.

Lim, H., Lee, J., Chon, H. & Sager, M., 2008. Heavy metal contamination and health risk assessment in the vicinity of the abandoned Songcheon Au–Ag mine in Korea. *Geochemical Exploration,* Volume 96, pp. 223-230.

MacKellar, N., Hewitson, B. & Tadross, M., 2007. Namaqualand's climate: Recent historical changes and future scenarios. *Arid Environments,* Volume 70, pp. 604-614.

Macpherson, G. L., 1992. Regional variation in formation water chemistry: major and minor elements, Frio Formation fluids, Texas. *American Association of Petroleum Geologists Bulletin,* Volume 76, pp. 740-757.

Marais, J., 1981. *Updated technical report on the Spektakel water scheme in the district of Springbok, Cape Province.,* s.l.: Unpublished Report on the O'kiep Copper Company Limited.

Marais, J. A. H., Agenbacht, A. L. D., Prinsloo, M. & Basson, W. A., 2001. *The Geology of Springbok Area, Explanation: Sheet 2916. Scale 1:250 000,* Pretoria, South Africa: Council for Geoscience.

Martin, J.-M. & Whitfield, M., 1983. The Significance of the River Input of Chemical Elements to the Ocean. *Trace Metals in Sea Water,* Volume 9, pp. 265-296.

McDowell, R., 2008. *Environmental Impacts of Pasture-Based Farming,* Oxford shire: CAB International.

McLeod, M. et al., 2010. Soil salinity in Aceh after the December 2004 Indian Ocean tsunami. *Agricultural Water Management,* Volume 97, pp. 605-613.

Miller, D., 1995. 2000 years of indigenous mining and metallurgy in Southern Africa - A Review. *South African Journal of Geology,* pp. 232-238.

Minkina, T. et al., 2011. Effect of the Particle-Size Distribution on the Adsorption od Copper, Lead, and Zinc by Chernozemic Soils of Rostov Oblast. *Eurasian Soil Science,* Volume 11, pp. 1304-1311.

Monjerezi, M., 2012. *Groundwater Salinity in lower Shire River valley (Malawi),* s.l.: PhD thesis, University of Oslo.

Moore, J. & Luoma, S., 1990. Hazardous wastes from large-scale metal extraction. *Environmental Science and Technology,* Volume 24, pp. 1279-1285.

Morris, J. et al., 2002. Responses of coastal wetlands to rising sea level. *Ecology,* Volume 83, pp. 2869-2877.

Muhammad, S., Shah, M. T. & Khan, S., 2011. Health risk assessment of heavy metals and their source apportionment in drinking water of Kohistan region, northern Pakistan. *Microchemical Journal,* Volume 98, pp. 334-343.

Mulligan, C., Yong, R. & Gibbs, B., 2001. Remediation technologies for metal-contaminated soils and groundwater: an evaluation. *Engineering Geology,* Volume 60, pp. 193-207.

Nakwafila, A. N., 2015. *Salinisation source(s) and mechanism(s) in shallow alluvial aquifers along the Buffels River, Northern Cape Province, South Africa,* Stellenbosch: Stellenbosch University.

Nriagu, J., 1989. A global assessment of natural sources of atmospheric trace metals. *Nature,* Volume 338, pp. 47-49.

Nriagu, J. & Pacyna, J., 1988. Quantitative assessment of worldwide contamination of air, water and soils with trace metals. *Nature,* Volume 333, pp. 134-139.

NSSC, 1995. *Soil Survey Laboratory Information Manual,* s.l.: National Soil Survey Centre .

Pacyna, J., Scholtz, M. & Li, Y., 1995. Global budget of trace metal sources. *Environmental Reviews,* Volume 3, pp. 145-159.

Park, S. et al., 2005. Regional hydrochemical study on salinization of coastal aquifers, western coastal area of South Korea. *Journal of Hydrology,* Volume 313, p. 182–194.

Partridge, T. & Maud, R., 1987. Geomorphic evolution of Southern Africa since the Mesozoic.. *South African Journal of Geology,* Issue 90, pp. 179-208.

Pestana, M., Formoso, M. & Teixeira, E., 1997. Heavy metals in stream sediments from copper and gold mining areas in southern Brazil. *Geochemical Exploration,* Volume 58, pp. 133-143.

Petterson, A., 2008. *Mesoproterozoic crustal evolution in Southern Africa,* Gothebburg, Sweden: University of Gothenburg.

Phillips, F., Hogan, J., Mills, S. & Hendrickx, J., 2003. Environmental tracers applied to quantifying causes of salinity in arid-region rivers: Preliminary results from the Rio Grande, Southwestern USA. *Developments in water science,* Volume 50, pp. 327-334.

Pietersen, K., Titus, R. & Cobbing, J., 2009. *Effective groundwater management in Namaqualand: Sustaining supplies,* s.l.: Water Research commission, Report No. TT 418/09.

Reid, D., Welke, H., Smith, C. & Moore, J., 1997. Lead isotope patterns inProterozoic stratiform mineralization in the Bushmanland Group, Namaqua Province, South Africa. *Economic geology,* Volume 92, pp. 248-258.

Rengasamy, P., 2006. World salinization with emphasis on Australia. *Experimental Botany,* Volume 57(5), pp. 1017-1023.

Richter, B. & Kreitler, C., 1993. *Geochemical techniques for identifying groundwater salinisation.* Florida, USA: CRC.

Rober, G. & Mari, G., 2003. *Human Health Effects of Metals, US Environmental Protection Agency Risk Assessment Forum,* Washington, DC: s.n.

Rose, C., 2004. *An Introduction to the Environmental Physics of Soil, Water and Watersheds.* Cambridge: Cambridge University Press.

SAWB, 2013. *Temperature, Wind and Precipitation Records,* s.l.: s.n.

Scanlon, B., Healy, R. & Cook, P., 2002. Choosing techniques for quantifying groundwater recharge. *Hydrogeology journal,* Volume 10, pp. 18-39.

Schoch, A. & Conradie, J., 1990. Petrochemical and mineralogical relationships in the Koperberg Suite, Namaqualand, South Africa. *American mineralogist,* Volume 75, pp. 27-36.

Shanyengana, E., Seely, M. & Sanderson, R., 2004. Major-ion chemistry and ground-water salinization in ephemeral floodplains in some arid regions of Namibia. *Arid Environments,* Volume 57, pp. 71-83.

Sharkey, K. & Lewin, S., 1971. Conditions governing the formation of atacamite and paracamite. *American Minerology,* Volume 56, pp. 179-191.

Slinger, D. & Tenison, K., 2007. *Salinity Glove Box Guide: NSW Murray & Murrumbidgee Catchments,* s.l.: NSW Department of Primary Industries.

Smalberger, J., 1975. *Aspects of the history of copper mining in Namaqualand.* Cape Town: Struik.

Smith, M., 2002. Copper Dump Leaching. *The Mining Journal,* pp. 21-27.

Smith, O., 2015. *Kleinzee membrane* [Interview] (28 May 2015).

Swartz, C., du Plessis, J., Burger, A. & Offringa, G., 2006. *A desalination guide for South African municipal engineers,* Durban: Water Institute of South Africa.

Thomas, R., 1989. A tale of two tectonic terranes. *South African Journal,* Volume 92, pp. 306-321.

Thomas, R., De Beer, C. & Bowring, S., 1996. A comparative study of the Mesoproterozoic late orogenic porphyritic granitoids of southwest Namaqualand and Natal, South Africa. *South African Journal of Earth Science,* Volume 23, pp. 485-508.

Thomas, R., von Veh, M. & McCourt, S., 1993. The tectonic evolution of southern Africa: an overview. *Journal of African Earth Sciences,* Volume 16, pp. 5-24.

Ujevic, I., Odzac, N. & Baric, A., 2000. Trace Metal Accumulation in Different Grain Size Fractions of the Sediments from Semi-enclosed Bay Heavily Contaminated by Urban and Industrial Wastewaters. *Water Resource,* Volume 34, pp. 3055-3061.

Van der Sommen, J. & Geirnaert, W., 1988. *On the continuity of the aquifer system on the crystalline basement of Burkina Faso. In I. Simmers (ed): Estimation of Natural Groundwater recharge,* s.l.: D. Reidel Publishing Company.

Van Weert, F., Van der Gun, J. & Reckman, J., 2009. *Global overview of saline groundwater occurence and genesis,* Utrecht: International Groundwater Assessment Centre (IGRAC).

Vengosh, A., Gill, J., Lee Davisson, M. & Bryant Hudson, G., 2002. A multi-isotope (B, Sr, O, H, and C) and age dating (3H–3He and 14C) study of groundwater from Salinas Valley, California: Hydrochemistry, dynamics, and contamination processes. *Water Resource Research,* Volume 38, pp. 1-9.

Wasserma, G. et al., 2006. Water manganese exposure and children's intellectual functions in Araihazar, Bangladesh. *Environmental health,* Volume 114, pp. 124-129.

Whitworth, T. & Fritz, S., 1994. Electrolyte-induced solute permeability effects in compacted smectite membranes. *Applied Geochemistry ,* Volume 9, p. 533–546.

WHO, 2008. *Chemical Fact sheet - Guidelines for drinking water quality,* Geneva: World Health Organisation.

Wicks, C. & Herman, J., 1996. Regional hydrogeochemistry of a modern coastal mixing zone. *Water Resource Research,* Volume 32, p. 401–407.

Wicks, C. M., Herman, J. S., Randazzo, A. F. & Jee, J. L., 1995.. Water–rock interactions in a modern coastal mixing zone. *Geological Society of America,* Volume 107, p. 1023–1032.

Woods, T. & Garrels, R., 1986. Use of oxidised copper minerals as environmental indicators.. *Applied Geochemistry,* Volume 1, pp. 181-187.

Yechieli, Y. & Wood, W., 2002. Hydrogeologic processes in saline systems: playas, sabkhas, and saline lakes. *Earth Science,* Volume 58, pp. 343-365.

Zhao, S. et al., 2013. Salinity increases the mobility of Cd, Cu, Mn, and Pb in the sediments of Yangtze Estuary: Relative role of sediments' properties and metal speciation. *Chemoshpere,* Volume 91, pp. 977-984.

Appendix 1 – Results

1. Saturated Paste Extracts (Sediments)

		Field measurements			Anions				Cations																
Sample Site	Depth of Sample	EC	Unit	pH	mg/l Chloride	mg/l Nitrite	mg/l Nitrate	mg/l Sulphate	mg/l Al	mg/l B	mg/l Ba	mg/l Ca	mg/l Co	mg/l Cr	mg/l Cu	mg/l Fe	mg/l K	mg/l Mg	mg/l Mn	mg/l Na	mg/l Ni	mg/l P	mg/l Pb	mg/l Si	mg/l Zn
Site 38	0-30cm	9.30	mS/cm	7.20	2167.2	16.6	-	1003.4	< 0.05	1.24	0.12	480.20	< 0.05	< 0.05	0.12	< 0.01	45.52	231.90	0.09	1103.0	< 0.05	0.70	< 0.05	10.32	< 0.05
Site 36	0-40cm	0.50	mS/cm	7.83	88.7	-	25.9	70.1	0.33	0.48	0.01	29.98	< 0.05	< 0.05	0.08	0.23	8.17	11.01	0.03	68.2	< 0.05	0.79	< 0.05	6.10	< 0.05
Site 44	0-15cm	26.40	mS/cm	7.35	7849.2	-	-	1933.0	< 0.05	1.10	0.27	1341.00	< 0.05	< 0.05	0.30	< 0.01	50.11	678.80	6.72	5255.0	< 0.05	0.66	< 0.05	6.50	0.13
Site 44	15-30cm	7.42	mS/cm	7.15	7727.2	-	-	2673.7	< 0.05	0.53	0.12	199.20	< 0.05	< 0.05	< 0.05	< 0.01	34.44	108.40	3.59	730.7	< 0.05	0.23	< 0.05	3.87	0.15
Site 45	0-15cm	37.70	mS/cm	7.16	16275.3	-	68364.8	5490.1	< 0.05	1.33	0.15	1235.00	< 0.05	< 0.05	0.11	< 0.01	98.68	910.20	3.29	5119.0	< 0.05	0.35	< 0.05	5.42	< 0.05
Site 45	15-30cm	6.36	mS/cm	7.05	6163.1	-	-	1736.6	< 0.05	1.15	0.27	992.90	< 0.05	< 0.05	< 0.05	< 0.01	85.05	551.50	6.97	3609.0	< 0.05	0.45	< 0.05	4.11	< 0.05
Site 51	0-50cm	20.00	mS/cm	7.70	1202.4	-	-	253.2	< 0.05	0.97	0.04	188.50	< 0.05	< 0.05	< 0.05	< 0.01	17.84	103.90	0.55	602.1	< 0.05	0.14	< 0.05	3.94	< 0.05
Site 21	0-30cm	22.90	mS/cm	7.01	7050.6	-	-	2208.1	< 0.05	1.49	0.33	1424.00	< 0.05	< 0.05	< 0.05	< 0.01	149.90	625.00	2.32	4367.0	< 0.05	0.57	< 0.05	13.26	< 0.05
Site 21	30-50cm	5.08	mS/cm	7.67	1026.8	-	-	741.1	< 0.05	0.78	0.10	262.00	< 0.05	< 0.05	< 0.05	< 0.01	28.06	81.05	0.41	649.9	< 0.05	0.35	< 0.05	10.38	< 0.05
Site 26	0-30cm	1.09	mS/cm	7.26	209.2	-	-	154.3	0.21	0.59	0.04	61.45	< 0.05	< 0.05	0.14	0.16	11.27	27.07	0.11	135.6	< 0.05	0.71	< 0.05	13.27	< 0.05
Site 35	0-30cm	0.29	mS/cm	6.90	59.9	0.8	5.8	17.1	1.88	0.63	0.01	14.34	< 0.05	< 0.05	0.12	1.18	16.30	8.55	0.03	38.4	< 0.05	1.18	< 0.05	15.91	< 0.05
Site 12	0-50cm	0.01	mS/cm	7.66	2.2	-	-	-	1.40	0.02	< 0.01	1.46	< 0.05	< 0.05	< 0.05	0.90	1.93	1.25	0.01	4.0	< 0.05	0.59	0.04	8.35	< 0.05
Site 12	50-90cm	0.07	mS/cm	7.68	10.2	-	-	-	4.42	< 0.05	0.01	2.17	< 0.05	< 0.05	0.02	2.87	2.99	1.85	0.02	17.8	< 0.05	0.82	< 0.05	13.38	0.01
Site 9	0-20cm	0.08	mS/cm	7.85	15.8	-	-	-	1.42	0.48	0.01	5.49	< 0.05	< 0.05	0.10	0.93	4.16	2.97	0.03	18.5	< 0.05	0.44	< 0.05	9.06	< 0.05
Site 9	20-40cm	0.05	mS/cm	7.67	5.0	-	2.5	-	1.91	< 0.05	0.01	2.18	< 0.05	< 0.05	0.02	1.27	3.02	1.58	0.02	9.6	< 0.05	0.70	< 0.05	9.26	< 0.05

2. Sediment Electrical conductivity and pH

Sample Site	Depth of Sample	EC	pH
Site 38	0-30cm	9.3 mS/cm	7.2
Site 36	0-40cm	0.504 mS/cm	7.83
Site 44	0-15cm	26.4 mS/cm	7.35
Site 44	15-30cm	7.42 mS/cm	7.15
Site 45	0-15cm	37.7 mS/cm	7.16
Site 45	15-30cm	6.36 mS/cm	7.05
Site 51	0-50cm	20 mS/cm	7.7
Site 21	0-30cm	22.9 mS/cm	7.01
Site 21	30-50cm	5.08 mS/cm	7.67
Site 26	0-30cm	1.086 mS/cm	7.26
Site 35	0-30cm	0.291 mS/cm	6.9
Site 12	0-50cm	0.01253 mS/cm	7.66
Site 12	50-90cm	0.0735 mS/cm	7.68
Site 9	0-20cm	0.0799 mS/cm	7.85
Site 9	20-40cm	0.0499 mS/cm	7.67

3. Grainsize analysis

	Sample Site	Depth of Sample	Sand	Silt	Clay	Total percentage
			Percentage			
Sample Trip 1	Site 1	0-50cm	99.89	0.00	0.11	100.00
	Site 1	50-100cm	99.94	0.00	0.06	100.00
	Site 2	0-10cm	99.91	0.02	0.07	100.00
	Site 2	10-30cm	99.86	0.08	0.06	100.00
	Site 3	0-15cm	99.85	0.02	0.13	100.00
	Site 3	15-30cm	99.79	0.07	0.14	100.00
	SIte 3	30-45cm	99.87	0.01	0.12	100.00
	Site 4	0-15cm	71.02	14.70	14.27	100.00
	Site 4	15-45cm	99.86	0.00	0.14	100.00
	Site 5	0-15cm	80.52	9.12	10.36	100.00
	Site 5	15-30cm	99.85	0.07	0.08	100.00
	Site 6	0-15cm	99.87	0.06	0.07	100.00
	Site 6	15-30cm	99.90	0.04	0.05	100.00
	Site 7	0-30cm	99.88	0.01	0.11	100.00
	Site 8	0-30cm	99.93	0.04	0.04	100.00
	Site 9	0-20cm	99.70	0.11	0.19	100.00
	Site 9	20-40cm	99.89	0.06	0.05	100.00
	Site 10	0-10cm	99.54	0.16	0.31	100.00
	Site 10	10-30cm	99.80	0.08	0.12	100.00
	Site 11	0-15cm	99.92	0.02	0.06	100.00
	Site 11	15-30cm	99.91	0.04	0.06	100.00
	Site 12	0-50cm	99.91	0.04	0.06	100.00
	Site 12	50-90cm	99.93	0.00	0.07	100.00
	Site 13	0-20cm	99.92	0.01	0.07	100.00
	Site 13	20-30cm	99.89	0.02	0.09	100.00
	Site 14	0-15cm	99.91	0.01	0.07	100.00
	Site 14	15-40cm	99.78	0.05	0.17	100.00
Sample Trip 2	Site 21	0-30cm	99.13	0.52	0.35	100.00
	Site 21	30-50cm	99.93	0.03	0.04	100.00
	Site 22	0-15cm	99.63	0.21	0.16	100.00
	Site 22	15-30cm	99.87	0.06	0.07	100.00
	Site 23	0-30cm	99.96	0.01	0.03	100.00
	Site 24	0-15cm	96.49	3.24	0.27	100.00
	Site 25	0-30cm	99.93	0.03	0.04	100.00
	Site 26	0-30cm	99.90	0.05	0.04	100.00
	Site 27	0-30cm	99.82	0.07	0.11	100.00
	Site 28	NONE	NONE	NONE	NONE	NONE
	Site 29	NONE	NONE	NONE	NONE	NONE
	Site 30	0-20cm	99.95	0.03	0.03	100.00
	Site 31	0-32cm	99.92	0.03	0.05	100.00
	Site 32	0-30cm	99.96	0.02	0.03	100.00
	Site 33	0-40cm	99.93	0.03	0.04	100.00
	Site 34	0-45cm	99.95	0.02	0.03	100.00
	Site 35	0-30cm	99.89	0.05	0.06	100.00
	Site 36	0-40cm	99.97	0.01	0.03	100.00
	Site 37	0-40cm	99.94	0.03	0.04	100.00
	Site 38	0-30cm	98.31	0.75	0.94	100.00
	Site 39	0-40cm	99.95	0.02	0.03	100.00
	Site 40	0-40cm	99.94	0.02	0.05	100.00
	Site 41	0-40cm	99.79	0.10	0.11	100.00
	Site 42	0-40cm	99.91	0.03	0.06	100.00
	Site 43	0-40cm	99.75	0.07	0.18	100.00
	Site 44	0-15cm	95.49	3.88	0.63	100.00
	Site 44	15-30cm	99.77	0.07	0.16	100.00
	Site 45	0-15cm	96.46	1.79	1.74	100.00
	Site 45	15-30cm	99.88	0.04	0.08	100.00
	Site 46	0-20cm	99.64	0.13	0.23	100.00
	Site 47	0-40cm	99.74	0.11	0.16	100.00
	Site 48	0-30cm	99.47	0.28	0.24	100.00
	Site 49	0-40cm	99.43	0.41	0.16	100.00
	Site 50	0-30cm	99.94	0.03	0.03	100.00
	Site 51	0-50cm	99.66	0.09	0.24	100.00
	Site 52	0-50cm	99.95	0.00	0.05	100.00
	Site 53	0-30cm	99.94	0.04	0.02	100.00
	Site 54	0-40cm	96.21	3.56	0.23	100.00
	Site 55	0-30cm	99.82	0.09	0.09	100.00
	Site 56	NONE	NONE	NONE	NONE	NONE

4. Site description

	Sample Site	Depth of Sample	Water	Colour	Description: Shape	Description: Size	Description: Description
Sample Trip 1	Site 1	0-50cm	No	Light brown	Mostly angular, some sligghtly rounded	Various (coarse to fine)	Sand material
	Site 1	50-100cm	No	Light brown	Mostly angular, some sligghtly rounded	Various (coarse to fine)	Sand Material
	Site 2	0-10cm	No	Light brown	Mostly angular, some sligghtly rounded	Various (coarse to fine)	Sand Material
	Site 2	10-30cm	No	Light brown	Mostly angular, some sligghtly rounded	Various (coarse to fine)	Sand Material
	Site 3	0-15cm	No	Brown	Rounded grains, some larger quartz grains (angular)	Med-fine grained	Moist sand
	Site 3	15-30cm	No	Brown	Rounded grains, some larger quartz grains (angular)	Rounded	Wet sand
	SIte 3	30-45cm	No	Brown	Rounded to sub-angular grains	Medium grained	Wet Sand
	Site 4	0-15cm	No	Dark brown	Fine grained Clay (rounded)	Fine grained	Clay Material
	Site 4	15-45cm	No	Brown	Well rounded sand grains, larger quartz grains	Med-fine grained	Clay/sand Material
	Site 5	0-15cm	No	Dark brown	Fine grained Clay (rounded)	Fine grained	Hard packed clay
	Site 5	15-30cm	No	Brown	Well rounded sand grains, larger quartz grains	Med-fine grained	sand
	Site 6	0-15cm	No	Light brown	Well rounded sand grains, larger quartz grains	Med-fine grained	Sand material
	Site 6	15-30cm	No	Light brown	Well rounded sand grains, larger quartz grains	Med-fine grained	Sand Material
	Site 7	0-30cm	No	Light brown	Mostly angular, some sligghtly rounded	Coarse to Med grained	Sand Material
	Site 8	0-30cm	No	Light brown	Mostly angular, some sligghtly rounded	Coarse grained	Sand Material
	Site 9	0-20cm	No	Light brown - Brown	Mostly angular, some sligghtly rounded	Various (coarse to fine)	Sand material
	Site 9	20-40cm	No	Light brown - Brown	Mostly angular, some sligghtly rounded	Various (coarse to fine)	Sand material
	Site 10	0-10cm	No	Light brown	Mostly rounded, Some angular larger quartz grains	Fine grained	Sand material
	Site 10	10-30cm	No	Light brown	Mostly rounded, Some angular larger quartz grains	Fine grained	Sand material
	Site 11	0-15cm	No	Light brown	Mostly rounded, Some angular larger quartz grains	Med-fine grained	Sand material
	Site 11	15-30cm	No	light brown	Mostly angular, some sligghtly rounded	Coarse to Med grained	Sand material
	Site 12	0-50cm	No	Light brown	Mostly rounded to sub-rounded	Coarse to Med grained	Sand material
	Site 12	50-90cm	No	Light brown	Mostly rounded, Some angular larger quartz grains	Med-fine grained	Sand material
	Site 13	0-20cm	No	Light brown	Mostly angular, some sligghtly rounded	Coarse-med grained	Sand material
	Site 13	20-30cm	No	brown	Mostly rounded, Some angular larger quartz grains	Med-fine grained	Sand material
	Site 14	0-15cm	No	Brown	Rounded grains	Fine-Medium grained	Sand material
	Site 14	15-40cm	No	Light Brown	Sub-angular to rounded grains	Medium grained	Sand material
Sample Trip 2	Site 21	0-30cm	Yes	Brown	Mostly angular, some sligghtly rounded	Various (coarse to fine)	Sand material
	Site 21	30-50cm	Yes	Brown	Mostly angular, some sligghtly rounded	Various (coarse to fine)	Sand Material
	Site 22	0-15cm	Yes	Brown, dark horizons	Mostly rounded to sub-rounded	Various (coarse to fine)	Sand and clay Material
	Site 22	15-30cm	Yes	Brown	Mostly rounded to sub-rounded	Medium grained	Sand Material
	Site 23	0-30cm	Yes	Brown	Mostly rounded to sub-rounded	Various (coarse to fine)	Sand Material
	Site 24	0-15cm	No	Brown	Mostly rounded to sub-rounded	Fine grained	Clay and sand
	Site 25	0-30cm	No	Light Brown	Mostly rounded, Some angular larger quartz grains	Coarse grained	Sand Material
	Site 26	0-30cm	No	Light Brown	Mostly rounded to sub-rounded	Fine grained	Sand Material
	Site 27	0-30cm	Yes	Brown, dark horizons	Mostly rounded, Some angular larger quartz grains	Coarse grained	Sand Material
	Site 28	NONE	Yes	NONE	NONE	NONE	NONE
	Site 29	NONE	Yes	NONE	NONE	NONE	NONE
	Site 30	0-20cm	No	Light Brown	Mostly rounded to sub-rounded	Medium grained	Sand Material
	Site 31	0-32cm	No	Light Brown	Mostly rounded to sub-rounded	Fine grained	Sand Material
	Site 32	0-30cm	No	Light Brown	Mostly rounded to sub-rounded	Medium grained	Sand Material
	Site 33	0-40cm	No	Light Brown	Mostly rounded to sub-rounded	Medium grained	Sand Material
	Site 34	0-45cm	No	Light Brown	Mostly rounded, Some angular larger quartz grains	Medium grained	Sand Material
	Site 35	0-30cm	No	Light Brown	Mostly rounded to sub-rounded	Fine grained	Sand Material
	Site 36	0-40cm	No	Light Brown	Mostly rounded, Some angular larger quartz grains	Medium grained	Sand Material
	Site 37	0-40cm	No	Light Brown	Mostly rounded, Some angular larger quartz grains	Coarse grained	Sand Material
	Site 38	0-30cm	No	Light Brown	Mostly rounded to sub-rounded	Fine grained	Sand Material
	Site 39	0-40cm	No	Light Brown	Mostly rounded, Some angular larger quartz grains	Medium grained	Sand Material
	Site 40	0-40cm	No	Light Brown	Mostly rounded to sub-rounded	Fine grained	Sand Material
	Site 41	0-40cm	No	Light Brown	Various	Various (coarse to fine)	Sand Material
	Site 42	0-40cm	No	Light Brown	Mostly rounded to sub-rounded	Medium grained	Sand Material
	Site 43	0-40cm	Yes	Light Brown	Fine grained Clay	Fine grained	Clay
	Site 44	0-15cm	Yes	Light Brown	Mostly rounded to sub-rounded	Fine grained	Sand material
	Site 44	15-30cm	Yes	Light Brown	Mostly rounded to sub-rounded	Fine grained	Sand material
	Site 45	0-15cm	No	Light Brown	Mostly rounded to sub-rounded	Fine grained	Sand material
	Site 45	15-30cm	No	Light Brown	Mostly rounded, Some angular larger quartz grains	Medium grained	Sand material
	Site 46	0-20cm	No	Light Brown	Mostly rounded to sub-rounded	Fine grained	Sand material
	Site 47	0-40cm	No	Light Brown	Mostly angular, some sligghtly rounded	Medium grained	Sand material
	Site 48	0-30cm	Yes	Light Brown	Mostly rounded to sub-rounded	Fine grained	Sand material
	Site 49	0-40cm	Yes	Light Brown	Mostly angular, some sligghtly rounded	Medium grained	Sand material
	Site 50	0-30cm	Yes	Light Brown	Mostly rounded to sub-rounded	Fine grained	Sand material
	Site 51	0-50cm	Yes	Light Brown	Mostly rounded to sub-rounded	Coarse grained	Sand material
	Site 52	0-50cm	No	Light Brown	Various	Coarse grained	Sand material
	Site 53	0-30cm	No	Light Brown	Various	Coarse grained	Sand material
	Site 54	0-40cm	Yes	Light Brown	Fine grained Clay	Fine grained	Clay and sand
	Site 55	0-30cm	No	Light Brown	Fine grained Clay	Fine grained	Clay and sand
	Site 56	NONE	Yes	NONE	NONE	NONE	NONE

		KCl							MgCl						
Site	**Depth**	Quartz	Albite	Kaolinite	Illite	Orthoclase	Calcite	Sylvite	Vermiculite	Quartz	Albite	Kaolinite	Illite	Orthoclase	Calcite	Sylvite	Vermiculite
Site 12	0-50cm	x	x	x	x	x			x	x	x	x	x	x			x
Site 12	50-90cm	x	x	x	x	x			x	x	x	x	x	x			x
Site 21	0-30cm	x	x	x	x	x	x			x	x	x	x	x		x	
Site 21	30-50cm	x	x	x	x	x				x	x	x	x	x			x
Site 26	0-30cm	x	x	x	x	x				x	x	x	x	x			x
Site 35	0-30cm	x	x	x	x	x				x	x	x	x	x			x
Site 36	0-40cm	x	x	x	x	x				x	x	x	x	x			x
Site 38	0-30cm	x	x	x	x	x		x		x	x	x	x	x			x
Site 44	0-15cm	x	x	x	x	x		x		x	x	x	x	x			x
Site 44	15-30cm	x	x	x	x	x				x	x	x	x	x			x
Site 45	0-15cm	x	x	x	x	x				x	x	x	x	x			x
Site 45	15-30cm	x	x	x	x	x		x		x	x	x	x	x			x
Site 51	0-50cm	x	x	x	x	x		x		x	x	x	x	x		x	
Site 9	0-20cm	x	x	x	x	x			x	x	x	x	x	x			x
Site 9	20-40cm																

6. XRF Results

Sample name		Al2O3 (%)	CaO (%)	Cr2O3 (%)	Fe2O3 (%)	K2O (%)	MgO (%)	MnO (%)	Na2O (%)	P2O5 (%)	SiO2 (%)	TiO2 (%)	L.O.I. (%)	Sum Of Conc. (%)
Site 38	0-30cm	14.34	1.05	0.01	4.07	4.4	1.14	0.09	1.62	0.15	68.22	0.68	5.25	101.02
Site 36	0-40cm	9.16	0.49	0	0.55	4.88	0.1	0.01	1.49	0.04	81.32	0.15	0.48	98.67
Site 44	0-15cm	16.32	1.38	0.01	5.8	4.05	1.75	0.14	1.66	0.21	59.42	0.9	8.02	99.66
Site 44	15-30cm	11.25	0.95	0	1.55	4.57	0.34	0.04	1.92	0.08	76.6	0.44	1.66	99.4
Site 45	0-15cm	15.57	1.45	0.01	5.5	3.97	1.61	0.13	1.76	0.18	60.84	0.96	7.59	99.57
Site 45	15-30cm	10.49	0.89	0	1.59	4.45	0.29	0.06	1.84	0.07	77.96	0.57	1.03	99.24
Site 51	0-50cm	11.02	1.25	0	2.2	4.58	0.65	0.06	1.83	0.08	73.74	0.44	4	99.85
Site 21	0-30cm	9.74	1.66	0	1.88	4.44	1.11	0.05	1.66	0.11	74.85	0.31	4.78	100.59
Site 21	30-50cm	9.55	0.64	0	0.78	4.9	0.17	0.02	1.61	0.04	80.48	0.22	0.88	99.29
Site 26	0-30cm	9.45	0.64	0	1.48	4.38	0.27	0.04	1.5	0.06	80.04	0.47	1.11	99.44
Site 35	0-30cm	10.33	0.61	0	0.93	4.87	0.22	0.02	1.64	0.05	79.22	0.15	1.15	99.19
Site 12	0-50cm	9.53	0.56	0	0.74	4.84	0.11	0.02	1.59	0.03	80.68	0.21	0.56	98.87
Site 12	50-90cm	9.58	0.57	0	0.82	4.86	0.12	0.02	1.6	0.04	80.54	0.26	0.58	98.99
Site 9	0-20cm	9.4	0.52	0	0.97	4.85	0.12	0.03	1.52	0.04	80.32	0.39	0.51	98.67
Site 9	20-40cm	9.25	0.5	0	1.09	4.86	0.11	0.04	1.53	0.05	80.3	0.48	0.46	98.67

	Field Measurements		Anions		Cations																											
			PPM	PPM	PPM	PPM	PPM	PPM	PPM	PPB	PPB	PPB	PPB	PPB	PPB	PPB	PPB	PPB	PPB	PPB	PPB	PPB	PPB	PPB	PPB	PPB	PPB	PPB	PPB	PPB	PPB	PPB
Sample Site	EC	Unit	pH	Chloride	Sulphate	Ca	K	Mg	Na	P	Si	B	Al	Ti	V	Cr	Mn	Fe	Co	Ni	Cu	Zn	As	Se	Mo	Cd	Sb	Ba	Hg	Pb
Site 43	3.88	mS/cm	7.39	2200.64	464.586	275	19.2	141.7	804	0.04	10.29	557.17	2.41	0.06	1.24		112.79	6.67	0.12	1.51	6.72	2.87	0.38		3.03	0.03	0.25	51.21	0.07	0.02
Site 44	5.67	mS/cm	6.75	3587.51	484.707	328.7	24.31	223	1196	0.04	9.31	645.23	5.18	0.45	1.46	0.41	11659.53	51.93	11.89	3.54	9.60	105.22	0.63		10.10	0.08	0.37	124.66	0.06	0.04
Site 48	4.37	mS/cm	6.62	2414.71	356.002	281.9	13.84	139.1	865	0.04	14.12	548.23	2.98	0.20	0.67		6140.05	992.08	2.93	1.06	0.31	7.34	1.43		1.77	0.00	0.22	159.11	0.04	0.03
Site 49	3.56	mS/cm	6.65	2091.54	445.16	211.9	24.06	119.1	783	0.03	10.70	513.40	5.24	0.64	0.58		836.42	754.65	0.65	1.10	0.34	5.01	1.60		4.41	0.01	0.26	111.15	0.04	0.02
Site 50	2.85	mS/cm	7.26	1788.86	441.424	161.7	18.58	103.6	629	0.14	1.60	475.49	4.45	0.25	8.62		83.10	16.99	0.97	2.25	1.58	2.51	0.77		11.74	0.01	0.29	39.43	0.03	0.03
Site 51	8.99	mS/cm	7.34	5375.13	1364.629	545.8	28.44	343.4	2176	0.14	11.91	1198.63	1.82	0.33	9.59	0.77	4.38	5.04	0.31	4.84	26.81	4.49	1.05		3.84	0.15	0.46	99.36	0.06	0.02
Site 54	15.79	mS/cm	7.15	10308.93	4306.005	2034	44.02	957.2	3796	0.03	19.29	2133.37	2.18	0.28	1.91	0.53	15110.20	30.77	21.73	12.18	9.63	9.02	1.69	1.49	10.27	0.21	0.77	137.36	0.08	0.05
Site 21	2.73	mS/cm	7.19	970.30	345.89	157.2	14.96	79.36	504	0.23	10.95	399.41	1.28	0.21	5.44	0.62	14.62	4.04	0.20	2.13	8.13	1.94	0.62	20.36	7.15	0.03	0.24	67.19	0.04	0.05
Site 22	2.44	mS/cm	6.72	1231.52	358.17	158.6	14.67	85.81	468	0.02	10.78	425.58	5.59	0.48	1.52		2154.58	8.41	13.61	4.80	24.89	7.50	0.47		7.86	0.26	0.25	74.13	0.04	0.04
Site 23	5.18	mS/cm	6.96	3015.56	985.439	352.5	24.43	176.7	1234	1.01	18.00	840.87	2.78	0.08	4.71		1817.68	13.07	5.54	15.61	29.39	3.26	1.62	22.32	11.43	0.38	0.33	119.41	0.05	0.04
Site 27	5.05	mS/cm	6.81	2549.56	770.527	326.3	37.59	153.8	1056	0.08	12.74	608.30	5.17	0.06	3.68		2332.39	7.13	6.46	4.06	11.86	5.92	1.18		3.67	0.21	0.35	267.16	0.05	0.07
Site 29	3.31	mS/cm	7.44	1525.02	330.398	218.5	18.46	117.9	655	0.04	9.91	548.12	2.57	0.40	0.79		10.21	4.77	0.05	1.09	5.48	53.11	0.16		3.85	0.11	0.22	56.08	0.08	0.02
Site 28	3.06	mS/cm	7.41	1965.3	413.99	181.5	15.75	100	547	0.08	9.46	466.47	3.09	0.06	0.77		2.80	5.40	0.03	1.15	10.43	172.84	0.31		2.73	0.07	0.21	40.85	0.04	0.02
Site 56	15.21	mS/cm	7.21	10008.32	2969.07	866.8	95.2	467.2	3966	0.02	14.58	4421.51	1.90	0.71	16.54	0.54	91.89	5.06	4.37	5.26	1.28	5.81	1.59	17.84	16.10	0.19	0.57	50.61	0.09	0.19

8. Groundwater TDS

Sample Site	TDS	unit
Site 43	2522	mg/l
Site 44	3685.5	mg/l
Site 48	2840.5	mg/l
Site 49	2314	mg/l
Site 50	1852.5	mg/l
Site 51	5843.5	mg/l
Site 54	10263.5	mg/l
Site 21	1774.5	mg/l
Site 22	1586	mg/l
Site 23	3367	mg/l
Site 27	3282.5	mg/l
Site 29	2151.5	mg/l
Site 28	1989	mg/l
Site 56	9886.5	mg/l

9. Groundwater Lab and Field Alkalinity

Sample Name	pH	Lab Alkalinity (mg/L)	Field Alkalinity (mg/L)
43	7.52	258.4	240.0
44	7.96	408.8	400.0
48	7.85	379.8	360.0
49	7.96	286.2	270.0
50	7.13	97.0	105.0
51	7.89	897.2	900.0
54	7.25	798.8	800.0
21	7.74	196.4	200.0
22	7.79	169.6	180.0
23	7.93	284.6	300.0
27	7.79	181.0	190.0
29	7.82	161.6	175.0
28	7.79	152.5	110.0
56	7.2	635.0	624.0

10. Leaching experiment

DI Water

	Days	1	2	3	4	5	6	7	8	9	10	11	12	13	14	15	16	17	18
A		5.16	5.22	5.36	5.47	5.51	5.61	5.34	5.25	5.56	5.59	5.69	5.65	5.55	5.68	5.76	5.59	5.78	5.58
B	pH	5.10	5.30	5.33	5.42	5.48	5.47	5.32	5.28	5.49	5.51	5.58	5.62	5.59	5.68	5.72	5.70	5.69	5.55
C		5.21	5.42	5.53	5.53	5.60	5.58	5.41	5.44	5.66	5.71	5.78	5.72	5.71	5.79	5.78	5.81	5.88	5.68
Average		5.16	5.31	5.41	5.47	5.53	5.55	5.36	5.32	5.57	5.60	5.68	5.66	5.62	5.72	5.75	5.70	5.78	5.60
A		108.00	91.00	80.50	73.40	70.20	63.30	61.80	59.10	56.20	54.90	53.10	47.80	46.20	44.90	43.50	40.80	39.40	39.80
B	Cu mg/l	87.20		77.60		67.40		67.00		60.90		55.80		50.80		47.80		41.80	
C		91.20		82.00		72.40		64.50		57.60		52.80		48.50		44.10		39.60	
Average		95.47	91.00	80.03	73.40	70.00	63.30	64.43	59.10	58.23	54.90	53.90	47.80	48.50	44.90	45.13	40.80	40.27	39.80

0.5 mol NaCl

	Days	1	2	3	4	5	6	7	8	9	10	11	12	13	14	15	16	17	18
D		4.87	4.98	5.00	5.07	5.22	5.18	5.27	5.29	5.35	5.41	5.44	5.51	5.41	5.53	5.55	5.66	5.62	5.50
E	pH	4.78	4.97	4.94	4.94	5.25	5.20	5.29	5.30	5.38	5.44	5.45	5.49	5.43	5.56	5.57	5.63	5.64	5.54
F		4.84	5.03	5.05	5.07	5.17	5.45	5.37	5.38	5.52	5.59	5.70	5.78	5.69	5.76	5.92	5.90	5.97	5.87
Average		4.83	4.99	5.00	5.03	5.21	5.28	5.31	5.32	5.42	5.48	5.53	5.59	5.51	5.62	5.68	5.73	5.74	5.64
D		151.20		88.30		55.20		37.00		27.50		21.30		17.60		14.50		12.80	
E	Cu mg/l	154.60	90.60	73.80	62.50	50.90	45.90	38.10	31.70	29.40	24.20	22.40	20.60	18.20	16.20	15.00	13.70	12.90	11.80
F		155.50		86.00		53.80		37.30		27.20		21.70		18.30		15.20		12.60	
Average		153.77	90.60	82.70	62.50	53.30	45.90	37.47	31.70	28.03	24.20	21.80	20.60	18.03	16.20	14.90	13.70	12.77	11.80

11. Reaction rate calculations for synthetic atacamite

	Initial reaction rate	Divide by two (/2)	Convert from L to grams (*0.1)	Grams to m2 (/18)	mmol to mol (/1000)
Synthetic DI Water					
Run 1	0.0084 mmol per l per s	0.0042 mmol per l per s	0.00042 mmol per g per s	2.33E-05 mmol per m2 per s	2.33E-08 mol per m2 per s
Run 2	0.0073 mmol per l per s	0.0037 mmol per l per s	0.00037 mmol per g per s	2.03E-05 mmol per m2 per s	2.03E-08 mol per m2 per s
Run 3	0.0106 mmol per l per s	0.0053 mmol per l per s	0.00053 mmol per g per s	2.94E-05 mmol per m2 per s	2.94E-08 mol per m2 per s
Average	0.0088 mmol per l per s	0.0044 mmol per l per s	0.00044 mmol per g per s	2.44E-05 mmol per m2 per s	2.44E-08 mol per m2 per s
Synthetic 0.5M NaCl					
Run 1	0.0061 mmol per l per s	0.0031 mmol per l per s	0.00031 mmol per g per s	1.69E-05 mmol per m2 per s	1.69E-08 mol per m2 per s
Run 2	0.0051 mmol per l per s	0.0026 mmol per l per s	0.00026 mmol per g per s	1.42E-05 mmol per m2 per s	1.42E-08 mol per m2 per s
Run 3	0.0033 mmol per l per s	0.0017 mmol per l per s	0.00017 mmol per g per s	9.17E-06 mmol per m2 per s	9.17E-09 mol per m2 per s
Average	0.0048 mmol per l per s	0.0024 mmol per l per s	0.00024 mmol per g per s	1.34E-05 mmol per m2 per s	1.34E-08 mol per m2 per s

Appendix 2 – Atacamite Paper

The dissolution kinetics of atacamite in the acid range and the stability of atacamite containing soils from Namaqualand, South Africa used the following experimental results from my work.

- Leaching experiments using atacamite soil.
- Auto titration work using synthetic atacamite, DI Water, 0.5M NaCl as the analyte and 0.5 $H2_5O_4$ as the titrant
- Auto titration using atacamite soil. DI Water. 0.5M NaCl, 1M NaCl as the analyte and 1M HNO_3 as the titrant.

Applied Geochemistry xxx (2015) 1–8

Contents lists available at ScienceDirect

Applied Geochemistry

journal homepage: www.elsevier.com/locate/apgeochem

The dissolution kinetics of atacamite in the acid range and the stability of atacamite containing soils from Namaqualand, South Africa

S.G. Le Roux [a], J.A. Miller [b], A.J. Dunford [b], C.E. Clarke [c, *]

[a] CT-scanner Facility, Central Analytical Facilities, Stellenbosch University, South Africa
[b] Department of Earth Sciences, Stellenbosch University, South Africa
[c] Department of Soil Science, Stellenbosch University, South Africa

ARTICLE INFO

Article history:
Received 12 February 2015
Received in revised form
4 August 2015
Accepted 2 September 2015
Available online xxx

Keywords:
Paratacamite
Reaction kinetics
Buffels river
Spektakel mine

ABSTRACT

The Cu hydroxy mineral, atacamite, is commonly associated with saline environments and is generally thought to dissolve rapidly in the presence of fresh water. A Cu contaminated soil from the arid Namaqualand region, South Africa, shows atacamite as the dominant Cu containing mineral. The stability of the Cu phase in this soil was determined through equilibrium and leaching studies using both deionised water (DI) and a concentrated (0.5 M) NaCl solution. Initially a high concentration of exchangeable Cu was released from the soils leached with NaCl. Continued leaching with NaCl resulted in a substantial decrease in Cu release as atacamite equilibria started to control dissolved Cu. This suggests that an initial spike of Cu laden water will leach from the soils at the onset of a large rainfall event. Further additions of water will result in a lower but sustained release of Cu from the soil. The Cu contaminated soils are exposed to acidic sulphate leachate thus the dissolution kinetics of synthetic atacamite in the acidic range (pH 5.5–4.0) was determined in both NaCl and DI solutions. The kinetic data showed that atacamite dissolution rates are significantly higher in DI than in NaCl but the rates converge at pH 4. In comparison to common acid soluble minerals, atacamite displays a moderate dissolution rate ($10^{-9.55}$–$10^{-7.14}$ mol m^{-2} s^{-1}) within the acid range (pH 5.5–4.0). The atacamite dissolution reaction order with respect to pH is 1.3 and 1.6 in DI and NaCl solutions, respectively, suggesting that dissolution rates of atacamite are highly pH dependent in the acid range. The type of acid used to lower the pH had no effect on the reaction kinetics, with HNO_3 and H_2SO_4 resulting in comparable dissolution rates of atacamite at pH 4.5.

1. Introduction

The Cu hydroxy mineral, atacamite [$Cu_2(OH)_3Cl$], occurs commonly in the oxidised zones of porphyry Cu deposits in the Atacama desert (Cameron et al., 2007; Reich et al., 2009; Sillitoe, 2005). It has also been observed in deep seafloor vents (Hannington, 1993), as a corrosion product of Cu-containing metals in coastal environments (Livingston, 1991) and in saline soils contaminated with Cu-bearing mine leachate (Clarke et al., 2014). Atacamite (used collectively hereafter to represent both atacamite and paratacamite) is a basic Cu hydroxide and is usually formed under neutral to alkaline conditions (Sharkey and Lewin, 1971) in high Cl environments (Woods and Garrels, 1986). Due to the high Cl requirement for the formation of atacamite, it is often regarded as unstable when exposed to fresh or low salinity solutions as Cu hydroxy minerals react rapidly to changes in their environment (Woods and Garrels, 1986).

Numerous studies, proposing the formation conditions of the atacamite deposits in Northern Chile, have highlighted the rapid dissolution and instability of atacamite in the presence of meteoric water (Cameron et al., 2007; Reich et al., 2008, 2009). However, the kinetics of atacamite dissolution in saline and non-saline waters have not been previously quantified. MacFarlane et al. (2005), included an atacamite containing ore material in their demonstration of a continuous leaching system. They observed that the majority of Cu was released from the ore during the initial water leach; however, the ore contained numerous Cu phases and thus direct information on atacamite dissolution was obscured. Most Cu hydroxy mineral dissolution studies are directed at ore processing techniques (Bingöl and Canbazoğlu, 2004; Quast, 2000). In these

* Corresponding author.
E-mail address: cdowding@sun.ac.za (C.E. Clarke).

http://dx.doi.org/10.1016/j.apgeochem.2015.09.003
0883-2927/

studies, minerals are subjected to harsh dissolution techniques using concentrated sulphuric acid, and the results cannot easily be extrapolated to environmental conditions. Thus the stability and dissolution kinetics of atacamite under environmental conditions has not been established.

In the historic Cu mining region of Namaqualand on the north west coast of South Africa (Fig. 1), atacamite and its polymorph, paratacamite have been identified as the sole secondary Cu minerals in the arid soil system surrounding the Spetakel Cu mine (Clarke et al., 2014). Copper has entered the soil system through the leaching of Cu-bearing acid mine drainage (AMD), which is generated in the unlined tailings heaps and ore processing ponds. The AMD is only mildly acidic (pH of 4.5) but contains an extremely high concentration of Cu (5700 ppm) (Clarke et al., 2014). Unabated leaching of the AMD into the surrounding soils has resulted in acute soil contamination with Cu concentrations of up to 14% being measured in the soil (Clarke et al., 2014). The use of saline groundwater during ore processing resulted in the soils also being contaminated with salts, especially Na and Cl. It was established that evaporative concentration of Cl^- in the soil pore waters is largely responsible for the formation of atacamite in the Spektakel soils (Clarke et al., 2014).

Current rainfall in the region is very low, typically less than 150 mm/yr with the majority of rain falling in the winter months (May–August) (Benito et al., 2011). Evapotranspiration is high and exceeds annual rainfall by between 12 and 22 times (Adams et al., 2004). Despite this, the region occasionally experiences very wet years with rainfall figures as high as 400 mm/yr being recorded (MacKeller et al., 2007). Rainfall patterns in the area are predicted to change as the region becomes hotter and drier in response to ongoing climate change (Hoerling et al., 2006). In particular, the likely change towards fewer but larger rainfall events may result in a temporary lowering of Cl^- activities, which could impact atacamite stability. In addition, unabated leaching of AMD has gradually exhausted the calcium carbonate buffering capacity of the soils and the soil pH is starting to attain equilibrium with the AMD (pH 4.5). Thus the stability of atacamite in these soils, which are gradually acidifying and exposed to periodic dilution changes, is uncertain.

The Spektakel mine is situated next to the ephemeral Buffels River, which is the major river system in Namaqualand (Fig. 1). Metal release from the contaminated soils is likely to impact water quality in the unconfined Buffels River aquifer, which supports numerous boreholes downstream. Given the prevalence of atacamite in the Spektakel soils, the stability and dissolution kinetics of atacamite in mildly acidic, NaCl solutions of various strengths is required. Thus the main objectives of the current study are: i) to determine the stability of Cu phases in the Spektakel soils in both pure water and a range of NaCl solutions, ii) to determine the Cu leaching potential of the Spektakel soils in both pure water and concentrated NaCl and finally iii) to determine the reaction kinetics of atacamite dissolution with respect to pH and acid type in both pure water and a concentrated NaCl solution.

2. Materials and methods

2.1. Atacamite preparation and sampling

Synthetic atacamite crystals were prepared according to the method of Sharkey and Lewin (1971) using the calcite replacement method. The atacamite minerals were washed with 0.5 M $Mg(NO_3)_2$ to remove excess Cu^{2+} and Cl^- from the mineral surface. The atacamite was washed until additions of $AgNO_3$ to the decanted wash water showed the absence of Cl^-. After washing with deionised water to remove salts, the crystals were dried overnight at 50 °C and gently crushed into a powder using an agate mortar and pestle. X-ray diffraction analysis (Fig. 2) and scanning electron microscope images (Supplementary Material; Fig. S1) confirmed the material to be a mixture of paratacamite and atacamite (collectively called atacamite hereafter). The Brunauer–Emmett–Teller (BET) surface area of the atacamite was determined to be 18 $m^2\ g^{-1}$.

A soil sample containing a high proportion of atacamite was collected from a subsurface horizon within the derelict mining compound of the Spektakel mine. This sample (SP 6) was fully characterised in an earlier study (Clarke et al., 2014). Briefly the sample (called Spektakel soil hereafter) contains 14% Cu and the

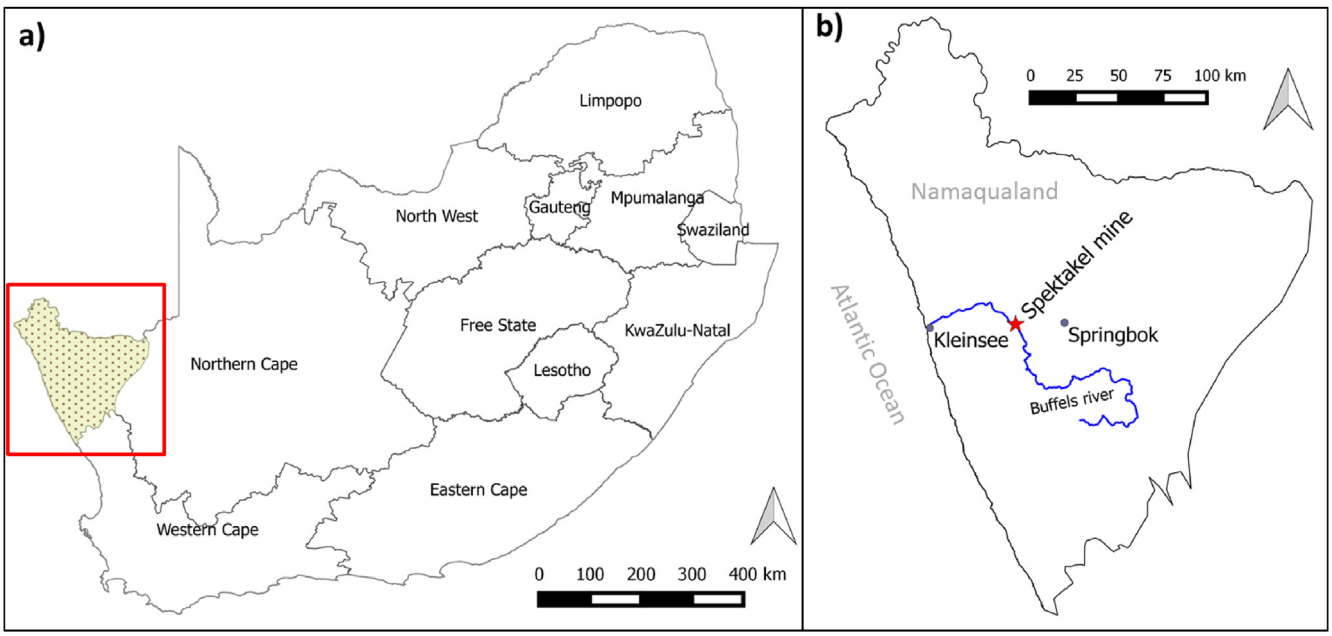

Fig. 1. a) Location of Namaqualand within South Africa and b) location of Spektakel mine within the Namaqualand region.

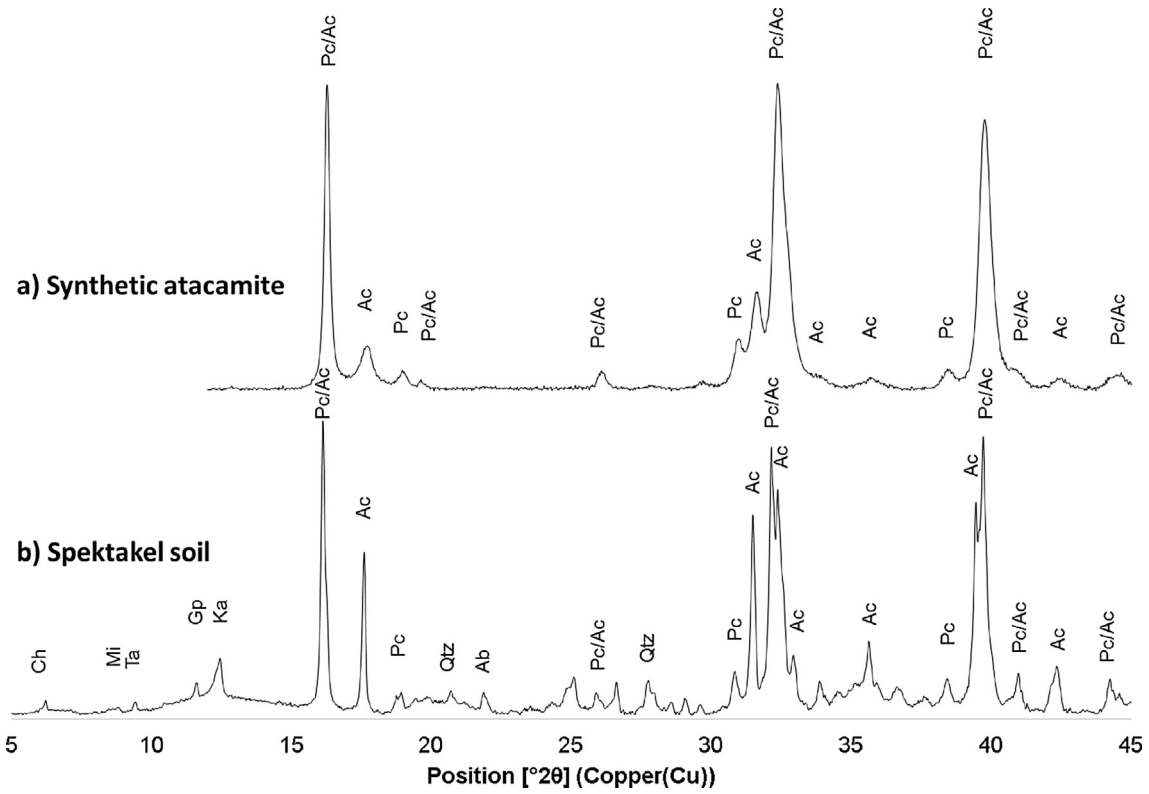

Fig. 2. X-ray diffraction patterns of a) the synthetic atacamite and b) the Spetakel soil (Ac = atacamite; Pc = paratacamite; Ch = chlorite; Mi = mica; Ta = talc; Gp = gypsum; ka = kaolinite; Qtz = quartz; Ab = albite).

mineralogy is dominated by atacamite minerals (atacamite and paratacamite) along with talc, chlorite, gypsum and other common soil minerals (Fig. 2).

2.2. Soil equilibrium experiments

In a batch experiment, 0.4 g of Spektakel soil was reacted with NaCl solutions of various strengths for 24 days. The following NaCl concentrations were used 0, 0.1, 0.25 and 0.5 M. The pH of the suspensions were measured daily and at the end of the 24 days the supernatants were analysed for soluble Cu using a Varian inductively coupled plasma atomic emission spectrometer (ICP-AES). All samples were prepared in triplicate. The experiment was also simulated using PHREEQC version 2.18 (Parkhurst and Appello, 1999) and the wateq4f.dat database, where atacamite was equilibrated with atmospheric CO_2 ($P_{CO2} = 10^{-3.5}$) and a range of NaCl containing solutions from 0 to 0.5 M in concentration (PHREEQC input file provided in Supplementary material S2).

2.3. Soil leaching experiments

The potential leachability of Cu from the Spektakel soils was determined by placing an 80 g subsample into a leaching column and leaching the soil with either deionised water (DI) or 0.5 M NaCl (NaCl). The amount of solution added was limited so that only soil pores were saturated and limited free water accumulated on top of the soil column. Initially soils were wetted with 45 mL of solution (either DI or NaCl). Thereafter 20 mL of solution was added to each column and allowed to equilibrate for 24 h before the solution was extracted under vacuum through a glass wool plug. Each extract was analysed for Cu^{2+} using a Varian 240 FS atomic absorption spectrometer. The leaching columns were prepared in triplicate for each solution.

2.4. Kinetic experiments

Two extreme cases of ionic strength were used for the kinetic experiments, deionised water and a 0.5 M NaCl solution. Although DI water represents an unrealistic natural solution, it is an extreme proxy for meteoric water, and thus can be used to determine the upper limit for the atacamite dissolution rate. A 0.5 M NaCl solution was selected as the upper salinity limit as this represents the maximum Cl^- concentration measured in the Spetakel soil solution (Clarke et al., 2014). Samples were prepared by weighing 0.4 g of synthetic atacamite into a 50 mL beaker. A 40 mL solution of NaCl or DI was then added to the atacamite. The pH of each suspension was adjusted to pH 5.5, 5.0. 4.5 or 4.0 with 1 N HNO_3 using a Metrohm 905 Titrando autotitrator. The use of buffers for such a study was not possible due to the complexation of Cu by buffering agents (Cardoso Fonseca et al., 1992). The kinetic measurements were only started once the target pH had been achieved. A 0.7 mL aliquot of suspension was collected at 60 s time intervals and immediately filtered through 0.2 μm syringe filters to stop the reaction. The filtered solutions were diluted 10 times before being analysed for Cu^{2+} with ICP-AES. The consumption of acid was also measured throughout the duration of the kinetic experiments. The kinetic experiments were conducted in triplicate at each pH in both the NaCl and DI solutions. Following the initial rate method of Lasaga (1981), only the initial linear portion of the dissolution curve was used for rate calculations. Kinetic experiments were conducted at 25 °C, under ambient pCO_2. The buffer capacity was estimated by determining the amount of acid required to bring the pH down to

Please cite this article in press as: Le Roux, S.G., et al., The dissolution kinetics of atacamite in the acid range and the stability of atacamite containing soils from Namaqualand, South Africa, Applied Geochemistry (2015), http://dx.doi.org/10.1016/j.apgeochem.2015.09.003

the respective starting pH. In order to establish the effect of acid type on dissolution kinetics the kinetic procedure was repeated at pH 4.5, using 1 N H_2SO_4.

The initial dissolution rate of atacamite in the Spektakel soil sample was determined by reacting the soil with DI and NaCl solutions acidified to pH 4.5 using 1 N HNO_3. Care was taken to ensure that the same amount of atacamite (calculated from the total Cu concentration in the soil) was used as in the synthetic atacamite experiments.

3. Results

3.1. The effect of salt concentration on atacamite dissolution

Fig. 3 shows the change in solution pH over time for the Spektakel soils equilibrated with solutions of different NaCl concentrations for 24 days. Initially the DI treatment (0 M) showed a substantially higher pH than the salt treatments, but the pH values for all solutions converged with time and after 4 days there was no significant difference between treatments. Modelling the pH of the four solutions equilibrated with atacamite in PHREEQC (Fig. 3) showed a similar trend to the initial pH of the experiment, with the pH in DI water being substantially higher than in any of the salt treatments. Copper release after 24 days equilibration in the four solutions is given in Fig. 4. Both the modelled and the experimental data show the same trend although the experimental concentrations are consistently higher. The experimental Cu concentration in DI is significantly higher ($p < 0.01$) than in the salt solutions. No significant difference was evident between the different salt solutions (0.1–0.5 M).

The leaching study results are shown in Fig. 5. Copper release is significantly higher in the first NaCl leachate, but further leaching reduces the Cu concentration and after the fourth leaching, the Cu in NaCl drops well below the level observed in the DI solution.

3.2. Atacamite dissolution kinetics

Atacamite dissolution in an acid medium is given by the following equation:

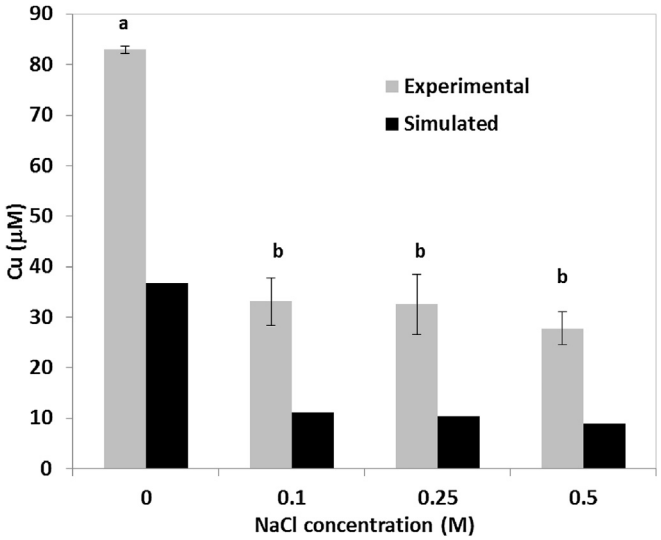

Fig. 4. Copper concentration in DI (0) and three NaCl solutions equilibrated with Spektakel soils for 24 days (grey) shown with simulated (PHREEQC) Cu concentrations after equilibration with atacamite (black). Different letters show concentrations that differ significantly at $p \leq 0.05$.

$$Cu_2(OH)_3Cl + 3H^+ \rightleftharpoons 2Cu^{2+} + Cl^- + 3H_2O \quad [1]$$

The $[H^+_{consumed}]/[Cu^{2+}_{released}]$ ratio observed in the dissolution experiments was 1.5 indicating that congruent dissolution of atacamite occurs in acid media (Brantley, 2008). The kinetics of the dissolution was measured both by the increase of Cu^{2+} in solution as well as the consumption of protons, although at pH 5 and 5.5 proton consumption was not sensitive enough for kinetic observations. Fig. 6 shows the release of Cu with time for DI and NaCl treatments in the pH 4.5 treatment. The initial rates for atacamite dissolution in both DI and NaCl between pH 5.5 and 4.0 are given in Table 1. Initial dissolution rates at pH 5.5 were highly variable (relative standard deviation (RSD) > 68%), which led to insignificant differences in the dissolution rates measured in DI and NaCl. The high variability at pH 5.5 is assigned to small differences in

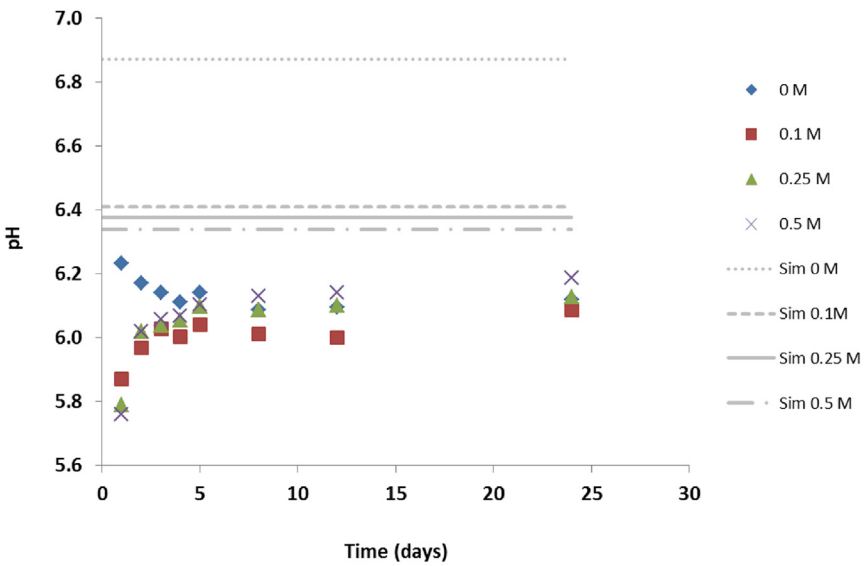

Fig. 3. Solution pH as a function of time for deionised water (0 M) and three NaCl solutions equilibrated with the Spektakel soil for 24 days. Grey lines give the simulated (Sim) pH for the solutions equilibrated with atacamite modelled using PHREEQC.

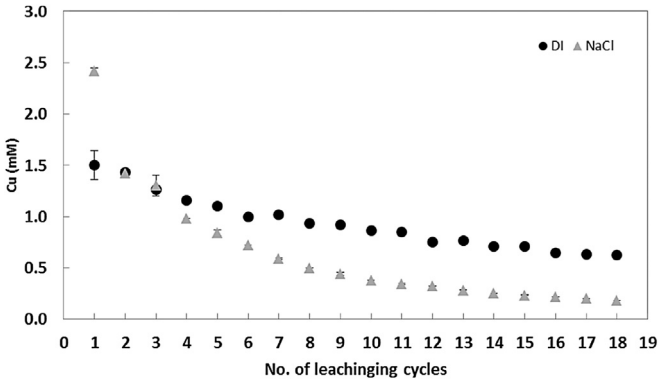

Fig. 5. Copper concentration (mM) measured in NaCl and deionised water (DI) leachates extracted from Spektakel soils every 24 h.

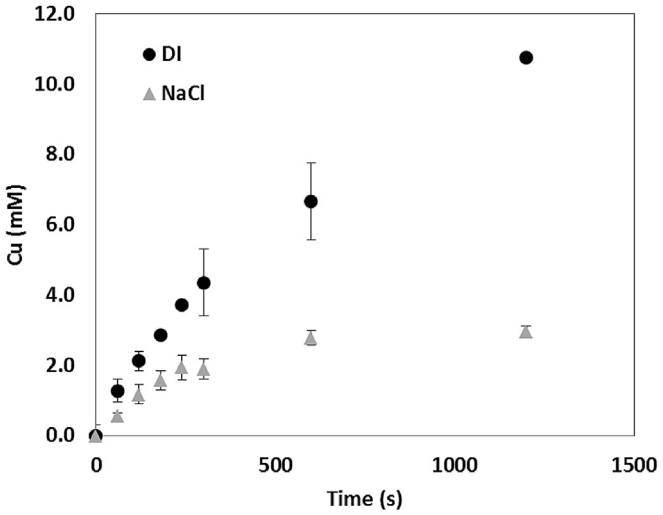

Fig. 6. Copper dissolution (mM) from atacamite as a function of time in deionised water (DI) and a 0.5 M NaCl solution acidified to pH 4.5.

Table 1
Initial dissolution rates (mol m^{-2} s^{-1}) of atacamite between pH 5.5 and 4.0 measured in deionised water (DI) and 0.5 M NaCl (NaCl) using HNO_3 or H_2SO_4 to acidify suspensions. Also included, initial dissolution rates of atacamite from the Spektakel soil acidified with HNO_3.

pH	HNO_3		H_2SO_4		Soil atacamite (HNO_3)	
	DI	NaCl	DI	NaCl	DI	NaCl
5.5	$10^{-8.91a}$	$10^{-9.55a}$				
5.0	$10^{-8.42a}$	$10^{-8.79b}$				
4.5	$10^{-7.34a}$	$10^{-7.68b}$	$10^{-7.33a}$	$10^{-7.60b}$	$10^{-7.93c}$	$10^{-8.35d}$
4.0	$10^{-7.14a}$	$10^{-7.18a}$				

*Different superscript letters show significant difference between DI and NaCl treatments at a $p \leq 0.05$.

homogenisation of the stirred samples as well as the low concentrations of Cu^{2+} released. The precision of the dissolution rate measurement improved at lower pH values (RSD < 29%). At pH 5.0 and 4.5 dissolution rates were significantly ($p \leq 0.05$) higher in DI than in NaCl while at pH 4 there was no significant difference ($p = 0.6$) in the rates despite a low RSD (<15%). Reaction rates in both DI and NaCl increased with decreasing pH. The pseudo reaction order with respect to pH was determined by plotting the log of the initial rate against pH (Lasaga, 1981) as shown in Fig. 7. The

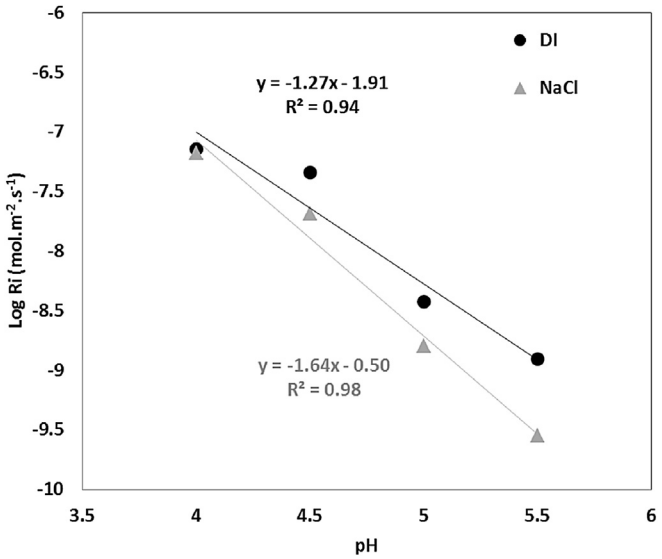

Fig. 7. Log of initial atacamite dissolution rate Ri (mol m^{-2} s^{-1}) plotted against pH for NaCl and deionised water (DI) solutions.

reaction order, across the experimental pH range, is 1.6 in NaCl and 1.3 in DI with respect to H^+ activity. Despite the high R^2 value for both curves ($R^2 > 0.90$) it may be possible that the order may not be linear across the experimental pH range. Fragmenting the experimental range into 4–4.5 and 5–5.5 still gives a higher pH-dependent reaction order in NaCl than in DI.

To establish the effect of acid type on dissolution rate, the initial rate of atacamite dissolution at pH 4.5 was determined using H_2SO_4 to acidify the solution (Table 1). Again a significant difference ($p = 0.03$) was obtained between the DI and NaCl treatments acidified with H_2SO_4, however acidification with different acids had no significant effect on the respective treatments.

Dissolution rates of atacamite in the Spektakel soil are provided in Table 1. Again dissolution rates are higher in the DI compared to the NaCl and both rates measured in the soil are slightly slower than those measured with the synthetic atacamite.

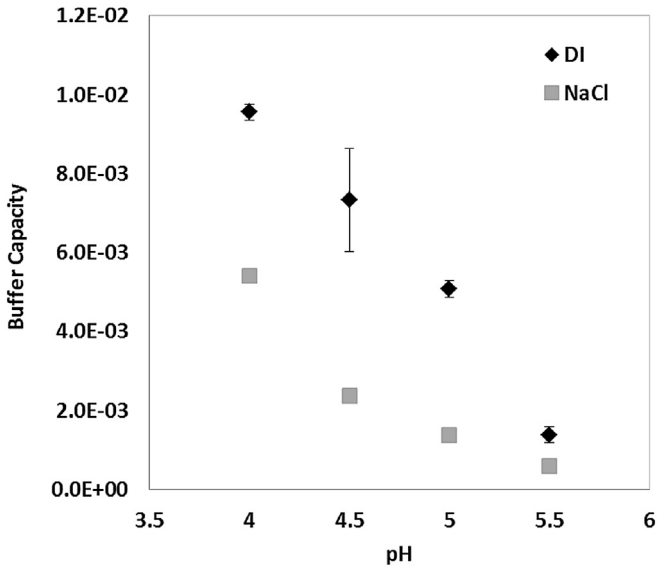

Fig. 8. Buffer capacity of pure atacamite in deionised water (DI) and 0.5 M NaCl.

3.3. The effect of salt concentration on atacamite pH buffer capacity

The amount of acid required to bring the atacamite suspensions to the desired pH was used as a proxy for the buffer capacity of the mineral-solution system (Fig. 8). The DI system showed a significantly ($p < 0.02$) higher buffer capacity than the NaCl system across the experimental pH range. The difference between the two treatments showed a decrease with decreasing pH.

4. Discussion

4.1. The effect of salt concentration on atacamite dissolution from the Spektakel soils

The concentration of NaCl has a significant influence on the solution pH in equilibrium with atacamite, with the simulated equilibrium showing a decreasing pH as the concentration of NaCl increases (Fig. 3). The pH at the beginning of the experimental period showed a similar trend, but pH evened out as the equilibrium time progressed. The higher pH in the DI water is likely to relate to the higher equilibrium Cu concentration in this solution (Fig. 4) which signifies increased atacamite dissolution. According to Equation (1) atacamite dissolution is an acid-consuming reaction, thus the increased dissolution of atacamite in DI will result in a pH increase. This also relates to the significantly higher buffer capacity of atacamite in water compared to NaCl (Fig. 8). The stoichiometric $[H^+_{consumed}]/[Cu^{2+}_{released}]$ ratio of 1.5, measured during the kinetic experiments, demonstrates that buffer capacity directly relates to the dissolution of the mineral. The reason for the pH change over time in the Spektakel soil (Fig. 3) is not clear but may relate to slower mineral equilibrium reactions controlling the pH over time. The lower equilibrium pH and higher Cu concentrations in the Spektakel soil sample compared to the modelled solutions, suggests that there are more labile Cu fractions (possibly exchangeable) in the soil as one would expect in a complex natural system. Although exchangeable Cu is difficult to determine, due to the reaction of NH_4OAc with Cu hydroxide phases (Künkül et al., 2013), a 1:5 KCl extract yielded an exchangeable Cu concentration of 1.6 mmol kg^{-1} confirming the presence of an exchangeable Cu fraction in the soil.

Fig. 5 shows the capacity for Cu release from the Spektakel soil with continual additions of pure and saline water. The Cu release in the first leaching cycle shows the opposite trend to what is observed in the equilibrium experiments (Fig. 4) with the NaCl solution releasing significantly more Cu than the DI treatment. The Cu concentration in subsequent NaCl leaching cycles decreases substantially and after the 4th cycle the Cu concentration in the NaCl leachates declines below that measured in the DI leachates. This suggests that the initial Cu released in the NaCl treatment may represent an exchangeable Cu phase, which is depleted after a single leaching cycle. Further cycles return to the pattern of higher Cu release in DI suggesting that after the removal of the more labile exchangeable phase, atacamite equilibrium starts to control Cu release. The apparent contradiction of the initial leaching results and the equilibrium experiment can be reconciled by the fact that the equilibrium experiment was left for 24 days before Cu was measured. This would have allowed for exchangeable Cu, initially released from the NaCl addition, to have equilibrated with atacamite in the chloride-rich solution. As shown by Woods and Garrels (1986) equilibrium reactions involving Cu hydroxyl minerals occur rapidly. The initial Cu release from the exchangeable phase may also partly explain the lower pH observed initially for the equilibrium experiment as a result of Cu hydrolysis reactions.

The leaching experiment (Fig. 5) was designed to assess Cu release from the Spektakel soils after a large rainfall event. The experiment was designed so that the added solutions only just saturated the soil. The high concentration of Cu initially released in the NaCl solution, means that a spike of Cu laden water is likely to move through the profile with the onset of a rainfall event. Further Cu mobilisation is likely to decrease as a rain event continues, yet a sustained release of Cu will occur as atacamite dissolves and the more the soil solution is diluted the higher the sustained release of Cu will be.

The Spektakel soils generally have a sandy loam texture, which gives them an approximate field capacity of 140 mm/m (Saxton et al., 1986). The atacamite is predominantly found in the top 20 cm of soil, thus a rainfall event of at least 30 mm is required to induce leaching through the Cu containing horizon. Nakwafila (2015) showed that within a one year period, two rainfall events occurred which exceeded 30 mm in a 24 h period. Although rainfall can be very erratic in this region, the occurence of these high rainfall events indicates that Cu can be leached from the Spektakel soils as a result of annual precipitation. Should these high rainfall events become more common in the future then the amount of Cu leached from the Spektakel soils will presumably increase.

4.2. The effect of pH, salt concentration and acid type on atacamite dissolution kinetics

The results given in Table 1 show the strong pH dependence of the atacamite dissolution rate over the pH range tested (5.5–4.0). The dissolution rates were higher in DI than in NaCl above pH 4, however at pH 4 the dissolution rates converged. The difference between dissolution rates in DI and NaCl can be explained by deviation from equilibrium conditions. The highest mineral dissolution rates are achieved under conditions furthest from equilibrium due to negligible influence of the reverse reaction (Brantley, 2008; Pokrovsky and Schott, 2004). Fig. 9 shows the composition of the first sample, collected after the pH had reached the desired value, plotted with the atacamite equilibrium lines in both NaCl and DI. The saturation index (SI) was consistently lower in DI than in NaCl, which would explain the higher dissolution rate in DI. At pH 4 both solutions are far from equilibrium with atacamite, which may explain why dissolution rates converged at this point. It is also apparent from the converging atacamite stability lines constructed in PHREEQC (Fig. 9) that at lower pH values, Cl^- activity plays a

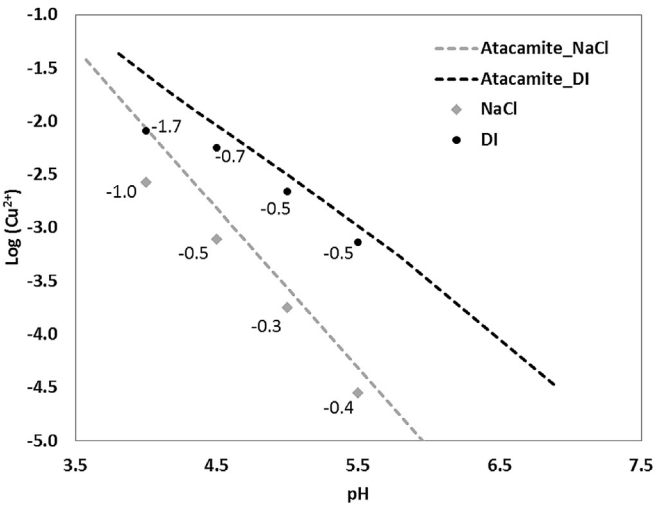

Fig. 9. Log Cu^{2+} activity of the first samples taken during the kinetic study in the NaCl and DI solutions, plotted with equilibrium lines modelled in PHREEQC for atacamite stability in NaCl (Atacamite_NaCl) and DI (Atacamite_DI) throughout the pH rage used. The saturation index for each point is given next to the symbol.

diminishing role in the stability of atacamite.

In order to establish how realistic the synthetic atacamite dissolution rates are for predicting atacamite dissolution in the environment, the atacamite dissolution rate in the Spektakel soil was measured at pH 4.5. The dissolution rates determined in the soil were, on average, four times slower than the synthetic atacamite dissolution rate. Although the dissolution rate is slower in the soil, it needs to be kept in mind that the soil contains water soluble Cl^- ions and thus a pure DI-soil system does not exist. In addition to this, the soil is a heterogeneous mix of minerals and the surface area measurement, required to determine the dissolution rate is, not specific to atacamite. Thus given the large scope for error when dealing with the soil, the dissolution rates of the synthetic and environmental samples of atacamite are very comparable. This suggests that the dissolution rates presented here give a realistic indication of atacamite dissolution kinetics in the acid range.

There has been very little work conducted on the dissolution kinetics of divalent hydroxides, making the comparison of atacamite dissolution rates to similar divalent oxides difficult. In order to put the atacamite dissolution rate into perspective it is useful to compare it to other acid soluble minerals. The fastest dissolution rate for atacamite was observed in DI water at pH 4 ($10^{-7.14}$ mol s^{-1} m^{-2}). This rate is substantially slower than the dissolution rate of calcite and dolomite at pH 4 ($10^{-4.25}$ and $10^{-5.7}$, respectively) as reported by Chou et al. (1989). Although caution needs to be exercised when comparing mineral dissolution rates, due to the large number of factors that influence reaction kinetics (Brantley, 2008), atacamite dissolution appears to be substantially slower than these common carbonate minerals. This suggests that even in an aggressive solution, such as acidified DI water, atacamite dissolution rate is only moderate at best. Bingöl and Canbazoğlu (2004), observed diffusion controlled kinetics for malachite dissolution in sulphuric acid, which suggests a rapid reaction rate (Brantley, 2008). Unfortunately the study on malachite did not actually calculate a rate, thus direct comparison to atacamite dissolution is not possible.

The reaction orders determined for both solutions are greater than 1 with respect to pH and across the investigated pH range a generalised rate expression for atacamite dissolution can be given as:

$$R_H = K_H\left[H^+\right]^{1.3-1.6}$$

Where R_H and K_H are the experimental dissolution rate and rate constant, respectively. These reaction orders are substantially higher than those reported for other oxyhydroxides, which often show fractional rate orders between 0 and 0.5 with respect to pH (Wieland et al., 1988). One reason for the high orders obtained in this study may relate to the narrow pH range investigated (Wieland et al., 1988) but may also relate to the nature of the mineral itself. For simple oxides the reaction order with respect to protonated surface species ($-M^{n+}OH_2^+$) has been shown to be equal to the oxidation state of the oxide metal for proton-promoted dissolution reactions (Furrer and Stumm, 1986; Pokrovsky and Schott, 2004). The high reaction order with respect to [H^+] concentration for atacamite dissolution suggests that atacamite hydroxyl groups protonate readily within the investigated pH range to form protonated surface species.

The higher reaction order observed for atacamite dissolution in NaCl compared to DI indicates that, in acidified solutions, reaction rates are more dependent on pH in NaCl than in DI. High electrolyte concentrations are known to increase surface protonation (McBride, 1994), which may contribute to the higher reaction order observed in NaCl, but the overriding factor is more likely to be a consequence of the diminishing effect of Cl^- ions on atacamite stability at low pH. In DI, dissolution at higher pH values is also affected by low Cl^- activities, thus pH is not the sole factor influencing dissolution.

It was hypothesised that sulphuric acid may result in a slower dissolution rate of atacamite than what was observed with nitric acid, due to potential equilibrium with the sulphate equivalent of atacamite, brochantite ($Cu_2(OH)_3SO_4$). Thermodynamic modelling (PHREEQC) of a solution acidified to pH 4.5 using sulphuric acid gives a brochantite saturation index of 1.2. The results, however, show no significant difference in dissolution rates between HNO_3 and H_2SO_4 (Table 1), suggesting that dissolution kinetics of atacamite dominate over brochantite precipitation kinetics in the acidic range.

Laboratory determined weathering rates are usually faster than field rates (White and Brantley, 2003). In addition deionised water is an aggressive dissolution agent and is an extreme proxy for meteoric water. Thus the conditions used in our kinetic experiments represent favourable conditions for mineral dissolution and should be considered as the upper limit for atacamite dissolution. The results imply that although atacamite dissolution will occur in acidic sulphate waters, the dissolution rate of atacamite is only moderate at best and thus with the slow movement of water in the arid Spektakel soil system large scale dissolution is unlikely even in a large rainfall event. This would suggest that the risk of extensive Cu pollution of the Buffels river aquifer is relatively low, under current climatic patterns.

5. Conclusions

The equilibrium pH and Cu release from atacamite minerals is higher in pure water than in concentrated NaCl solutions as a result of increased atacamite dissolution in pure water. Equilibrium Cu concentrations in the Spektakel soil are higher than thermodynamically predicted, indicating there may be more labile Cu phases in the soils. Leaching the soil with a concentrated NaCl solution initially releases more Cu than in pure water, suggesting that the initial water percolating through the soil profile will have a high Cu spike but Cu concentrations will decrease with further additions of water as atacamite starts to control Cu release.

Atacamite shows a moderate dissolution rate in the acidic pH range. Atacamite dissolution rates are dependent on NaCl concentration and pH with higher rates observed in pure water compared to concentrated NaCl. Reaction rates in both solutions converge at pH 4 suggesting atacamite is far from equilibrium in either solution. The dissolution of atacamite is unaffected by the presence of sulphate ions when sulphuric acid is used to acidify the system, suggesting that atacamite dissolution is faster than brochantite formation in acid conditions.

Currently, the western coastal region of South Africa is characterised by low rainfall, indicating that atacamite dissolution would be limited. Most global climate models predict a reduction in precipitation rates throughout large parts of south western Africa but an increase in the incidence of extreme rainfall events (Fauchereau et al., 2003). On-going monitoring of rainfall events would therefore be necessary to determine whether climate change might lead to an increase in the amount of Cu being dissolved during extreme rainfall events and how this might impact on water quality in the region.

Acknowledgements

We would like to thank Prof. Roychoudhury for the generous use of his autotitrator and Matt Gordon for Cu analyses. This research was funded by the South African National Research Foundation

Please cite this article in press as: Le Roux, S.G., et al., The dissolution kinetics of atacamite in the acid range and the stability of atacamite containing soils from Namaqualand, South Africa, Applied Geochemistry (2015), http://dx.doi.org/10.1016/j.apgeochem.2015.09.003

(grant number 80400). A student bursary (S.G. le Roux) was provided by Inkaba ye Africa. This is Inkaba ye Africa publication number 83.

Appendix A. Supplementary material

Supplementary material related to this article can be found at http://dx.doi.org/10.1016/j.apgeochem.2015.09.003.

References

Adams, S., Titus, R., Xu, Y., 2004. Groundwater Recharge Assessment of the Basement Aquifers of Central Namaqualand. Water Research Commission Report No. 1093/1/04, Pretoria, South Africa.

Benito, G., Botero, B.A., Thorndycraft, V.R., Rico, M., Sanchez-Moya, Y., Sopena, A., Machado1, M.J., Dahan, O., 2011. Rainfall-runoff modelling and palaeoflood hydrology applied to reconstruct centennial scale records of flooding and aquifer recharge in ungauged ephemeral rivers. Hydrol. Earth Syst. Sci. 15, 1185–1196.

Bingöl, D., Canbazoğlu, M., 2004. Dissolution kinetics of malachite in sulphuric acid. Hydrometallurgy 72, 159–165.

Brantley, S.L., 2008. Kinetics of Mineral Dissolution, Kinetics of Water–Rock Interaction. Springer, pp. 151–210.

Cameron, E., Leybourne, M., Palacios, C., 2007. Atacamite in the oxide zone of copper deposits in northern Chile: involvement of deep formation waters? Min. Depos. 42, 205–218.

Cardoso Fonseca, E., Claudino Cardoso, J., Estela Martins, M., Margarida Vairinho, M., 1992. Selective chemical extraction of Cu from selected mineral and soil samples: enhancement of Cu geochemical anomalies in Southern Portugal. J. Geochem. Explor. 43, 249–263.

Chou, L., Garrels, R.M., Wollast, R., 1989. Comparative study of the kinetics and mechanisms of dissolution of carbonate minerals. Chem. Geol. 78, 269–282.

Clarke, C.E., le Roux, S.G., Roychoudhury, A.N., 2014. The role of evaporation in the formation of secondary Cu-hydroxy minerals in the arid Namaqualand soil system. South Afr. Appl. Geochem. 47, 52–60.

Fauchereau, N., Trzaska, S., Rouault, M., Richard, Y., 2003. Rainfall variability and changes in southern Africa during the 20th century in the global warming context. Nat. Hazards 29, 139–154.

Furrer, G., Stumm, W., 1986. The coordination chemistry of weathering: I. Dissolution kinetics of δ-Al_2O_3 and BeO. Geochim. Cosmochim. Acta 50, 1847–1860.

Hannington, M.D., 1993. The formation of atacamite during weathering of sulfides on the modern seafloor. Can. Mineral. 31, 945–956.

Hoerling, M., Hurrell, J., Eischeid, J., Phillips, A., 2006. Detection and attribution of twentieth century northern and southern African rainfall change. J. Clim. 19, 3989–4008.

Künkül, A., Gülezgin, A., Demirkiran, N., 2013. Investigation of the use of ammonium acetate as an alternative lixiviant in the leaching of malachite ore. Chem. Ind. Chem. Eng. Q. 19, 25–34. http://dx.doi.org/10.2298/CICEQ120113039K.

Lasaga, A.C., 1981. Rate laws of chemical reactions. In: Lasaga, A.C., Kirkpatrick, R.J. (Eds.), Kinetics of Geochemical Processes. Reviews in Mineralogy, vol. 8. Mineralogical Society America, Washington, DC, pp. 1–68.

Livingston, R.A., 1991. Influence of the environment on the patina of the Statue of Liberty. Environ. Sci. Technol. 25, 1400–1408.

MacFarlane, W.R., Kyser, T.K., Chipley, D., Beauchemin, D., Oates, C., 2005. Continuous leach inductively coupled plasma mass spectrometry: applications for exploration and environmental geochemistry. Geochem. Explor. Environ. Anal. 5, 123–134.

MacKeller, N.C., Hewitson, B.C., Tadross, M.A., 2007. Namaqualand's climate: recent historical changes and future scenarios. J. Arid. Environ. 70, 604–614.

McBride, M.B., 1994. Environmental Chemistry of Soils. Oxford University Press, New York.

Nakwafila, A.N., 2015. Salinisation Source(s) and Mechanism(s) in Shallow Alluvial Aquifers along the Buffels River, Northern Cape Province, South Africa, Earth Science. Stellenbosch University.

Parkhurst, D.L., Appello, C.A.J., 1999. Users Guide to PHREEQC (Version 2)-A Computer Program for Speciation, Batch-reaction, One-dimensional Transport and Inverse Geochemical Calculations, pp. 99–4259. U.S. Geological Survey Water-Resources Investigations Report.

Pokrovsky, O.S., Schott, J., 2004. Experimental study of brucite dissolution and precipitation in aqueous solutions: surface speciation and chemical affinity control. Geochim. Cosmochim. Acta 68, 31–45.

Quast, K.B., 2000. Leaching of atacamite ($Cu_2(OH)_3Cl$) using dilute sulphuric acid. Miner. Eng. 13, 1647–1652.

Reich, M., Palacios, C., Parada, M.A., Fehn, U., Cameron, E.M., Leybourne, M.I., Zúñiga, A., 2008. Atacamite formation by deep saline waters in copper deposits from the Atacama Desert, Chile: evidence from fluid inclusions, groundwater geochemistry, TEM, and 36Cl data. Miner. Depos. 43, 663–675.

Reich, M., Palacios, C., Vargas, G., Luo, S., Cameron, E., Leybourne, M., Parada, M., Zuniga, A., You, C.-F., 2009. Supergene enrichment of copper deposits since the onset of modern hyperaridity in the Atacama Desert, Chile. Miner. Depos. 44, 497–504.

Saxton, K.E., Rawls, W.J., Romberger, J.S., Papendick, R.I., 1986. Estimating generalized soil-water characteristics from texture. Soil Sci. Soc. Am. J. 50, 1031–1036.

Sharkey, J.B., Lewin, S.Z., 1971. Conditions governing the formation of atacamite and paratacamite. Am. Mineral. 56, 179–191.

Sillitoe, R.H., 2005. Supergene oxidized and enriched porphyry copper and related deposits. In: Economic Geology 100th Anniversary Volume, pp. 723–768.

White, A.F., Brantley, S.L., 2003. The effect of time on the weathering of silicate minerals: why do weathering rates differ in the laboratory and field? Chem. Geol. 202, 479–506.

Wieland, E., Wehrli, B., Stumm, W., 1988. The coordination chemistry of weathering: III. A generalization on the dissolution rates of minerals. Geochim. Cosmochim. Acta 52, 1969–1981.

Woods, T.L., Garrels, R.M., 1986. Use of oxidised copper minerals as environmental indicators. Appl. Geochem. 1, 181–187.

Please cite this article in press as: Le Roux, S.G., et al., The dissolution kinetics of atacamite in the acid range and the stability of atacamite containing soils from Namaqualand, South Africa, Applied Geochemistry (2015), http://dx.doi.org/10.1016/j.apgeochem.2015.09.003